OAK RIDGE
NATIONAL LABORATORY
MANAGED BY UT-BATTELLE
FOR THE DEPARTMENT OF ENERGY

ORNL/TM-2010/199

Pre-Conceptual Design of a Fluoride-Salt-Cooled Small Modular Advanced High-Temperature Reactor (SmAHTR)

December 2010

Prepared by

S. R. Greene
J. C. Gehin
D. E. Holcomb
J. J. Carbajo
D. Ilas
A. T. Cisneros
V. K. Varma
W. R. Corwin
D. F. Wilson
G. L. Yoder Jr.
A. L. Qualls
F. J. Peretz
G. F. Flanagan
D. A. Clayton
E. C. Bradley
G. L. Bell
J. D. Hunn
P. J. Pappano
M. S. Cetiner

UT-BATTELLE
ORNL-27 (4-00)

DOCUMENT AVAILABILITY

Reports produced after January 1, 1996, are generally available free via the U.S. Department of Energy (DOE) Information Bridge.

Website http://www.osti.gov/bridge

Reports produced before January 1, 1996, may be purchased by members of the public from the following source.

National Technical Information Service
5285 Port Royal Road
Springfield, VA 22161
Telephone 703-605-6000 (1-800-553-6847)
TDD 703-487-4639
Fax 703-605-6900
E-mail info@ntis.gov
Website http://www.ntis.gov/support/ordernowabout.htm

Reports are available to DOE employees, DOE contractors, Energy Technology Data Exchange (ETDE) representatives, and International Nuclear Information System (INIS) representatives from the following source.

Office of Scientific and Technical Information
P.O. Box 62
Oak Ridge, TN 37831
Telephone 865-576-8401
Fax 865-576-5728
E-mail reports@osti.gov
Website http://www.osti.gov/contact.html

This report was prepared as an account of work sponsored by an agency of the United States Government. Neither the United States Government nor any agency thereof, nor any of their employees, makes any warranty, express or implied, or assumes any legal liability or responsibility for the accuracy, completeness, or usefulness of any information, apparatus, product, or process disclosed, or represents that its use would not infringe privately owned rights. Reference herein to any specific commercial product, process, or service by trade name, trademark, manufacturer, or otherwise, does not necessarily constitute or imply its endorsement, recommendation, or favoring by the United States Government or any agency thereof. The views and opinions of authors expressed herein do not necessarily state or reflect those of the United States Government or any agency thereof.

ORNL/TM-2010/199

PRE-CONCEPTUAL DESIGN OF A FLUORIDE-SALT-COOLED SMALL MODULAR ADVANCED HIGH-TEMPERATURE REACTOR (SmAHTR)

S. R. Greene
J. C. Gehin
D. E. Holcomb
J. J. Carbajo
D. Ilas
A. T. Cisneros
V. K. Varma
W. R. Corwin
D. F. Wilson
G. L. Yoder Jr.
A. L. Qualls
F. J. Peretz
G. F. Flanagan
D. A. Clayton
E. C. Bradley
G. L. Bell
J. D. Hunn
P. J. Pappano
M. S. Cetiner

Date Published: December 2010

Prepared by
OAK RIDGE NATIONAL LABORATORY
Oak Ridge, Tennessee 37831-6283
managed by
UT-BATTELLE, LLC
for the
U.S. DEPARTMENT OF ENERGY
under contract DE-AC05-00OR22725

CONTENTS

Page

LIST OF FIGURES

LIST OF TABLES

ACRONYMS AND ABBREVIATIONS

AEC	U.S. Atomic Energy Commission
AHTR	Advanced High-Temperature Reactor
AHX	air heat exchanger
ASME	American Society of Mechanical Engineers
B&PV	boiler and pressure vessel
BOL	beginning of life
DAR	DRACS air radiator
DHX	DRACS heat exchanger
DOE NE	U.S. Department of Energy Office of Nuclear Energy
DOE	U.S. Department of Energy
DOT	U.S. Department of Transportation
DRACS	direct reactor auxiliary cooling system
FHR	fluoride-salt-cooled high-temperature reactor
GCR	gas-cooled reactor
GDC	general design criteria
GEN-III+	generation III+
GT-MHR	Gas-Turbine Modular Helium Reactor
GWe	gigawatt (electric)
HWR	heavy water reactor
ICL	intermediate cooling loop
IHX	intermediate heat exchanger
ILP	intermediate loop pump
iPWR	integral pressurized water reactor
kWe	kilowatt (electric)
LBLOCA	large break loss-of-coolant accident
LMR	liquid metal reactor
LWR	light water reactor
MCL	main circulating loop
MCP	main circulating pump
MSBR	Molten Salt Breeder Reactor
MSR	molten salt reactor
MSRE	Molten Salt Reactor Experiment
MWe	megawatt (electric)
MWt	megawatt (thermal)
NASA	National Aeronautics and Space Administration
NGNP	Next-Generation Nuclear Plant
NRC	U.S. Nuclear Regulatory Commission
O&M	operations and maintenance
ORC	organic Rankine cycle
ORNL	Oak Ridge National Laboratory
PBMR	Pebble-Bed Modular Reactor
pcm	percent mille (10^{-5})
PHX	primary heat exchanger
PIRT	phenomena identification and ranking table
PRA	probabilistic risk assessment
PRISM	Power Reactor Innovative Small Module
psia	pounds per square inch (absolute)
RCS	reactivity control system
RPM	revolutions per minute
RPV	reactor pressure vessel

SAFR	Sodium Advanced Fast Reactor
S-CO_2	supercritical carbon dioxide
SSC	systems, structures, and components
SHX	secondary heat exchanger
SmAHTR	Small modular Advanced High-Temperature Reactor
SMR	small modular reactor
TRISO	tri-isotropic
UCO	uranium oxicarbide

FOREWORD

During the spring of 2010, a multidisciplinary team of reactor systems specialists and nuclear technologists was assembled at Oak Ridge National Laboratory to explore the feasibility of a small modular fluoride-salt-cooled high-temperature reactor, or FHR. The goal of the team was to explore the technology and system architecture trade-space for this new reactor type and to develop a pre-conceptual design. This document and the design presented here are the products of this effort. However, the team went beyond simply defining a reactor concept, also proposing an innovative thermal energy system based on the clustering of multiple small FHR units together with an advanced energy storage system to deliver benefits not otherwise attainable from reactor units operating independently.

The fluorine-salt-cooled Small modular Advanced High-Temperature Reactor (SmAHTR) and energy system concept described in this report are but a first step in making tangible the possibilities afforded by new technologies, new ways of employing "old" technologies, and new approaches to old challenges. They provide a tantalizing glimpse at what might be possible should the decision be made to develop and deploy small modular high-temperature and very-high-temperature reactors.

This preliminary effort has drawn upon the skills and innovative creativity of a team of dedicated individuals. Reactor systems are complex creations, and reactor system concept development is a highly iterative, collaborative process that draws on the technical skills, life experiences, intuitive inspirations, and interpersonal chemistry of the individuals working together. Success depends upon the team's ability to collectively exercise "disciplined fearlessness" in questioning the status quo, while humbly respecting the limits of our knowledge and the collective wisdom of our technical community. It is my belief the SmAHTR concept development team has achieved a measure of success in this regard. We look forward to the continuing evolution and improvement of the concept we have birthed.

Sherrell R. Greene, Leader
SmAHTR Concept Development Team
Oak Ridge, Tennessee
December 2010

EXECUTIVE SUMMARY

Fluoride-salt-cooled high-temperature reactors, or FHRs, are a new class of thermal-spectrum nuclear reactors defined by their use of liquid-fluoride-salt coolants, together with tri-isotropic (TRISO)-coated particle fuels and graphite moderator materials. FHRs operate with primary system pressures near atmospheric pressure and at coolant temperatures in the range of 600°C to ~1000°C. FHRs combine and leverage technologies and system architectures originally developed for molten salt reactors, gas-cooled reactors, and liquid-metal-cooled reactors to provide functionalities not otherwise attainable with traditional reactor concepts.

This report summarizes the results of work conducted at Oak Ridge National Laboratory during 2010 to explore the design space and technology trade issues associated with small modular FHRs. The small modular FHR concept described in this report, termed SmAHTR for Small modular Advanced High-Temperature Reactor, builds upon work conducted between 2002 and 2006, during which time the original large FHR concept, the Advanced High-Temperature Reactor (AHTR), was developed.

SmAHTR is a 125 MWt, integral primary system FHR concept (Figs. ES.1 and ES.2). The design goals for SmAHTR are to deliver safe, affordable, and reliable high-temperature process heat and electricity from a small plant that can be easily transported to and assembled at remote sites. The initial SmAHTR concept is designed to operate with a core outlet temperature of 700°C, but with a system architecture and overall design approach that can be adapted to much higher temperatures as higher-temperature structural materials become available. The SmAHTR reactor vessel is transportable via standard tractor-trailer vehicles to its deployment location (Fig. ES.3). Tables ES.1 and ES.2 provide SmAHTR's principal design and operating parameters.

SmAHTR employs a "two-out-of-three system" philosophy for operational and shutdown decay-heat removal. Transition from operational power production to shutdown decay-heat removal is accomplished without active components.

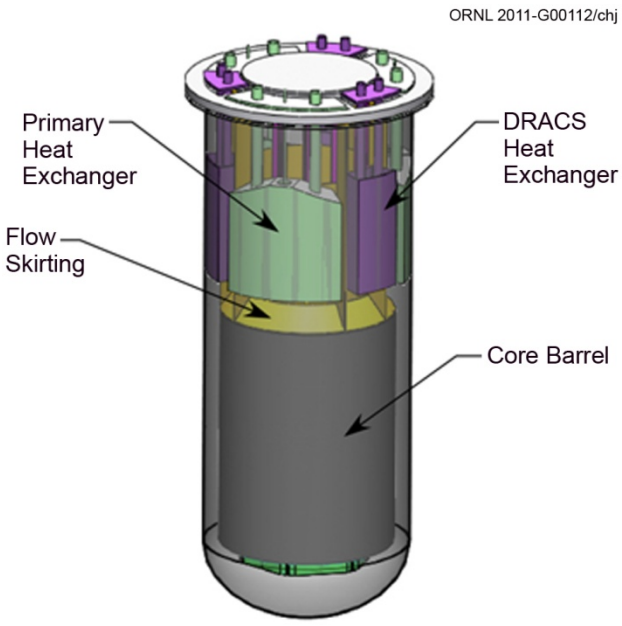

Fig. ES.1. SmAHTR integral primary system concept.

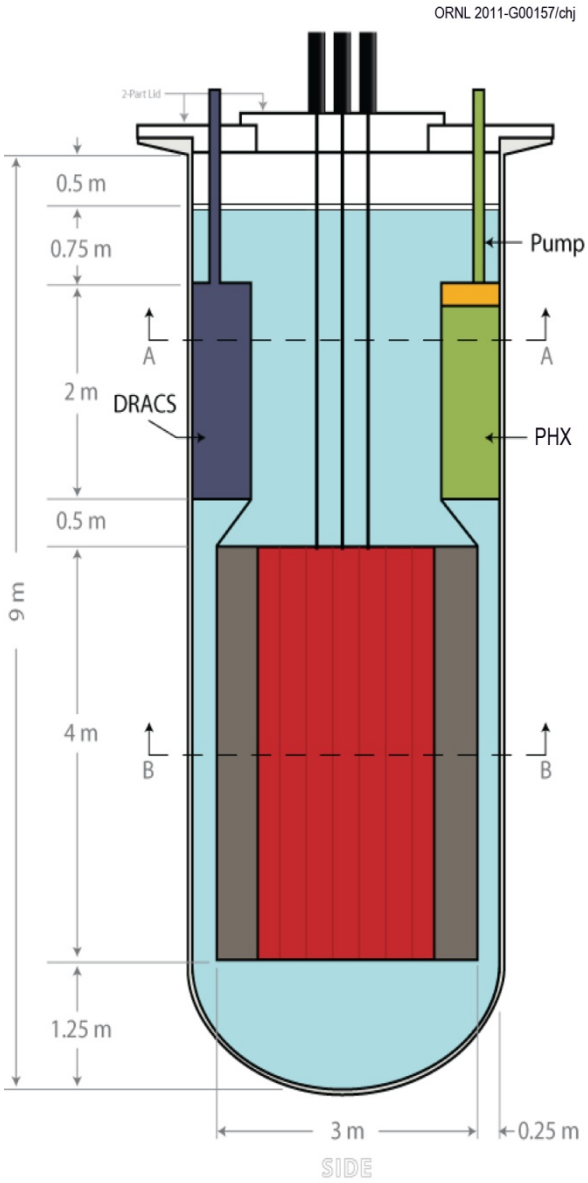

Fig. ES.2. SmAHTR dimensions.

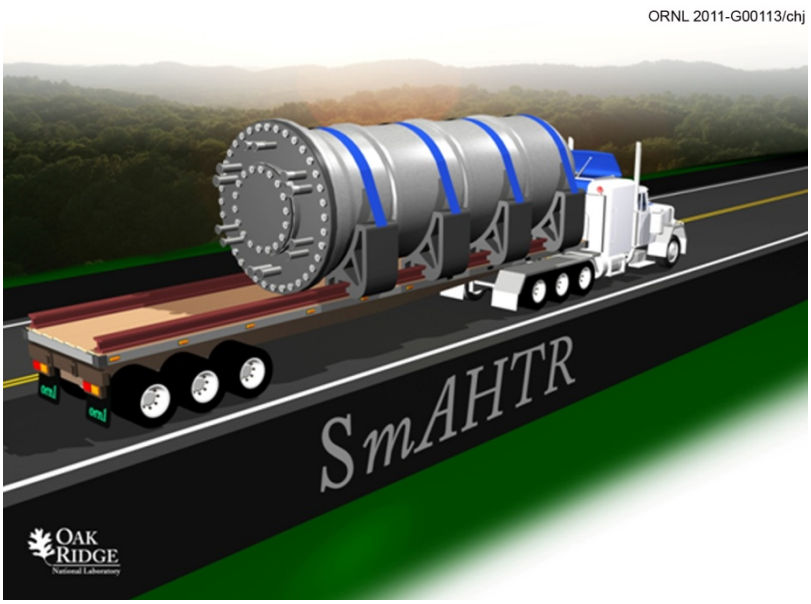

Fig. ES.3. SmAHTR reactor vessel can be transported via tractor-trailer.

Table ES.1. SmAHTR overall design values

Variable	Value
Reactor power, MW(t)	125
Core volumetric power density, MW(t)/m^3	9.4
Primary coolant salt	FLiBe
Fuel type	TRISO, low enriched uranium
TRISO packing fraction, vol. %	50
Fuel enrichment, wt %	19.75
Core uranium loading at BOL,[a] kg	1600–2020[b]
Core life, years	4.19
Fuel configuration	Annular pins
Fuel pin diameters (inside, outside), cm	2.2, 6.5
Fuel surface coating thickness, cm	0.3
Moderator material	Graphite
Moderator configuration	Pins and blocks
Moderator pin diameter, cm	6.16
Number of total fuel assemblies/blocks	19
Number of core assembly rings	3
Number of fuel pins/assembly	15
Number of graphite pins/assembly	4
Core height, m	4
Core effective diameter, m	~2.2
Reflector configuration and material	Radial, graphite blocks
Reflector diameter, effective inside, outside, m	~2.2, 3
Vessel height, m	9
Vessel diameter, m	3.5

Table ES.1. (continued)

Variable	Value
Vessel wall thickness, cm	2.5
Vessel weight (empty, no lid), kg	22,516
Vessel and skirt material	Hastelloy-N
Secondary coolant salt	FLiNaK
Core cooling mode	Forced convection
Core flow direction	Upward
IHX/downcomer flow direction[a]	Downward
Number of main coolant pumps	3
Number of PHXs[a]	3
Number of DRACS[a]	3
PHX/DRACS annulus, height, m	2
PHX/DRACS annulus, diameter-inner, m	2.365
PHX/DRACS annulus, diameter-outer, m	3.5

[a]BOL = beginning of life; IHX = intermediate heat exchanger; PHX = primary heat exchanger; DRACS = director reactor auxiliary cooling system.

[b]Core uranium loading depends upon the fuel concept employed and the refueling interval requirement. The range presented encompasses all fuel concepts and refueling intervals considered to date in the trade study.

Table ES.2. SmAHTR thermal hydraulic parameters

Variable	Units	Value
Reactor power	MW(t)	125
Primary coolant salt		FLiBe
Flow/pump (3 operating)	kg/s	510
Flow/pump (2 operating)	kg/s	765
Vortex valve diodicity		50
Bypass flow/DRACS[a]	kg/s	68
Bypass flow, total (3 DRACS)	kg/s	205
Total core flow	kg/s	1325
Total core flow area	m^2	0.6226
Core coolant velocity	m/s	1.1
Coolant temperature at core inlet	°C	650
Core outlet coolant temperature—inner, middle, outer radial zones	°C	703, 692, 689
Coolant temperature, upper plenum (mixed)	°C	692
Coolant temperature, top plenum	°C	687
Maximum fuel temperature, centerline	°C	1027
Maximum fuel temperature, surface	°C	988
Maximum fuel surface coating temperature	°C	786
Maximum fuel heat flux	W/m^2	6.3×10^5
Fuel/Coolant heat transfer coefficient	$W/(m^2 \cdot °C)$	4700–6380
Core pressure drop	kPa	15
Pumping power main pump	kW	10
PHX capacity, 3 operating/2 operating[a]	MW	42/63
PHX secondary salt		FliNaK
PHX secondary flow, each, 3 operating/2 operating	kg/s	247/370
DRACS heat losses (per DRACS)	MW	0.45
DRACS heat losses, total (3 DRACS)	MW	1.35

[a]DRACS = direct reactor auxiliary cooling system; PHX = primary heat exchanger.

Several fuel and core design options for SmAHTR were investigated during the design evolution. These designs included solid cylindrical fuel "pins" in stringer fuel assemblies (which was the baseline design for the AHTR), hollow annular fuel pins in stringer fuel assemblies, and solid plate or "plank"-type fuel elements. The most developed and analyzed configuration, and current baseline design, is based on the annular fuel pin design. However, the plank-type fuel assembly in a "cartridge core" configuration appears to offer many operational advantages and is being further investigated at this time. Additional work is needed to arrive at an operational fuel assembly design that simultaneously accomplishes all of the required functions. A pebble-bed variant is also possible.

The SmAHTR design takes advantage of the existing safety philosophy of several small modular reactors. The reactor employs passive decay-heat removal systems relying on natural convection, and the core is designed with large negative reactivity feedback coefficients. The core and all primary components are contained in the reactor vessel (integral design). This design eliminates the large break loss-of-coolant accident (LBLOCA) scenario. Only intermediate-loop piping carrying non-radioactive coolant penetrates the vessel. The passive decay-heat removal design eliminates the reliance on off-site power, which is necessary if the reactor is to be sited in remote locations, and the need for safety-related emergency on-site AC power. The reactor can be seen as having several barriers to fission product release in the case of an accident: coated particle fuel, the graphite moderator, the reactor vessel/guard vessel, and the containment.

The SmAHTR concept has been developed with three potential operating modes and applications in mind: (1) process heat production, (2) electricity production, and (3) a combined cogeneration mode in which both electricity and process heat are produced. The capability to cluster multiple reactors to meet energy demands greater than those which can be met by a single reactor unit is an important design consideration for small modular reactors. This is certainly the case for any reactor concept designed for both electricity production and process heat applications. However, numerous questions and issues arise whenever multiple reactor units are interconnected. Only integration methods that do not compromise system safety or reliability can be considered. The interconnection or "ganging" of multiple reactor units to drive shared electrical power conversion systems has been widely discussed by reactor vendors and advanced concept developers for many years. However, the matter of the correct approach for clustering multiple small reactor units to meet intermediate-to-large process heat loads has received much less attention.

The use of an innovative liquid-salt thermal energy storage system, or "salt vault," notionally depicted in Fig. ES.4, expands the flexibility and applicability of the SmAHTR reactor for all applications. The salt vault offers three distinct functionalities: (1) the potential to combine multiple SmAHTR reactor modules to meet thermal energy and electrical power generation demands much greater than 125 MWt, (2) a robust capability to buffer the reactors and the process heat load from transients (such as reactor shutdown or time-varying heat demand) on either side of the salt vault interface, and (3) the ability to buffer multi-reactor module installations from upsets within a single reactor.

As a high-temperature system, SmAHTR is potentially compatible with several highly efficient (>40% thermal efficiency) power conversion technologies. The most attractive options for power conversion systems are Rankine and Brayton cycle technologies. One particularly appealing option is to couple the system to a high-efficiency closed-cycle supercritical carbon dioxide (S-CO_2) power conversion system. S-CO_2 power conversion is an emerging technology that can potentially provide a combination of small system components and high operating efficiency even at modest operating temperatures. Multi-reheat helium Brayton systems are also viable options, though they are less compact than the supercritical Brayton systems.

Based on work to date, it appears small modular FHRs are technically feasible. Additionally, it appears small FHRs, such as SmAHTR, would provide siting and applications flexibility unparalleled by other types of reactors.

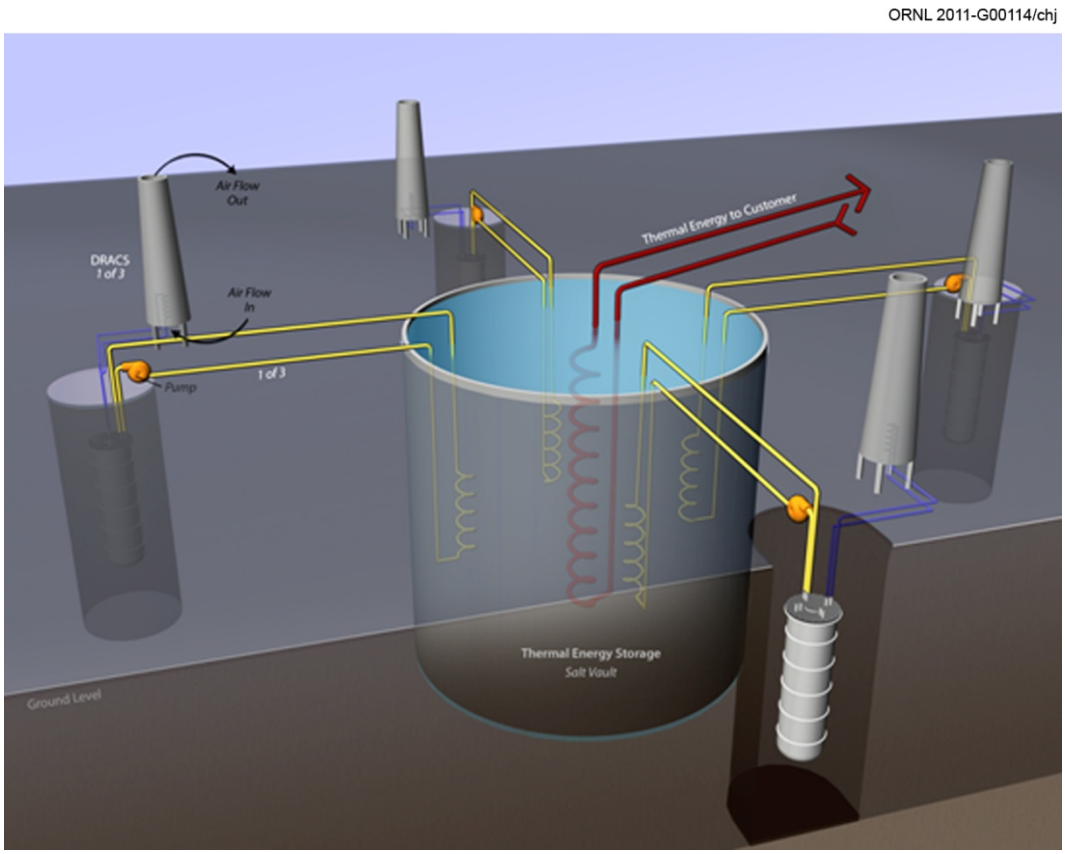

Fig. ES.4. SmAHTR salt vault thermal energy storage system.

Though a detailed SmAHTR cost and economic analysis cannot yet be performed due to the relative immaturity of the concept, there are reasons to expect that SmAHTR would be an economically attractive system from both capital cost and operating cost standpoints. The intrinsic virtues of FHR systems and technologies (low pressure, high volumetric heat capacity coolant, high-fuel-temperature thermal margins, etc.), when coupled with the potential for further capital cost reductions stemming from factory fabrication of small reactor modules, hold much promise. Significant potential offsetting considerations include the cost of high-temperature nuclear structural materials and the fabrication techniques required to produce complex components (such as heat exchangers) from them.

The SmAHTR concept presented here is but a snapshot of a complex technology and system architecture trade space. SmAHTR and the SmAHTR salt vault thermal energy system described in this report are not optimized systems. Additional concept definition work to be done includes the following.

- Optimization of the fuel and core design
- Further definition of the reactivity and instrumentation and control system
- Expanded transient and safety analyses (including generation of a pre-conceptual phenomena identification and ranking table, or PIRT, as soon as the concept is sufficiently defined to enable the exercise)
- Optimization of the in-vessel primary heat exchanger and direct reactor auxiliary cooling system heat exchanger designs
- Optimization of the salt vault system design and its interface with the reactors

- optimization of the SmAHTR electrical power conversion system design and the interface to it
- Preliminary SmAHTR capital cost estimates

Modest investment in these activities will significantly expand our understanding of the feasibility of the SmAHTR concept, its performance attributes, and its principal development challenges.

System concept development activities are essential elements of integrated advanced reactor development programs because *it is in the system concept that the value and promise of scientific research and technology development are made manifest*. Concept development activities provide the basis for prioritizing and guiding both basic technology development and enabling component development activities. With this in mind, a focused research, technology development, and component demonstration program is needed to enable FHR and SmAHTR development. A focused R&D program would include the development and optimization of fluoride-salt coolants, TRISO fuel forms, salt-compatible structural materials (graphites, composites, metals), critical components (pumps, heat exchangers, and valves), and high-temperature instrumentation. One insight that stands out from the work performed to date is the priority that must be placed on the development of compact salt-to-salt and salt-to-gas heat exchangers. Additional key component development priorities include liquid salt pumps and the vortex diodes that can tolerate a high-temperature liquid salt environment. All of these activities are supported by a basic focus on the development of high-performance, high-temperature nuclear materials, as discussed previously.

ABSTRACT

This report presents the results of a study conducted at Oak Ridge National Laboratory during 2010 to explore the feasibility of fluoride-salt-cooled small modular high-temperature reactors. A preliminary reactor system concept, SmAHTR (for Small modular Advanced High-Temperature Reactor) is described, along with an integrated high-temperature thermal energy storage or "salt vault" system. The SmAHTR is a 125 MWt, integral primary, liquid-salt-cooled, coated-particle-fueled, graphite-moderated, low-pressure system operating at 700°C. The system employs passive decay-heat removal and "two-out-of-three" subsystem redundancy for critical functions. The reactor vessel is sufficiently small to be transportable on standard commercial tractor-trailer vehicles. Initial transient analyses indicated the transition from normal reactor operations to passive decay-heat removal is accomplished in a manner that preserves robust safety margins throughout the transient. Numerous trade studies and trade-space considerations are discussed, along with the resultant initial system concept. However, the current concept has not yet been optimized, and work remains to more completely define the overall system—with particular attention given to refining the final fuel/core configuration, salt vault configuration, and integrated system dynamics and safety behavior.

1. INTRODUCTION

1.1 BACKGROUND

Fluoride-salt high-temperature reactors (FHRs) are characterized by their use of fluoride-salt coolants together with solid fuel forms. Currently, the preferred FHR fuel form is tri-isotropic (TRISO)-coated particle graphite fuel similar to that employed in today's high-temperature gas-cooled reactors (GCRs). FHRs differ from molten salt reactors (MSRs) in that MSRs employ a fissile-material-bearing, multicomponent fluid as both a coolant and a fuel. Unlike the MSRs, FHRs contain no fissile or fertile material in the coolant.

This report presents the initial technology trade study and pre-conceptual design evolution of a small modular high-temperature reactor system developed at Oak Ridge National Laboratory. This **S**mall **m**odular **A**dvanced **H**igh-**T**emperature **R**eactor (SmAHTR) employs liquid-fluoride-salt coolant together with TRISO-coated particle fuel technology in an integral primary system architecture.[1] These key technologies are joined with an innovative thermal energy storage system and Brayton power conversion technology to deliver high-temperature (>600°C) process heat and highly efficient electricity production from a small integral reactor capable of being transported via a standard tractor-trailer truck to remote destinations for permanent installation.

1.2 REPORT ORGANIZATION

This report provides a description the pre-conceptual design of SmAHTR and is organized into 12 chapters. Chapter 1 provides background information on early work on fluoride-salt-cooled reactors and an introduction to the SmAHTR concept, and Chap. 2 presents the system design philosophy and functional requirements adopted for the SmAHTR design trade study. Chapter 3 provides a high-level overview of the SmAHTR concept as an introduction to the more detailed system descriptions in Chaps. 4 and 5. Chapter 4 describes the primary in-vessel structures, along with key reactor system mechanical design details, and Chap. 5 discusses the major systems that interface directly to the reactor vessel. Chapter 6 summarizes very preliminary SmAHTR transient and safety analysis results, and Chap. 7 presents the salt vault concept, an innovative high-temperature thermal energy storage system that enables clustering of multiple SmAHTR reactors to meet a broad range of high-temperature thermal energy system loads. Candidate electrical power conversion systems are discussed in Chap. 8, and SmAHTR operational considerations (salt management, refueling, etc.) are described in Chap. 9. Chapter 10 briefly discusses SmAHTR economic performance considerations, and Chap. 11 summarizes the principal SmAHTR technology development challenges. Chapter 12 provides a summary of the report, and Appendices A and B contain ancillary data and information.

The original U.S. FHR concept, termed the Advanced High-Temperature Reactor (AHTR), was developed in 2004[2, 3] and was subsequently updated in 2006.[4] The AHTR embodied the basic elements of the FHR and was targeted for large (GWe-class) central station electricity production. Unlike the AHTR, the SmAHTR concept presented in this report is targeted for deployment in remote locations, where smaller amounts of power/energy are needed, for situations in which additional power/energy capacity is needed in an incremental manner rather than all at once, or where cooling water constraints preclude large GW-class nuclear power plants.

This report documents the initial concept evolution of SmAHTR. As will be discussed, several significant technology and system architecture design trades are yet to be performed, and several SmAHTR design variants are evident. Thus, the current SmAHTR concept is best considered to be a tool for exploring the small fluoride-salt high-temperature reactor design space, rather than as an optimized system concept. The details of the concept will, no doubt, evolve as various technology trade and system optimization studies are completed.

1.3 REFERENCES

1. S. R. Greene, D. E. Holcomb, J. C. Gehin et al., "SmAHTR—A Concept for a Small, Modular Advanced high Temperature Reactor," Paper 205, Proceedings of HTR 2010, Prague, Czech Republic, October 18–20, 2010.

2. C. W. Forsberg, P. F. Peterson, and P. S. Pickard, "Molten-salt-cooled Advanced High-Temperature Reactor for Production of Hydrogen and Electricity," *Nuclear Technology* **144**, 289–302 (December 2003).

3. D. T. Ingersoll et al., *Status of Preconceptual Design of the Advanced High-Temperature Reactor (AHTR)*, ORNL/TM-2004/104 (May 2004).

4. D. T. Ingersoll et al., *Trade Studies for the Liquid-Salt-Cooled Very High-Temperature Reactor: Fiscal Year 2006 Progress Report*, ORNL/TM-2006/140, Oak Ridge National Laboratory (February 2007).

2. SmAHTR SYSTEM APPLICATIONS, DESIGN GOALS, AND FUNCTIONAL REQUIREMENTS

2.1 NUCLEAR PROCESS HEAT REQUIREMENTS AND POTENTIAL SmAHTR SYSTEM APPLICATIONS

The SmAHTR concept described in this report is being designed to be a system capable of providing reliable, economically attractive electricity and process heat. The potential value of such a system improves significantly as the reactor outlet temperature rises above 600°C but requires that fundamental material challenges above this temperature be addressed. In terms of electricity production, thermal-to-electric power conversion efficiencies increase from the mid-thirty percent range at light-water-reactor operating temperatures (~300°C) to the mid-fifty percent range as reactor operating temperatures rise to 750°C—with still higher efficiencies as operating temperatures rise above this level.

With regard to process heat applications, numerous petrochemical refining processes require high-quality heat in the 600–700°C range.[1] Small reactor systems operating in the 750°C range would be well suited for remote production of high-pressure steam to enable petroleum extraction from oil sands.[2] Hydrogen production via high-temperature electrolysis and steam–methane reforming becomes practical at temperatures in the 800–850°C range (and is currently produced via natural gas combustion).[2] The attainment of reactor core outlet temperatures of 900–1000°C would enable a variety of thermal chemical processes for the production of hydrogen from water, gasification of hard coal and lignite, etc.[3] Thus, the development of a reliable, economical, and flexible reactor system capable of delivering heat at 600–1000°C would revolutionize highly efficient electrical power production and the production of liquid fuels for transportation and other applications.

Finally, the power level (MWt or MWe) required from an individual reactor unit can be determined by several factors. The broad range of industrial process heat applications presents a variety of process heat loads. Typical heat loads are in the range of ~100 to few hundred MWt. (An example of a forward-looking nuclear process heat application is presented in Ref. 4, where it is concluded the optimal size reactor for powering future biorefineries would be on the order of ~100 MWt.) On the other hand, until recently the trend in reactor sizing for electricity production has focused on larger and larger reactors. The largest reactors currently envisioned by reactor vendors are on the order of ~1.7 GWe. This growth in unit size has been driven by classical “economy of scale” considerations based on traditional plant manufacturing and construction techniques. More recently, interest has grown in the use of “small modular reactors” (SMRs), with power levels in the ~50–200 MWe range. This interest is driven by a multitude of factors including the very large unit capital cost of the larger plants, the desire to meet smaller electricity demand market needs, the ability to match generation capacity growth more closely with load growth, and the expectation that factory fabrication of larger numbers of smaller reactor units will deliver economies of production that offset the traditional “economy of scale” considerations.

2.2 SmAHTR DESIGN GOALS AND DESIGN TRADE SPACE ATTRIBUTES

The design goals for SmAHTR are to deliver safe, affordable, and reliable high-temperature process heat and electricity in a small plant that can be easily transported to and assembled at remote sites.

A design deemed to be unsafe by regulatory bodies will not be certified and, therefore, will never come to market. A plant that is not affordable from the unit capital cost perspective will not be purchased and will never achieve significant market penetration. A plant that is not reliable and does not offer very high levels of unit operational availability will not present favorable long-term value to its owner and is destined for a short operating lifetime. Reactor system designs (and their companion

fuel cycles) that exhibit unacceptable proliferation vulnerability will not be supported by the U.S. government. Therefore, the SmAHTR design goals also include the delivery of acceptable levels of safety, affordability and economic viability from both the plant capital cost and electricity/process heat cost perspectives, and favorable nonproliferation characteristics.

The ability to deliver the desired system performance attributes and functionalities discussed above requires the designer to make numerous decisions relating to the selection and integration of a large number of technologies, structures, components, and architectures. The primary design trade-space variables considered to date in the SmAHTR development activity include the following.

- reactor power level
- reactor operating temperature
- system architecture (integral primary system vs. classical distributed loop system)
- core architecture (cartridge core vs. individual fuel assemblies vs. pebble fuel)
- safety system actuation mode (active vs. passive)
- coolant
- power conversion system technology
- manner of fabrication and deployment (on-site vs. factory produced and truck transported)

The details of some of the more important trade analyses conducted to date are presented in Chap. 3.

2.3 SmAHTR FUNCTIONAL REQUIREMENTS

After consideration of the work previously conducted on the original AHTR concept, and in view of challenges faced by those seeking to develop and deploy any radical reactor technology that is significantly different from today's commercial light water reactors, the following principal SmAHTR functional requirements were adopted to guide the initial concept evolution activities.

1. Reactor power level: 125 MWt
2. Maximum operational fuel temperature: 1250°C
3. Reactor core outlet temperature: 700°C
4. Passive decay-heat removal capacity: 1% of full power
5. Reactor vessel and internals transportable via standard 53 ft commercial tractor-trailer vehicles
6. Thermal-to-electric power conversion efficiency: >40%
7. System architecture and technology suite that can be adapted to higher temperatures

Requirements 1–4 are related to the technical performance of the reactor subsystem. The 125 MWt size ensures a single SmAHTR module could support a number of different process heat applications, and the cluster of a few SmAHTR modules could support the majority of high-temperature and very-high-temperature-process heat applications envisioned well into this century. Requirement 2 ensures there should be no unacceptable release of radioactive fission products from the SmAHTR fuel during normal operations. Requirement 3 ensures that the early SmAHTR systems should be able to utilize Hastelloy-N structure materials in the core and reduces the probably that new structural alloy development will be an obstacle to development of the SmAHTR prototype. The passive decay-heat removal requirement (Requirement 4) establishes both the size of the decay-heat removal systems and sets requirements for SmAHTR system transient behavior during any event leading to reactor scram or shutdown.

Requirement 5 ensures the SmAHTR reactor vessel and internals can be delivered to virtually any location within North America. Use of the U.S. interstate highway system is governed by U.S. Department of Transportation (DOT) regulations. These regulations stipulate that transport vehicles

shall not exceed 2.6 m (102 in.) in width, 4.1 m (13.5 ft) in height, and 36,000 kg (80,000 lb) in gross weight. However, these regulations may be temporarily suspended by individual states to allow movement of oversize and/or overweight payloads, and variances are routinely granted by states throughout the country. Thus, an optimal SmAHTR reactor vessel would not exceed these dimensional and mass parameters.

Requirement 6 applies to the overall SmAHTR electrical energy system and has the effect of requiring the SmAHTR reactor to be joined to a Brayton power conversion system for electricity supply applications.

Requirement 7 acknowledges that SmAHTR is but the first step in a long-term goal to deliver very-high-temperature nuclear energy to the world. This goal is best served by adopting evolvable design approaches, system architectures, and wherever possible, technology suites that have the potential to function at temperatures as high as 800–1,000°C for applications later in this century as technical barriers are overcome.

2.4 REFERENCES

1. C. W. Forsberg, "Nuclear Energy for a Low-Carbon-Dioxide-Emission Transportation System with Liquid Fuels," *Nuclear Technology* **164**, 348–366 (December 2008).
2. R. A. Matzie, A. Paterson, R. Kuhr, and G. Claasen, "Beyond Electricity—Nuclear Process heat," presented at the 32nd Annual World Nuclear Association Symposium.
3. W. vonLensa and K. Verfondern, "20 Years of German R&D on Nuclear Heat Applications," 4th International Freiberg Conference on IGCC & XtL Technologies—IFC2010, Dresden, Germany, May 3–6, 2010.
4. S. R. Greene, G. F. Flanagan, and A. P. Borole, *Integration of Biorefineries and Nuclear Cogeneration Power Plants—A Preliminary Analysis*, ORNL/TM-2008/102 (August 2008).

3. SmAHTR SYSTEM CONCEPT OVERVIEW

SmAHTR is a small liquid-fluoride-salt-cooled, very-high-temperature reactor that employs an integral primary system concept in which all major components required to interface the reactor with the rest of plant are placed inside a single reactor vessel. Figure 3.1 is a depiction of a SmAHTR reactor vessel in transient on a standard commercial flat-bed tractor-trailer rig. Figure 3.2 provides an overall schematic of the SmAHTR system, and Fig. 3.3 shows the dimensions of the vessel and internals. Table 3.1 summarizes the key SmAHTR system parameters, and Table 3.2 summarizes the thermal hydraulic parameters of the SmAHTR.

SmAHTR employs three in-vessel primary heat exchangers (PHXs). Each PHX is coupled with a main circulating pump (MCP) that directs primary coolant salt from the common riser region above the reactor core down through the shell side of the PHX into a common downcomer region located between the outside of the core reflector and the inside of the reactor vessel. The coolant flows down through the downcomer annulus region to the lower head region of the reactor vessel and then up through the core and back to the common riser region, thus completing the main circulating loop. Each of these in-vessel cooling loops is termed a main circulating loop (MCL).

The secondary (tube) side of each PHX is an integral element of a companion intermediate cooling loop (ICL). Each ICL consists of the secondary side of the PHX, a companion intermediate loop pump (ILP), and an intermediate heat exchanger (IHX) that transfers the heat to the ultimate load (either the electrical power conversion system or the process heat storage system and load). During normal operations, all three MCLs and ICLs are active, each removing one-third of the heat produced by the reactor. This is accomplished by adjusting the in-vessel MCP flow and the companion ILP in each of the three ICLs. SmAHTR can operate at full power with only two of the MCL/ICL loops operational by simply increasing the MCP/ILP flow in the two operational cooling trains.

SmAHTR can be employed in three different energy production modes: (1) electricity production only, (2) process heat production only, or (3) cogeneration mode (both electricity and process heat production). If dedicated electricity production is the objective, the secondary side of the SmAHTR

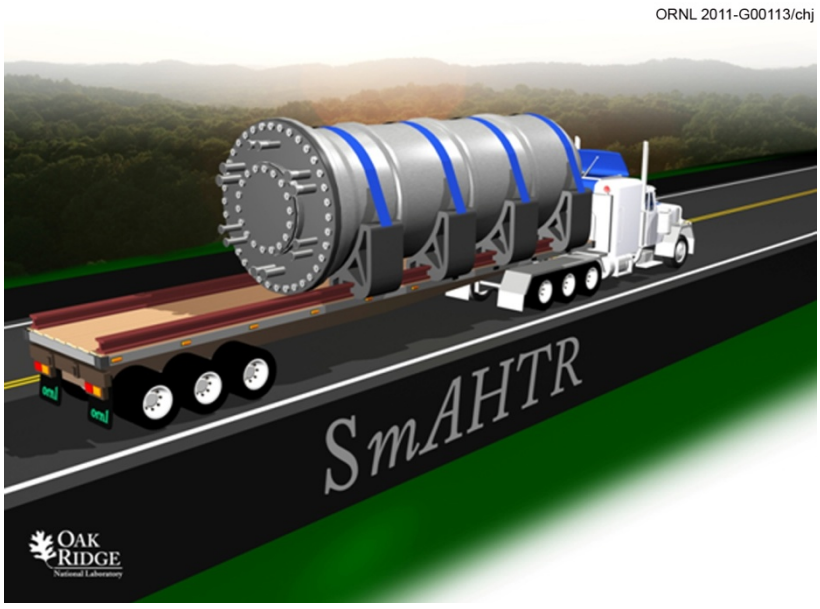

Fig. 3.1. SmAHTR reactor vessel in transient on commercial flat-bed tractor-trailer.

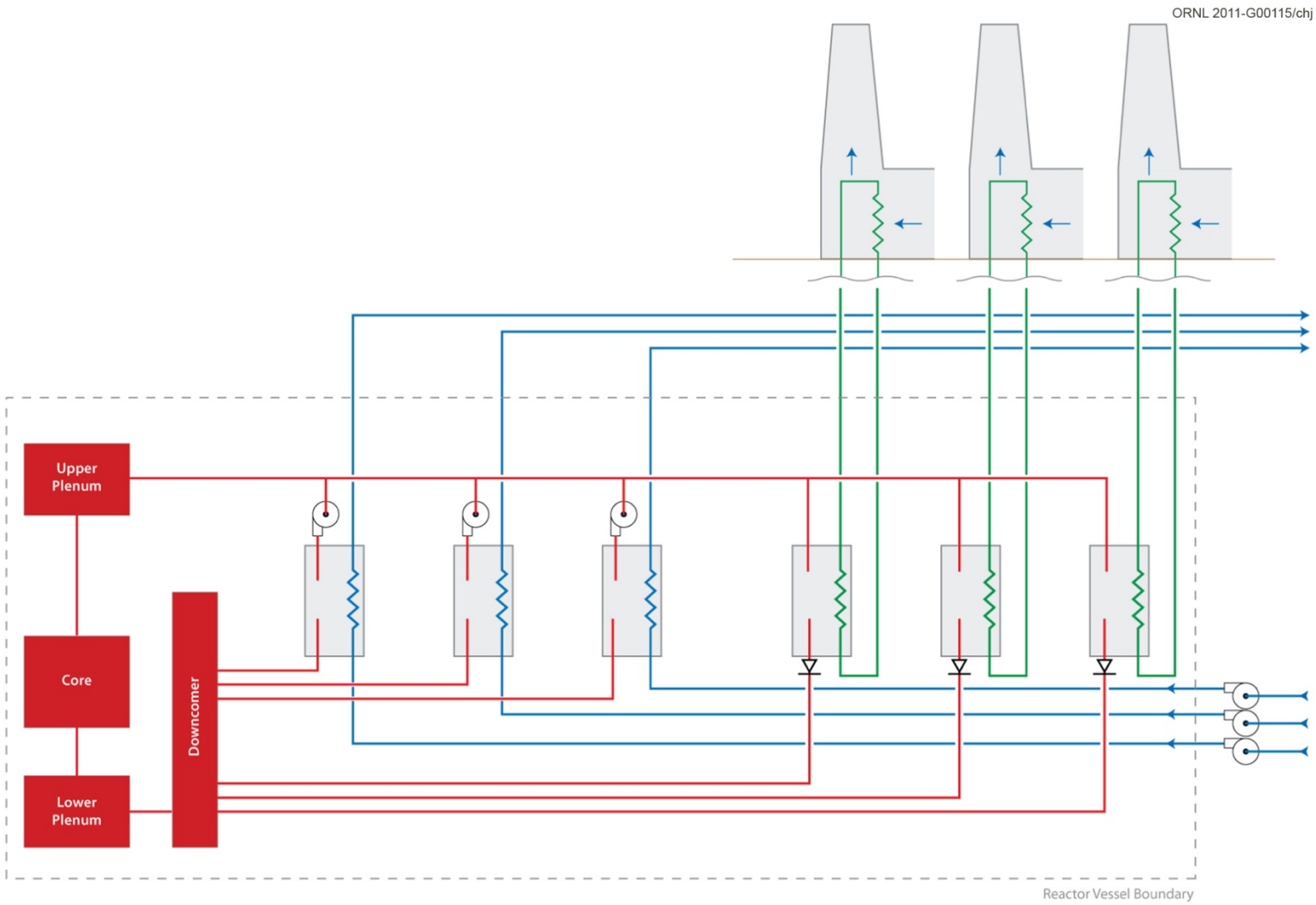

Fig. 3.2. SmAHTR system configuration.

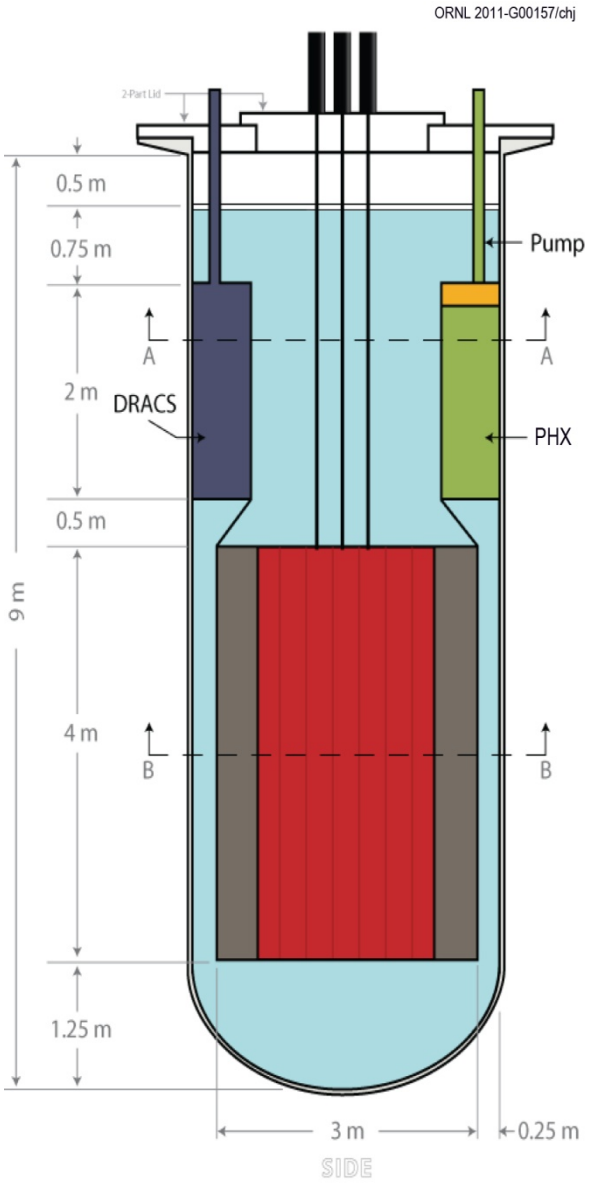

Fig. 3.3. SmAHTR vessel and internal dimensions.

Table 3.1. SmAHTR overall design values

Variable	Value
Reactor power, MW(t)	125
Primary coolant salt	FLiBe
Secondary coolant salt	FLiNaK
Core cooling mode	Forced convection
Core flow direction	Upward
IHX/downcomer flow direction	Downward
Fuel type	TRISO
TRISO packing fraction, %	50
Fuel enrichment, %	19.75
Core uranium loading at BOL, kg[a]	1600–2020[b]
Core life, years	4.19
Fuel configuration	Annular pins
Fuel pin diameters (inside, outside), cm	2.2, 6.5
Fuel surface coating thickness, cm	0.3
Moderator material	Graphite
Moderator configuration	Pins and blocks
Moderator pin diameter, cm	6.16
Number of total fuel assemblies/blocks	19
Number of core assembly rings	3
Number of fuel pins/assembly	15
Number of graphite pins/assembly	4
Graphite reflector and material	Radial, graphite blocks
Reflector diameter, inside, outside, m	~2.2, 3
Number of main pumps	3
Number of PHXs[a]	3
Number of DRACS	3
Vessel height, m	9
Vessel diameter, m	3.5
Vessel wall thickness, cm	2.5
Vessel weight (empty, no lid), kg	22,516
Vessel and skirt material	Hastelloy-N
Core height, m	4
Core diameter, m	~2.2
PHX/DRACS annulus, height, m	2
PHX/DRACS annulus, diameter-in, m	2.365
PHX/DRACS annulus, diameter-out, m	3.5

[a]BOL = beginning of life; PHX = primary heat exchanger; DRACS = director reactor auxiliary cooling system

[b]Core uranium loading depends upon the fuel concept employed and the refueling interval requirement. The range presented encompasses all fuel concepts and refueling intervals considered to date in the trade study.

Table 3.2. Thermal hydraulic parameters of the SmAHTR

Variable	Units	Value
Reactor power	MW(t)	125
Primary coolant salt		FLiBe
Flow/pump (3 operating)	kg/s	510
Flow/pump (2 operating)	kg/s	765
Vortex valve diodicity		50
Bypass flow/DRACS[a]	kg/s	68
Bypass flow, total (three DRACS)	kg/s	205
Total core flow	kg/s	1325
Total core flow area	m^2	0.623
Core coolant velocity	m/s	1.
Coolant temperature into core (cold)	°C	650
Core outlet coolant temperature—inner, middle, outer radial zones	°C	703, 692, 689
Coolant temperature, upper plenum (mixed)	°C	692
Coolant temperature, top plenum	°C	687
Maximum fuel temperature, centerline	°C	1027
Maximum fuel temperature, surface	°C	988
Maximum fuel surface coating temperature	°C	786
Maximum fuel heat flux	W/m^2	6.3×10^5
Fuel/Coolant heat transfer coefficient	$W/(m^2\ °C)$	4700–6380
Core pressure drop	kPa	15
Pumping power main pump	kW	10
PHX capacity, 3/2 operating[a]	MW	42/63
PHX secondary salt		FliNaK
PHX secondary flow, each, 3/2 operating	kg/s	247/370
DRACS heat losses (per DRACS)	MW	0.45
DRACS heat losses, total (3 DRACS)	MW	1.35

[a]DRACS = director reactor auxiliary cooling system; PHX = primary heat exchanger.

primary heat exchangers could be connected directly to the Brayton power conversion system heat exchangers to provide a very compact electricity production power block. Alternatively, if process heat production is the intended application, the secondary side of each primary heat exchanger would most likely be connected via its ICL to an IHX. The working fluid in this intermediate loop would be fluoride salt with thermal properties to match the application temperatures. Each IHX would, in turn, transfer the thermal energy either directly to the process heat load or to a thermal energy storage device. As will be discussed later in this report, the use of a common thermal energy storage device, coupled with multiple SmAHTR units, offers many operational advantages. A thermal energy storage tank, termed a salt vault, is envisioned here and discussed in Sect. 7. Multiple SmAHTR units could be clustered together to thermally "pump" or "charge" the salt vault to meet higher thermal energy loads, provide robust load following capability, decouple the thermal energy load from the reactors when desirable, and provide a degree of decoupling between the individual SmAHTR units.

SmAHTR employs three passive direct reactor auxiliary cooling system (DRACS) cooling loops to remove post-scram shutdown decay heat from the reactor. Only two of the three loops are required for safe operations. During normal operations, reverse flow of reactor coolant through the in-vessel's DRACS heat exchangers (DHXs) is reduced to the minimum necessary to keep the DRACS loop at working temperature by the use of a passive vortex diode at the outlets of the shell side of each of the

in-vessel DHXs. The vortex diode restricts (“reverses”) flow of reactor coolant through the DHX (and the associated parasitic heat loses through the DRACS systems) during normal operation. Upon trip of the MCPs, natural convection is established within both the reactor vessel and within the DRACS loop. Within the reactor vessel, reactor coolant flows up through the core and down (forward) through the primary (shell) side of the DHXs, thus removing the decay heat produced by the reactor. Within the DRACS system, the DRACS working fluid (an optimized fluoride salt) is heated within the DHX and flows up to its DRACS air radiator in an external structure, where the fluid is cooled by dumping its heat load to air in an induced-draft natural convection chimney structure.

4. SmAHTR NUCLEAR ISLAND STRUCTURES AND REACTOR MECHANICAL DESIGN

4.1 FLUORIDE SALT SELECTION

The SmAHTR reactor has three distinct working fluid loops: (1) the reactor primary loop, (2) the intermediate cooling loop (ICL), and (3) the DRACS decay-heat-removal loop. Additional working fluids are necessary for both the electricity generation and heat storage configuration options. The additional working fluids and their selection criteria are discussed in the Brayton power cycle and salt storage sections of this report. An evaluation of potential FHR primary coolant salts is available as an ORNL report.[1] Similarly, an evaluation of potential heat transport salts was recently performed.[2] The information summarized here is derived primarily from the more detailed assessments.

4.1.1 Primary Coolant Salt Selection

In an FHR, the primary coolant serves several interrelated functions. The coolant's primary function is to move heat generated in the fuel and transfer it to the PHXs, but it also provides neutron moderation, serves as a radionuclide containment, and provides gamma shielding. Therefore, the coolant salt selection must consider the salt's thermal, nuclear, and chemical properties.

The primary coolant must have a melting point well below the coldest point in the primary circuit. For the SmAHTR, the primary coolant melt point must be below ~550°C, providing 100°C of margin to any refreezing accident. The primary coolant must also be thermally stable well above any credible accident conditions. The primary coolant vapor pressure must remain below 1 atmosphere in all temperature regimes anticipated to occur in any credible accidents. Similarly, the primary coolant must have a boiling point well above any credible accident condition temperatures. In addition, to function as an effective coolant, the primary fluid must have a low viscosity at operating temperature and have a large heat capacity. Finally, the primary coolant needs to have a large change in specific volume with temperature to effectively drive natural circulation cooling.

From a neutronics perspective, while the majority of the neutron moderation is provided by the in-core carbon structures, the light elements in the primary coolant provide significant neutron moderation. Removing the coolant from the core will change the core reactivity due to the change of the neutron spectrum resulting from the loss of neutron moderation as well as the lost of absorbing materials. In order to ensure that coolant loss or voiding does not result in reactivity excursions resulting in loss of fuel, it is desirable to design the system to be in an under-moderated configuration such that the loss of the moderating coolant results in a negative reactivity. Note that in addition to the coolant reactivity, the uranium-based fuel has a large negative fuel temperature coefficient, so any potential increases in temperature due to loss of coolant will also result in a large negative reactivity effect from the fuel.

The primary coolant should have a low neutron-absorption cross section or become unstable under intense radiation. The requirement to have a low neutron-absorption cross section eliminates most isotopes from consideration. Fluoride salts are among the most stable compounds in radiation fields due to their strong ionic bonding and the resultant rapid chemical recomposition following radiolysis. In-service inspection and fuel manipulation would be simplified by a low-activity primary coolant. Further, having a large volume of highly radioactive fluid would increase the containment building structural requirements. Both zirconium and rubidium have significant activation products with multiday half-lives and energetic associated gamma rays greatly increasing the operational difficulty of employing either in the primary coolant. Similarly, sodium activates to ^{24}Na ($T_{½} \approx 15$ hr) and emits energetic gamma rays during decay.

The elements in the primary coolant need to be chemically compatible with the core and primary loop materials. Both bismuth and lead fluorides are eliminated from consideration due to their

corrosive nature with available alloys. Also, boron-11 fluorides are not useful due to the toxicity of BF_3, the high vapor pressure of BF_3 at accident temperatures, the tendency of BF_3 to separate from the remainder of the salt and locally raising the melting point, and BF_3's strong tendency to rapidly oxidize in the presence of trace amounts of water vapor.

Only lithium-7 beryllium fluorides meet all the requirements for the SmAHTR primary coolant. Pure beryllium fluoride has too high a viscosity at SmAHTR operating temperatures. The 2:1 ^{7}LiF to BeF_2 ratio (known as FLiBe) is selected as the SmAHTR primary coolant to provide a low melting temperature while minimizing the melt viscosity.

Tritium is produced by several reactions when using FLiBe as a primary coolant: ^{6}Li(n,α)t, ^{9}Be(n,α)^{6}Li → ^{6}Li(n,α)t, ^{7}Li(n,αn)t, and ^{19}F(n,^{17}O)t. The Molten Salt Breeder Reactor (MSBR) design estimate was that at a 99.995% ^{7}Li purity in the primary coolant, roughly 1 Ci of tritium would be produced per day per megawatt (thermal) of reactor size.[3] For comparison, a large light water reactor (LWR) produces ~50 Ci/day, and a typical heavy water reactor (HWR) produces 3,500–6,000 Ci/day. The largest fraction of the tritium produced will become a dissolved species in the primary salt. Most of the remainder will be trapped in the nearby core graphite. However, tritium will rapidly permeate through metals at high temperatures. Consequently, the tritium will need to be removed from the primary and secondary salts through a combination of chemical and physical degassing. Also, a cool tritium container shell surrounding the hot system components will likely be necessary.

While the lithium fluoride will require special production, the beryllium fluoride is anticipated to be available from commercial sources, although quality improvements may be necessary to meet purity requirements. The SmAHTR primary coolant salt will be expected to meet the Molten Salt Reactor Experiment (MSRE) minimum impurity levels, which are shown in Ref. 4, and were based on minimizing nuclear poisons and on analyses of samples of the best commercially available fluoride salts at that time. The coolant salts will be synthesized by first purifying the component salts to remove water and oxygen by heating under vacuum. Next the correct ratios of the constituent fluoride salts will be combined and melted. The resultant salt will then be processed to remove bound oxygen and water, sulfur, and metal ions by sparging with mixtures of hydrogen fluoride and hydrogen. Associated with the chemistry control process will be vacuum, hydrogen fluoride, helium, and hydrogen supply systems. The SmAHTR chemical control system will also mechanically filter the salt to remove any entrained particulates such as graphite dust using a nickel filter.

4.1.2 Fluoride-Salt Corrosion Chemistry

As discussed previously, SmAHTR will employ FLiBe as its primary coolant and either FLiNaK or KF-ZrF_4 as its intermediate and DRACS coolants. Corrosion of structural metals in liquid-fluoride-salt systems typically begins with oxidation of a structural constituent metal atom to an ion in solution. Thermodynamic stability of the alloy constituents versus fluoride salt constituents is, thus, quite important to minimize this corrosion mechanism. For example, chromium, which has one of the more thermodynamically stable fluorides, can react with available oxidants in the system. Chemically available fluorine atoms typically arise due to electronegative impurities within the otherwise strongly ionically bound fluoride melt. In other words, because of the strong chemical bonding of alkali metal and beryllium fluorides, the corrosion potential of liquid fluoride salts is generally controlled by redox equilibria involving impurities in the liquid salt or gas phase above the liquid salt.

Temperature differences within a single thermal loop cause gradients in the chemical activities of the loop constituents and can result in dissolution of metal in one region of the system with subsequent deposition in other portions of the system. The degree of attack will depend on the thermodynamic driving force of the reaction, the dissolution and deposition kinetics, and the temperature distribution, as well as the loop hydraulic properties. Essentially, the saturation concentration of the corrosion product fluoride depends upon its temperature, resulting in deposition of the corroded species in the cooler regions of a loop.

The presence of spatially distributed, dissimilar structural materials within the same system can also lead to mass transfer even at isothermal conditions. Two conditions are required for dissimilar material-based concentration-gradient mass transfer to be a factor. First, an element contained in one of the materials has to have a strong tendency to form an alloy or compound with an element in the second material. More importantly, an element in one of the materials must be subject to oxidative attack or suffer dissolution within the salt solution. The oxidative attack can be either by reaction with impurities or, if a reactive element, with the salt constituents. In either event, once the element goes into solution, it will be carried along with the coolant and form a solid product if the chemical driving force is sufficient. As the solid product forms, the concentration of the dissolved species within the fluoride salt melt decreases, enabling the corrosive attack or dissolution to continue. Solid-state diffusion kinetics may limit the rate at which this corrosion mechanism occurs. Further, if the attack, via any of the corrosion mechanisms, is mediated by reaction with impurities, the corrosion may inherently dramatically slow with time as the impurities are consumed.

SmAHTR corrosion will be minimized both by using high-purity starting materials as well as actively managing the salt chemical state. The salt redox condition, and thus its corrosivity, will be affected by impurities in the salt and impurity ingress from the atmosphere and the container materials. In addition to initially removing impurities from the salt before use, the electrochemical potential of the salt will be adjusted on-line to compensate for changes during operation. The essence of redox control in a liquid fluoride salt is minimization of the non-strongly bound fluoride by providing plentiful, energetically preferential reaction sites within the melt for any less strongly bound fluorine that develops. In other words, the redox potential of the salt is kept highly reducing to prevent oxidation of the container by fluorine atoms. Methods for redox control include setting the ratio of two different oxidation states of a particular multivalent element within the salt such as Ce(III)/Ce(IV).[5] The multivalent element initially reacts with the salt to become a fluoride and is then reduced within the salt by contacting it with a non-blocking electrode maintained at a negative voltage. The redox condition of a fluoride salt is also impacted by the chemical structure of the particular salt. Some fluoride salts (e.g., BeF_2), referred to as Lewis acids, can accept pairs of electrons, forming a weak complex (BeF_4^{2-}). This method of corrosion control will be implemented at SmAHTR by allowing the primary coolant FLiBe to corrode metallic beryllium, much as was done in the MSRE secondary loop, both providing an excess of an electropositive element as well as a Lewis acid to complex fluoride ions.

A continuous flowing cover gas will be employed over the primary salt in the reactor vessel. This cover gas will act as the transport medium to move tritium (which will be produced via neutron transmutation of the salt) and ingress gases (especially oxygen and moisture) away from the liquid salt coolants to cleanup systems. Helium will be employed as the cover gas, and either somewhat less pure helium or dry nitrogen will be employed within containment. Argon is avoided as a cover gas to minimize the production of ^{41}Ar during reactor operation. Some oxygen will unavoidably be present in containment and will leak into the gas volume above the coolant salt. A small amount of oxygen contacting the salt surface is not a high consequence issue. While oxygen contacting the salt surface will dissolve into the salt and need to be removed by the salt chemistry control system to maintain the salt redox condition, fluoride salts do not have energetic reactions with oxygen. Note that tritium will diffuse through the reactor vessel at temperature, and thus the tritium collection system will be required to envelop the entire reactor vessel and intermediate piping. While the addition of hydrogen to the cover gas would aid in maintaining a low oxidation potential above the salt, hydrogen cannot be readily separated from tritium and hence will not be employed.

4.2 REACTOR VESSEL AND VESSEL CLOSURE

The SmAHTR reactor vessel is a free-hanging cylindrical vessel with an integral annular flange at the top which is supported by the surrounding reinforced concrete structure. The reactor vessel will be made from Hastelloy-N, which has a maximum allowable stress of 3.5 ksi at 704°C.[6] Calculations

based on the hydrostatic loading of the vessel, and its weight under static condition, result in a maximum stress on the vessel with a thickness of 2.5 cm to be 1.4 ksi, which is well below the 3.5 ksi value that already includes most of the factor of safety in arriving at the number (see Fig. 4.1 showing the vessel and the stress distribution).

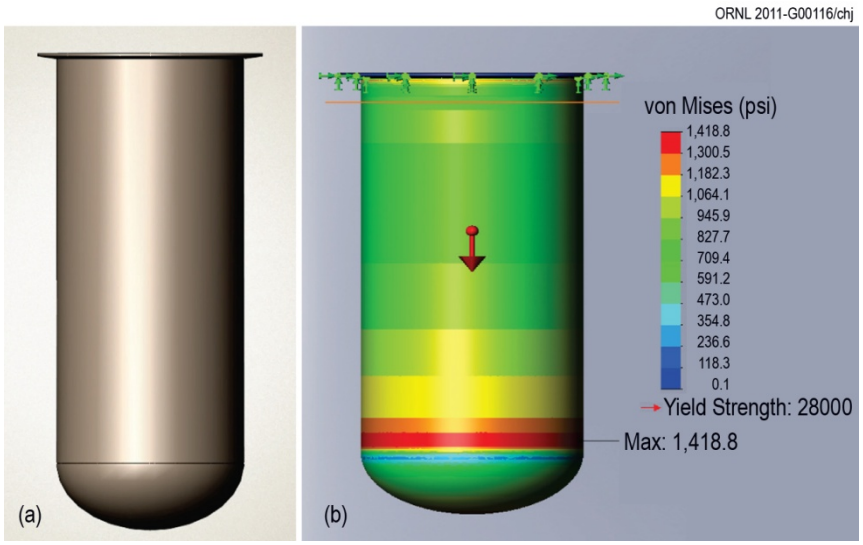

Fig. 4.1. (a) Reactor vessel and (b) reactor vessel stress distribution under load.

The reactor vessel is attached to the external load-bearing concrete structure by support brackets that allow for lateral motion that may occur during operation, installation, or removal.[7] By using Lubrite plate and an interstitial gap between the anchoring bolts that attach the reactor vessel and concrete, small lateral motion can be accommodated without transmitting large forces. Similar design is incorporated on the bolts that make the vertical support connection. The reactor will be designed to account for operational basis earthquake at the deployment site.

The overall reactor design philosophy is to make the design as modular as possible. All components of the reactor are introduced from the top (Fig. 4.2). The IHX and DRACS heat exchangers, the reactor core, the reflector, and the control rods have flanged entry points at the top of the reactor. This series of flanges in three concentric circles interlock to form the top closure of the reactor vessel. An outermost top closure flange rests on top of the reactor vessel flange which, in turn, rests on the supporting reinforced concrete pad (Figs. 4.2 and 4.3).

This top closure flange supports the weight of all the reactor vessel internals and transfers this load to the surrounding reactor vessel flange. The core reflector, the PHXs, the DRACS heat exchangers, and the downcomer "skirt" that constitutes the inner boundary of the annular downcomer are all suspended directly from this closure flange. The central closure plate or "core bonnet" supports the reactor core and transfers the resulting load to the top closure flange. The control rods are inserted through this central closure plate but have the ability to be raised or lowered independently of the central plate.

4.3 REACTOR FUEL AND CORE

4.3.1 Introduction

Three different SmAHTR fuel compact mechanical configurations have been evaluated: cylindrical, annular, and plate form. The SmAHTR design could also accommodate a pebble-bed-type core, although this core form has not yet been evaluated.

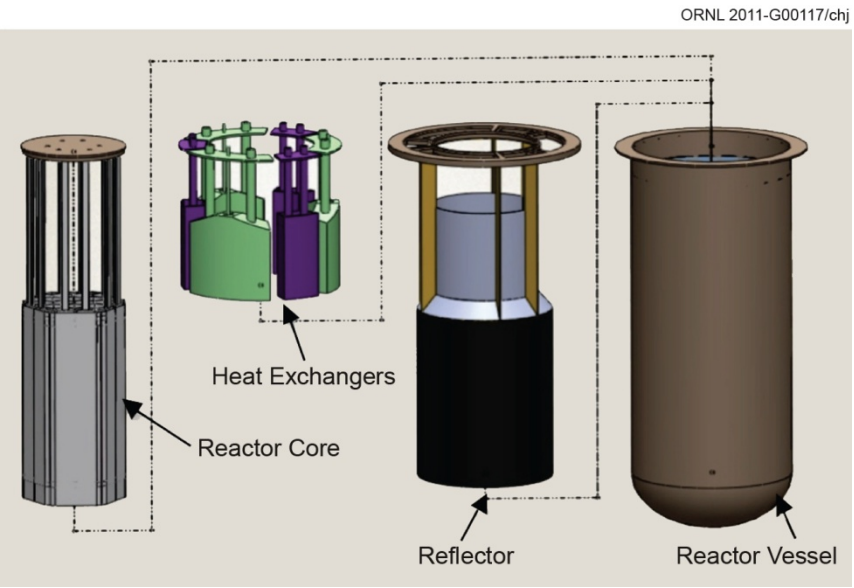

Fig. 4.2. Reactor core bonnet assembly, heat exchanger, top closure flange, and vessel flange.

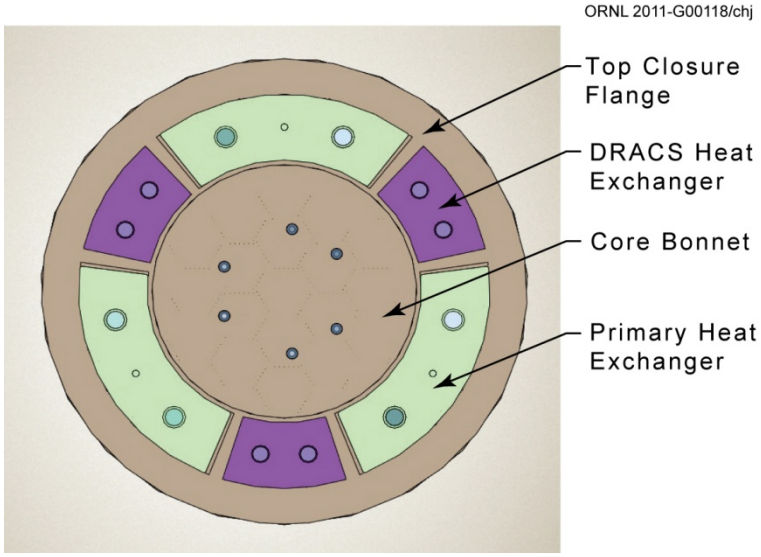

Fig. 4.3. Reactor vessel flange, top closure flange, and core bonnet (top view).

SmAHTR employs uranium oxicarbide (UCO), tri-isotropic (TRISO) particle fuel that closely resembles that being developed and demonstrated by the Department of Energy Office of Nuclear Energy (DOE NE) advanced gas reactor program.[8] TRISO fuel has an extensive reactor pedigree[9] and remains the only high-temperature fuel form with near-term availability for nuclear power deployment. In TRISO particle fuel, the fuel material (in this case $UC_{0.5}O_{1.5}$) is in the form of small spheres that are sequentially overcoated with a series of protective layers. The particles are embedded within a graphitic material to form fuel compacts. Unlike in GCRs, where the compacts are embedded within graphite structures (to provide conduction cooldown under loss of forced flow conditions),

FHR fuel compacts are placed into direct contact with the coolant to maximize their heat transfer under both forced and natural convection cooling conditions.

The peak TRISO temperature during normal operation is limited to 1,250°C for the current SmAHTR design evolution. This temperature matches the irradiation temperature of the current advanced gas reactor fuel-testing program.[10] Moreover the compact power density of the Advanced Gas Reactor-1 (AGR-1) test program (≈30–130 W/cm^3) bounds the SmAHTR fueled region power density.

The focus and depth of analysis for the three different fuel forms have not been uniform. The cylindrical fuel form was evaluated first. While a neutronically and thermally acceptable core form was developed, the cylindrical compacts have two technical difficulties. First, the long cylindrical fuel form would be difficult to fabricate and, second, technically challenging to robustly mount while preserving the thermal coupling to the coolant. In an FHR, a primary fuel configuration metric is the distance between the fuel particles and the coolant, as this heat conduction distance strongly influences the fuel operating temperature. Any external mechanical mounting structure would increase this distance and thus increase the fuel operating temperature.

An annular fuel concept was next investigated as a means to improve the thermal coupling between the fuel and coolant. The annular fuel form also enables the use of a central carbon–carbon composite mounting rod to hold shorter fuel segments. The annular fuel form decreases the fuel peak operating temperature as compared to the cylindrical form. Also, the shorter annular fuel pieces are suitable for manufacturing using known methods. However, a central tie rod is by itself insufficient to prevent the individual fuel compacts from moving as the coolant is pumped through the core. Movement of individual fuel compacts due to flow-induced vibration, along with potential physical interaction with other core structures, would be deleterious to fuel lifetime.

In order to provide strong mechanical mounting of the fuel, a plate or "plank" fuel form was next considered. The plank fuel form represents an evolution of the graphite moderator structure originally proposed for the MSR.[11] In this case, the fuel is embedded within vertically oriented planks configured into hexagonal fuel bundles that are directly emplaced within the coolant.

The plank mechanical fuel configuration appears to be superior to either the cylindrical or annular fuel forms. However, the hydraulic, thermal, and neutronic core models for the plank fuel form were not as advanced as with the earlier fuel forms at the conclusion of this project, and the predicted core lifetime and peak fuel temperatures remained shorter and higher, respectively, than those for the annular fuel form at the end of the evaluation effort. Additional design and modeling of the plank fuel design would be required before it could be recommended as the baseline core configuration.

The remainder of this section presents the results of the analysis conducted to date for each of the three fuel forms discussed. As previously noted, though a pebble-bed fuel/core form is clearly a candidate for SmAHTR applications, time and resource constraints precluded analysis of the pebble-bed core variant in this initial design evolution exercise.

4.3.2 Solid Cylindrical Fuel Option

The cylindrical fuel core consists of stacked prismatic blocks containing stringer fuel bundles. In the cylindrical fuel option, the TRISO particles are uniformly loaded at a 50% volumetric packing density into fuel cylinders. The TRISO UCO fuel kernels are 500 microns in diameter. A total of 1,556.4 kg of uranium (19.75 wt % ^{235}U) is loaded into the core. The stringer fuel bundles design is derived from the stringer fuel assemblies considered during 2006 for the AHTR[12] and are horizontally surrounded by hexagonal graphite blocks. The hexagonal graphite blocks and fuel cylinders are both 80 cm in height. The dimensions of the cylindrical fuel variant of the SmAHTR core are provided in Table 4.1. The graphite blocks are 45 cm across the flats. Each fuel block contains 72 fuel pins and 19 graphite pins. Figure 4.4 shows a cross section of a single fuel block.

Table 4.1. Solid cylindrical fuel SmAHTR core component dimensions

Component	Subcomponent	Dimension	Size (cm)
Fuel pins (72 fuel pins per fuel bundle)	Fuel pin	Radius	1.1
		Pitch	3.08
		Height	80
	Fuel pin clad (graphite)	Outer radius	1.4
Graphite pins (19 fuel pins per fuel bundle)	Graphite pin	Radius	1.4
		Pitch	3.08
		Height	80
Graphite fuel block	Coolant cylinder	Radius	16.94
		Height	80
		Pitch	45
Radial reflector	Coolant holes	Radius	6
	Graphite	Outer radius	150
		Height	400

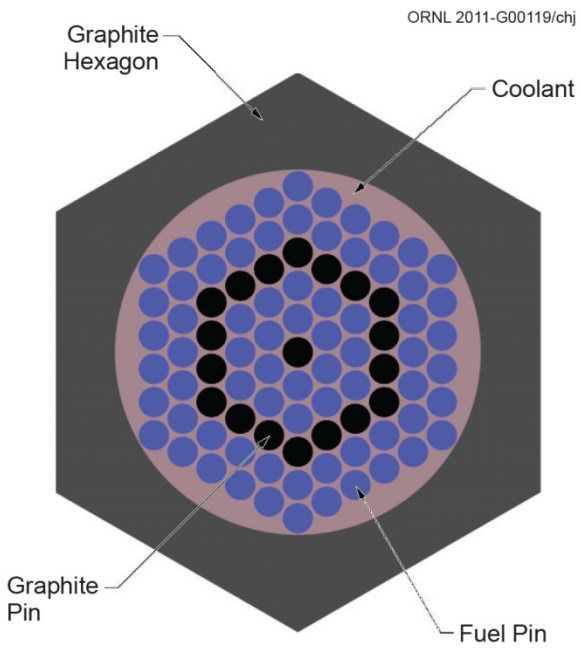

Fig. 4.4. Fuel block configuration cross section.

Figure 4.5 is a cross section of the entire SmAHTR core consisting 19 hexagonally close packed fuel blocks.

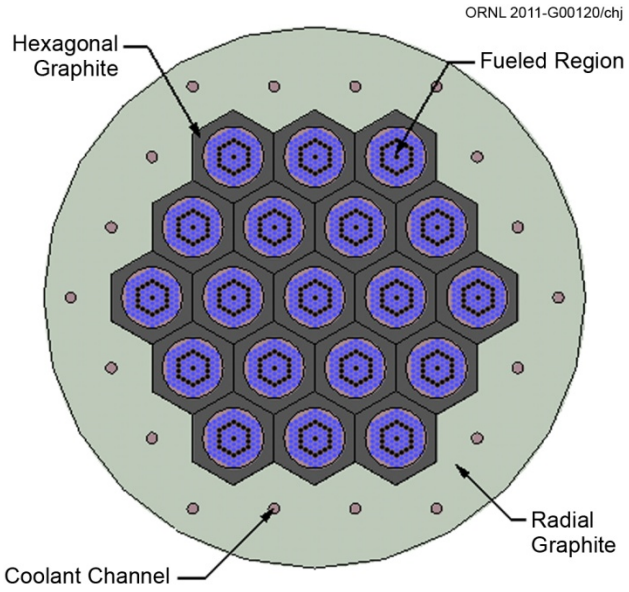

Fig. 4.5. SmAHTR core cross section.

Five fuel block layers are stacked to create the SmAHTR core, giving a total core height of 4 m. Figure 4.6 depicts the SmAHTR core along with the radial reflector graphite.

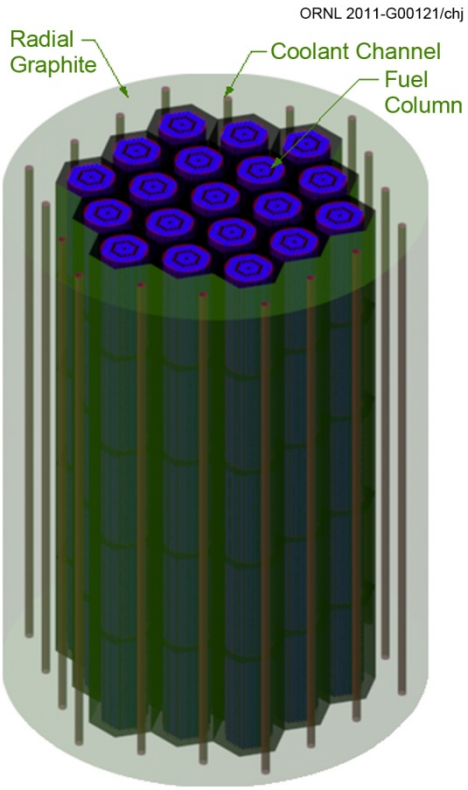

Fig. 4.6. SmAHTR core with radial reflector.

The evaluation of the lifespan of the SmAHTR core was performed using the Monte Carlo three-dimensional TRITON depletion sequence in SCALE6, the configuration controlled version of SCALE, which includes the latest updates.

The core model predicts an excess reactivity of $(k_{eff} - 1)/k_{eff}$ = 26,940 pcm for the fresh core. The core power density is 9.379 MW/m^3. The depletion was performed at constant power, using smaller time steps at the beginning of the simulation and increasing the magnitude of these steps as the depletion progresses. The depletion calculations were carried out for a total of 60 time steps, covering a span of ~4.5 years. The core becomes subcritical after 3.52 years.

The temperature coefficients of reactivity for the fresh core were estimated from the variation of k_{eff} over the temperature interval (1,100–1,500°C). A temperature coefficient of reactivity is defined as $\frac{\partial \rho}{\partial T}$, where ρ is the reactivity, and T can be the fuel temperature (for the fuel coefficient of reactivity), the moderator temperature (for the moderator coefficient of reactivity), the coolant temperature (for the coolant coefficient of reactivity), or an average core temperature (for the isothermal coefficient of reactivity).

The values calculated for the four coefficients are summarized in Table 4.2.

The variation of the coolant density with temperature was also included in the coolant temperature coefficient analysis.

Table 4.2. Solid cylindrical fuel reactivity coefficients

Component	Reactivity coefficient (pcm/K)
Fuel	–2.49
Graphite	+0.11
Coolant (T + ρ)	–0.30
Overall average	–2.70

4.3.3 Annular Cylindrical Fuel Option

The annular SmAHTR core resembles the cylindrical fuel core in overall geometry using the same 80 cm tall hexagonal fuel blocks stacked five high. In the annular fuel SmAHTR core variant, the fuel is configured into annular compacts roughly 5 cm high that are strung along a carbon–carbon composite vertical tie rod. The fuel compact beads have inner and outer 3 mm thick graphite sleeves to protect the fueled bead interior from erosion. A total of 1,806.7 kg of uranium (19.75 wt % ^{235}U) is loaded into the core with a 50% volumetric packing fraction. The overall annular fuel compact geometry is illustrated in Fig 4.7, and an annular fuel bundle is shown as Fig. 4.8.

A cross section view of an annular fuel bundle within its graphite channel is shown as Fig. 4.9. The graphite channels of the annular fuel variant are identical to those for the cylindrical fuel variant. Thus the overall core cross section is quite similar between the two design variants. The annular fuel core variant was calculated to become subcritical after 4.19 years.

The dimensions of the annular fuel bundle components are provided in Table 4.3.

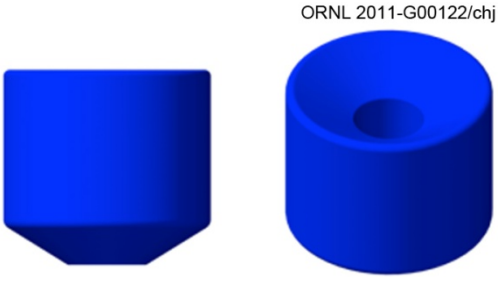

Fig. 4.7. Front and isometric views of a single annular fuel bead.

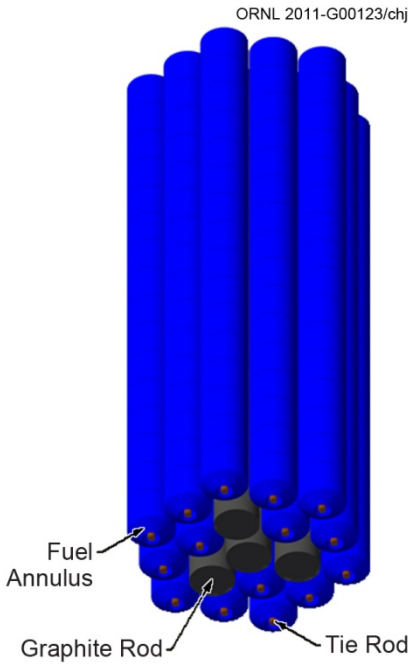

Fig. 4.8. Annular fuel bundle isometric view.

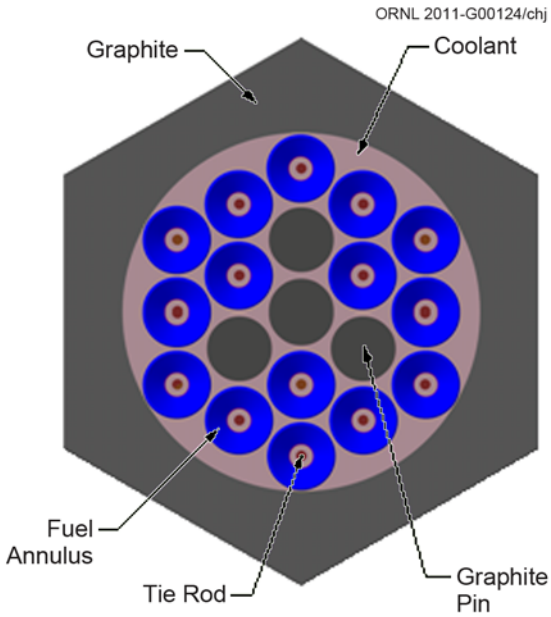

Fig. 4.9. Annular fuel bundle cross section with graphite channel.

Table 4.3. Annular cylindrical fuel compact dimensions

Parameter	Value
Pitch (cm)	6.78
Radius of tie rod (cm)	0.5
Inner radius of inner sleeve (cm)	1.1
Inner radius of active region (cm)	1.4
Outer radius of active region (cm)	2.95
Outer radius of outer sleeve (cm)	3.25
Radius of moderator pins (cm)	3.08
Fuel pins per fuel channel	15
Moderator pins per fuel channel	4

The values for the annular fuel temperature coefficients of reactivity are shown in Table 4.4.

Table 4.4. Annular cylindrical fuel reactivity fuel temperature coefficients of reactivity

Component	Reactivity coefficient (pcm/K)
Fuel	–2.61
Graphite	+0.02
Coolant (T + ρ)	–0.53
Overall average	–3.12

4.3.4 Plank Fuel Option

In the plank-fuel SmAHTR core design variant, the fuel is configured into full core height planks that are mounted into a carbon–carbon composite frame. The top and bottom 15 cm of the planks are unfueled and are notched to accommodate a retention band. Each fuel plate has unfueled wear ridges running along its length to provide positive mechanical spacing and thereby prevent flow-induced vibration. Several different plank-fuel configuration variants were analyzed by changing the number and thickness of the planks as well as their fuel loadings. A representative fuel plank bundle is shown as Fig. 4.10. The plank fuel bundles also are 45 cm across the flats, so they are geometrically similar to the fuel channels of the alternate core designs. A cross section of a plank fuel bundle is shown as Fig. 4.11.

Control rods were incorporated into the plank fuel core. Six rods were located within the middle ring of fuel bundles, as shown in the core cross section in Fig. 4.12. The different coloring of the plank fuel bundles in Fig. 4.12 are intended to illustrate the three rings of fuel bundles that constitute the core. The fuel bundles, however, are identical except for the control rods within the middle ring. Control rod position is adjusted from the top of the reactor.

The longest core lifetime achieved with the plank fuel to date was 3.08 years with a 40% volumetric fuel packing fraction and using identical UCO TRISO kernels as with the annular and cylindrical core variants. A total of 2015.4 kg of uranium (19.75 wt % ^{235}U) is loaded into the core.

Fuel is uniformly loaded within the planks, and each plank has a 2 mm unfueled sleeve surrounding it to protect against erosion. Each third of a neutronically optimized fuel bundle consists of six planks. Every other plank is fueled, so each one-third bundle section consists of three fueled planks and three graphite planks. The coolant channel spacing between planks is 6.8 mm. Geometrical information for the six-plank fuel bundles is provided in Table 4.5.

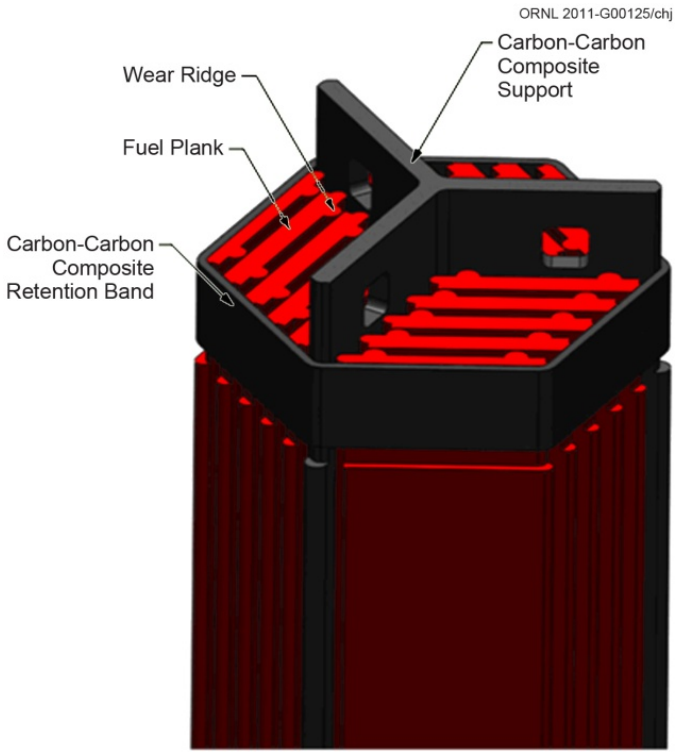

Fig. 4.10. Top of five-plank fuel bundle showing carbon–carbon composite support piece and retention band.

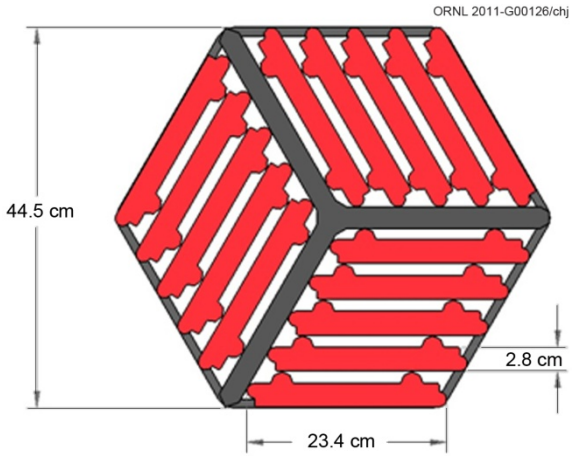

Fig. 4.11. Cross section of a five-plank fuel bundle.

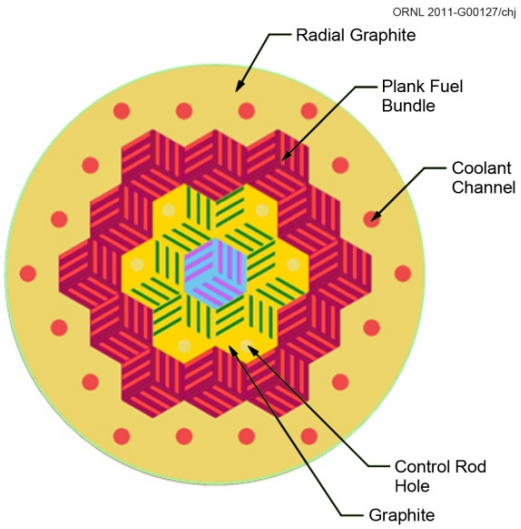

Fig. 4.12. Plank-fuel-core cross section.

Table 4.5. Six-plank bundle core component geometry

Core properties	
Number of slabs per one-third fuel block	6
Number of fuel slabs per one-third fuel block	3
Number of graphite slabs per one-third fuel block	3
Number of control rods	6
Control rod hole radius (cm)	5
Fuel slab thickness (cm)	2.4
Sleeve thickness (mm)	2.0
Coolant thickness (mm)	6.8

The fuel planks themselves are not load-bearing members. The fuel bundles are supported from below by a lower support honeycomb structure made from carbon–carbon composite that mimics the "*Y*" structure of the individual fuel bundles. A similar honeycomb structure is also employed at the top of the core to provide lateral positioning of the fuel assemblies. SiC–SiC composite rods from the top honeycomb connect the fuel assembly to the core bonnet. A SiC–SiC composite sheath connects the bottom and the top honeycomb structure. The core geometry is shown in Fig. 4.13. In this manner, the fuel assemblies rest on the bottom honeycomb, which is connected to an outer sheath that is, in turn, suspended from the top honeycomb structure. This top honeycomb has support rods that connect it to the removable core bonnet and transfer the load of the core to the core bonnet.

4.3.5 Fuel Assembly Thermal Performance

As discussed in Sect. 2, SmAHTR Functional Requirement 2 mandates that the peak fuel temperature anywhere in the core will not exceed 1250°C during normal operations, while Requirement 3 limits the peak core outlet coolant temperature for normal operations to 700°C. The three fuel assembly concepts discussed previously were analyzed to evaluate their respective performance with regard to these two key requirements.

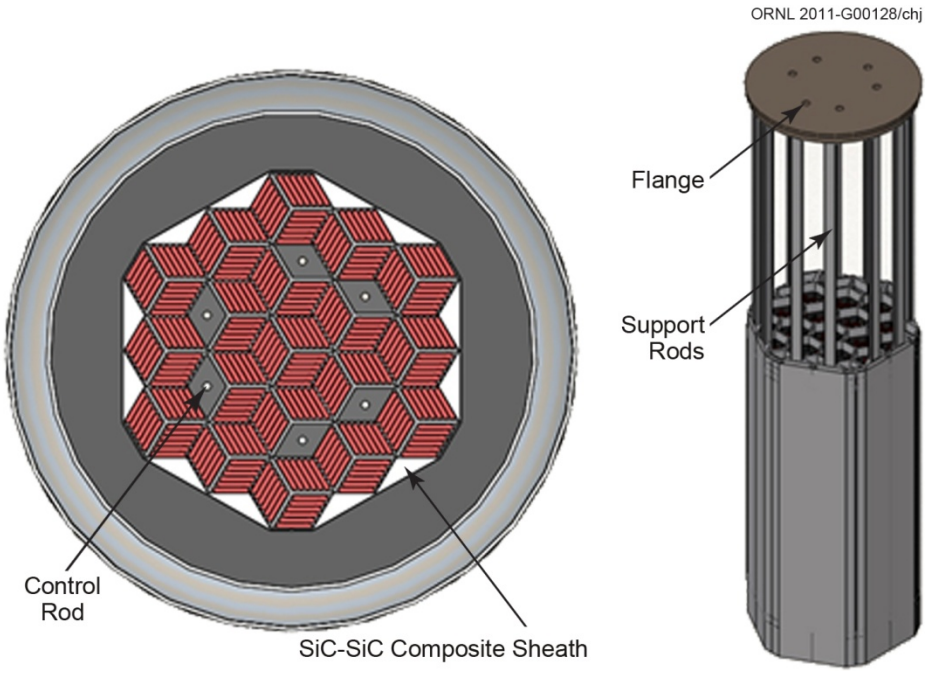

Fig. 4.13. Plank-fuel-assembly core cross section and removable core subassembly.

All of the fixed fuel SmAHTR core mechanical configurations were analyzed in steady state using RELAP5-3D. Table 4.6 shows some thermal hydraulic results for the three different fuels analyzed with different flow conditions. The central conclusion of the analysis is that with reasonable variance in the coolant flow through the core (900–1,400 kg/s) any of the fuel configurations evaluated will perform adequately in terms of both maximum fuel temperature and maximum coolant outlet temperature. The neutronic and structural core design constraints are more limiting than the steady-state thermal and hydraulic configurations. In general, minimizing the distance that heat must be conducted through the fuel to its surface is the primary fuel thermal design optimization parameter to minimize the fuel peak temperature.

Bypass flow could be mixed with the core outlet flow above the core, enabling a somewhat higher power output while maintaining the average coolant temperature below 700°C at all locations where it impacts metal structures.

4.4 REFLECTOR AND DOWNCOMER SKIRT

The reactor core has a radial graphite reflector as part of the neutronics design to thermalize and return neutrons to the fueled section of the core as well as to reduce the neutron fluence rate in the vessel. Because of the core's aspect ratio and the fact that the salt itself can serve as a reflector, no axial reflectors are contained in the current design, which results in a shorter overall vessel height. As discussed in Sect. 4.2, each PHX and DRACS heat exchanger is supported individually by the reactor closure flange. The heat exchangers receive the hot coolant discharging from the top of the reactor core while pumping the cold coolant down the annular space between the reflector and the reactor vessel. To separate the outlet coolant flow from the heat exchangers and the coolant at the top of the reactor, a "downcomer skirt" is designed to channel the flow (Fig. 4.14). The skirt is attached from the top of the reflector between the support rods up to the top of the heat exchangers. Although there may be small gaps that may not fully isolate the cold and hot coolant, for the most part, mixing of the coolant is avoided by this design.

Table 4.6. RELAP5-3D thermal hydraulic results for different fuels and flow conditions[a]

Fuel configuration	Diameter or thickness (cm)	Total number of pins or plates in the core		Coolant temperature (°C)			Max fuel temp. (°C)	Flow (kg/s)			Vortex valve diodicity
		Fuel	Graphite	Lower plenum	Max	Top plenum		Pump	Core	Bypass	
Cylindrical pins/stringers	2.8	72 × 19	19 × 19	650	700	695	1,178	350	1018	32	400
				650	715	700	1,182	350	969	81	50
Annular pins	**2.2–6.5**	**15 × 19**	**4 × 19**	650	737	700	1,143	350	905	145	50
				650	**703**	**687**	**1,027**	**510**	**1325**	**205**	**50**
Plates	2.6	18 × 19	0	650	703	700	975	350	1003	47	50
	2.8	9 × 17	9 ×17	650	706	700	1,240	350	949	101	50
	2.8	12 × 17	12 × 17	650	719	700	1,023	350	757	293	50
	2.8	12 × 17	12 × 17	653	700	686	1,002	530	1096	494	50
	2.8	12 × 17	9 × 17	651	700	694	1,061	410	1100	130	50

[a]Cylindrical and annular pins are located inside hexagonal graphite blocks. Plate fuel does not have the hexagonal graphite blocks. The total number of assemblies in the core is 19. For the four last cases (plate fuel), 6 control rods occupy 2 full assemblies; thus, the total number of fueled assemblies is only 17. The *Reference Design fuel* is in **bold**: fourth line—Annular Pins with high pump/core flow and reduced coolant temperatures.

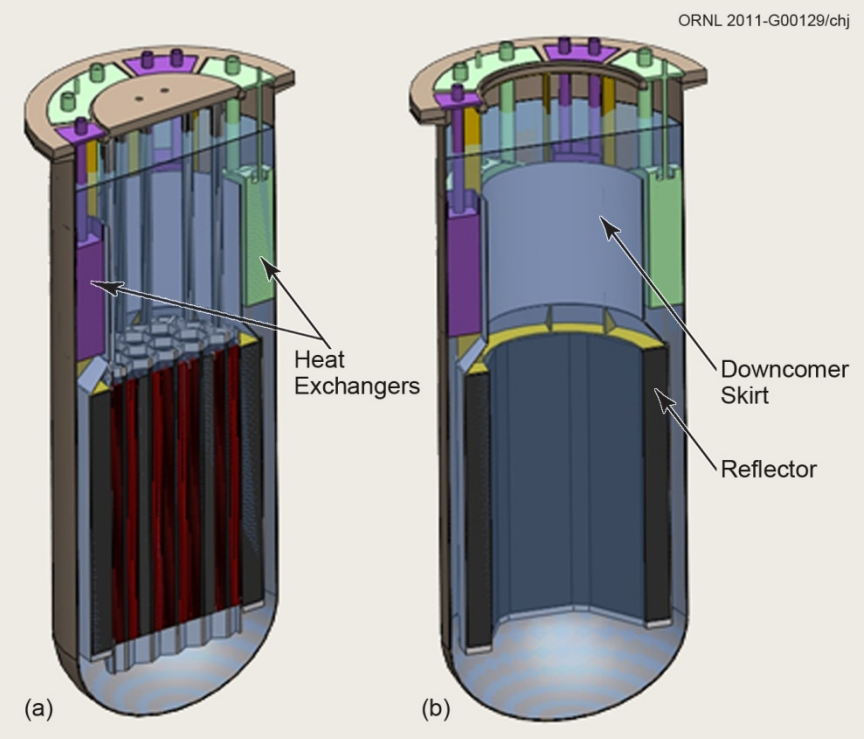

Fig. 4.14. (a) Downcomer skirt and (b) graphite reflector and support.

The reflector is located just outside the reactor core and is comprised of graphite. The reflector load is supported by the same SiC–SiC lower support plate (suspended from the reactor closure flange) that supports the reactor core. A SiC–SiC composite sheath connects this bottom SiC–SiC member to a similar structural piece at the top. Another set of SiC rods is used to connect these to the reflector flange at the top. The reflector can be removed only after the reactor core, and the heat exchangers have been removed from the vessel.

4.5 REFERENCES

1. D. F. Williams, L. M. Toth, and K. T. Clarno, *Assessment of Candidate Molten Salt Coolants for the Advanced High Temperature Reactor (AHTR)*, ORNL/TM-2006/12 (March 2006).
2. D. F. Williams, *Assessment of Candidate Molten Salt Coolants for the NGNP/NHI Heat-Transfer Loop*, ORNL/TM-2006-69 (June 2006).
3. R. B. Briggs, "Tritium in Molten-Salt Reactors," *Reactor Technology* **14**(4), 335–352 (Winter 1971–1972).
4. R. E. Thoma, *Chemical Aspects of MSRE Operations*, ORNL-4658 (December 1971).
5. G. D. Del Cul, D. F. Williams, L. M. Toth, and J. Caja, "Redox Potential of Novel Electrochemical Buffers useful for Corrosion Prevention in Molten Fluorides," in *Proceedings of the Thirteenth International Symposium on Molten Salts*, held during the 201st meeting of the Electrochemical Society, Philadelphia, Pennsylvania, May 12–17, 2002.
6. 2010 ASME Boiler & Pressure Vessel Code, Section II, Part D Properties, Table 1B, pp. 238–241.
7. E. L. Gluekler, editor, "Summary Plant Design Description," GEFR-000941, GE Nuclear Energy, March 1995.
8. J. A. Phillips, C. M. Barnes, and J. D. Hunn, *Fabrication and Comparison of Fuels for Advanced Gas Reactor Irradiation Tests*, HTR 2010, October 18–20, 2010, Prague, Czech Republic.

9. R. N. Morris, D. A. Petti, D. A. Powers, and B. E. Boyack, *TRISO-Coated Particle Fuel Phenomenon Identification and Ranking Tables (PIRTs) for Fission Product Transport Due to Manufacturing, Operations, and Accidents*, Volume 1, NUREG-6844 (July 2004).

10. AGR-1 Irradiation Experiment Test Plan, INL/EXT-05-00593, Revision 3 (October 2009).

11. Ebasco Services, Inc., *1000MW(e) Molten Salt Breeder Reactor Conceptual Design Study, Final Report Task 1*, TID-26156 (February 1972).

12. C. W. Forsberg, *Refueling Options and Considerations for Liquid-Salt- Cooled Very High-Temperature Reactors*, ORNL/TM-2006-92 (June 2006).

5. SmAHTR NUCLEAR ISLAND SYSTEMS

5.1 INTRODUCTION

In addition to the reactor vessel and its internal structures, the principal systems comprising the SmAHTR nuclear island are the

- intermediate heat transport system (including the in-vessel PHXs),
- direct reactor auxiliary cooling system (including the in-vessel DRACS heat exchangers),
- instrumentation and control system, and the
- reactivity control system.

These systems are described in this chapter.

5.2 INTERMEDIATE HEAT TRANSPORT SYSTEM

5.2.1 Intermediate-Cooling-Loop Overview

SmAHTR utilizes three PHXs coupled to three ICLs to remove heat from the reactor vessel and transport heat to either a power conversion system or to the thermal energy storage salt vault. Figure 5.1 is a simplified schematic representation of one of three identical SmAHTR in-vessel main circulating heat transfer loops, together with the associated in-vessel PHX, and the associated intermediate heat transport loop.

The PHXs are located at the top of the vessel, inside the annulus formed by the downcomer skirt and the inner surface of the reactor vessel. The pumps are located at the top of the PHXs, and each PHX has a corresponding pump. Figures 5.2 and 5.3 show the location of the PHXs. Each PHX alternates with each DHX. The three PHXs and the three DHXs occupy the complete annular space between the core barrel skirt and the vessel.

Each PHX (Fig. 5.4) is designed to remove 50% of the total reactor power (62.5 MW), so that only two heat exchangers are required to remove 100% reactor power. This is the design philosophy of "two-out-of-three," with redundancy of one component. During normal operation, all three loops with the three PHXs and the three main pumps will be operating, so each PHX will remove 33% of the total reactor power (41.7 MW). Likewise, each main pump flow is 350 kg/s (510 kg/s for the annular pin fuel when all three pumps are operating). If only two PHXs and two pumps are operating, then each main pump flow will be increased to 525 kg/s (765 k/s for the annular pin fuel). The total pump flow

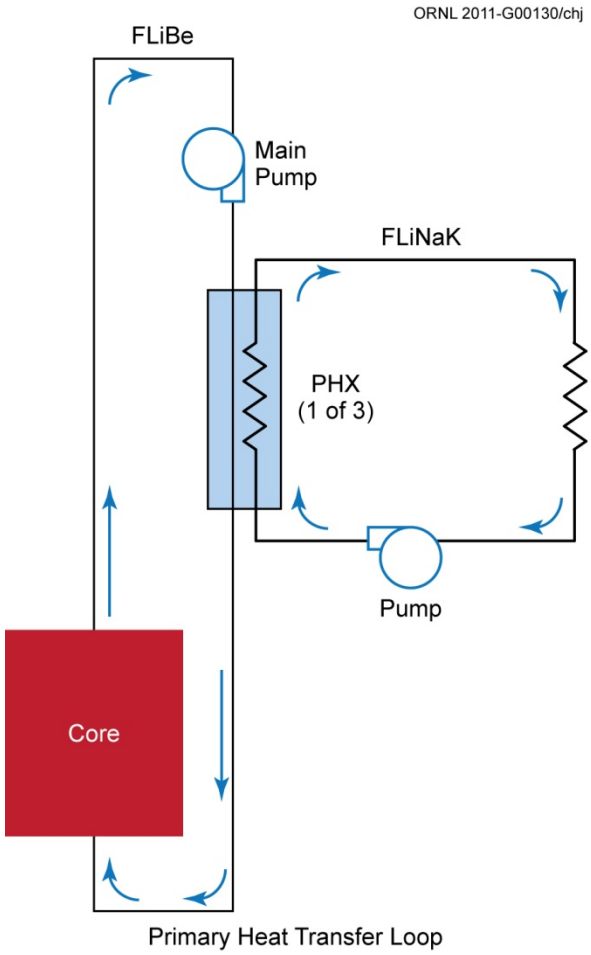

Fig. 5.1. SmAHTR operational heat removal system (one of three).

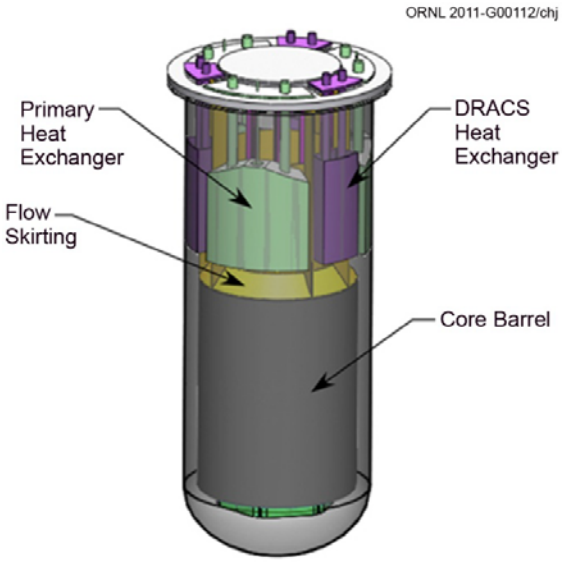

Fig. 5.2. Location of the PHX and DHX at the top of the vessel.

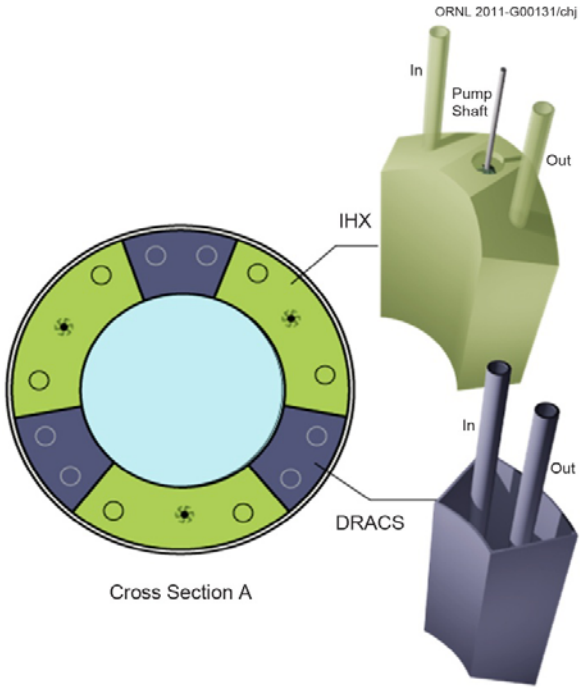

Fig. 5.3. Top view of the vessel closure flange and PHX and DHX.

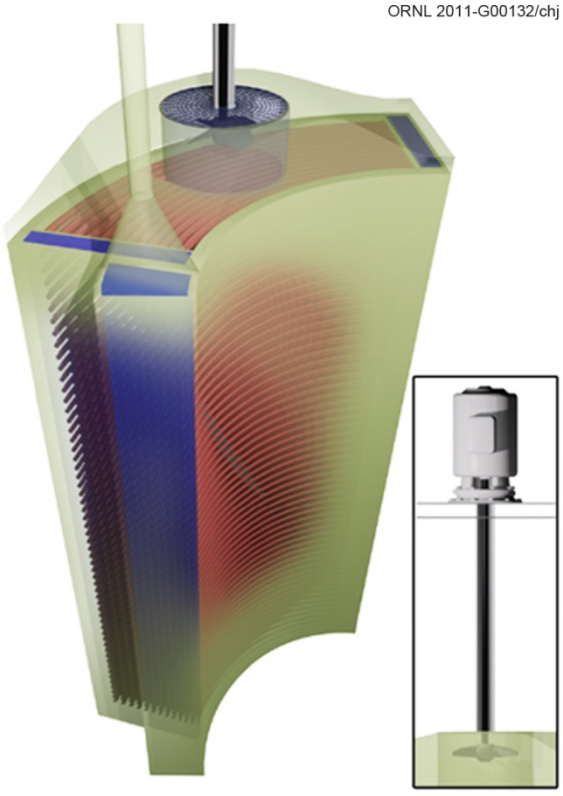

Fig. 5.4. PHX design with main pump.

in both cases is the same, 1,050 kg/s (1,530 kg/s for the annular pin fuel), with either three or two pumps in operation. The core flow is also the same with either two or three pumps in operation.

5.2.2 Intermediate-Cooling-Loop Salt Selection

The secondary coolant transports the reactor's heat from the PHX to a secondary heat exchanger (SHX). As such, the secondary salt evaluation criteria are almost entirely heat transport performance based. Only fluorides are candidates for SmAHTR secondary coolant since the primary coolant salt on the other side of the PHX is a fluoride salt. Having a different chemical system (such as a chloride) on one side of the heat exchanger and a fluoride on the other would require employing an alloy compatible with two different chemical systems at temperature. A proven alloy that is compatible with chloride and fluoride salt is not currently available.

The secondary coolant does not have a nuclear performance requirement, thus

expanding the salt options. The secondary coolant salt needs to have a melting point below ~500°C to minimize the potential for freeze-up events. The boiling point for the secondary salt must be above SmAHTR's core outlet temperature to maintain low pressure. Similarly, the vapor pressure of each of the salt components must remain below 1 atmosphere at operating conditions and preferably much lower to avoid depleting the salt in any species. The secondary coolant must also be thermally stable above any credible accident conditions. In addition, the secondary fluid must have a low viscosity at operating temperature and a large heat capacity. The secondary salt needs to be chemically compatible with the secondary loop structural alloy. For ease of operations, the secondary salt also should not be highly toxic.

Lighter low-Z salts (salts containing elements with low atomic number) tend to exhibit better heat-transfer performance metrics. However, almost all of the fluoride salts exhibit good heat-transport performance. Further, all of the candidate heat-transfer fluoride salts have similar corrosive properties when contaminated, and thus structural alloy compatibility is not a primary discriminator among candidate fluoride salts.

With respect to heat-transfer performance, the FLiNaK (46.5-11.5-42 mol % and 454°C melting point) eutectic is superior to all identified fluoride salts and for this reason has been selected as the SmAHTR secondary coolant salt. The leading alternative intermediate heat-transfer salt is KF-ZrF_4 (43–57 mol %) due to its acceptable heat transfer performance and lower melting point (430°C). One issue for the use of FLiNaK containing non-enriched lithium in the secondary loop is the potential for a leakage into the primary system. A principal part of the cost of the primary salt is for the removal of lithium-6. If a major leak from the secondary salt to the primary salt develops, the lithium isotopes will mix and require significant expense to reseparate. Thus, the secondary loop should not be at a significantly higher pressure than the primary system.

5.2.3 Primary Heat Exchangers and Pumps

The PHX (Fig. 5.4 and Table 5.1) is shell-and-tube, countercurrent flow design, with the primary fluid (FLiBe) circulating in the shell and the secondary fluid (FLiNaK) circulating inside the tubes.

The tubes are arranged horizontally, with four horizontal passes. Each pass consists of 354 tubes—the total number of tubes for the four passes is 1,416 tubes. There are 12 tubes per row, with a total of 114 rows. The total height of the HX is 2 m, which is the height of the annulus. The tube OD is 25.4 mm, and the wall is 1.6 mm thick. Tube pitch is 1.2. All the material in contact with the salt is Hastelloy-N. Welding and joining technologies for Hastelloy-N heat exchangers were developed for the MSRE project. A rendering of a single PHX and pump system is shown in Fig. 5.4. The secondary coolant, FLiNaK, is supplied to the bottom of the PHX through a down tube located at the left of the figure. Baffles are incorporated in each tube header to provide the appropriate number of tube passes. The secondary flow exits at the right side of the heat exchanger. An axial flow pump, located at the top of the PHX, provides forced-down flow on the primary side of the heat exchanger, drawing hot coolant from the upper plenum of the reactor and forcing coolant through the PHX. An overhung impeller allows the motor to be located outside of the reactor vessel and the pump bearings to operate in the cover gas at the top of the vessel. A rotating dry gas seal is used on the pump shaft between the cover gas and atmosphere.

The primary mass flow rate is 525 kg/s of FLiBe entering at the top (with only two PHXs operating and cylindrical pin fuel configuration) at a temperature of 700°C. The primary coolant leaves the PHX at the bottom at 650°C. The secondary coolant, FLiNaK, flows at a rate of 370 kg/s, entering at the bottom at a cold temperature of 600°C and leaving at the top at a hot temperature of 690°C. When three PHXs and three main circulating pumps are operating, the primary coolant flow is 350 kg/s and the secondary flow is 247 kg/s. Each PHX will be transferring ~42 MW of power.

Table 5.1. PHX design parameters

Variable	Units	Value
Capacity, max (two operating), each	MW	63
Capacity, nominal (three operating), each	MW	42
HX type		Shell and tube Multi-pass Countercurrent flow
Configuration		Horizontal tubes
Primary fluid salt		FLiBe
Secondary fluid salt		FLiNaK
Secondary fluid flows		Inside tubes
Number of tubes		1,416
Number of passes		4
Tubes/pass		354
Primary flow, nominal/max (3/2)	kg/s	350/525
Secondary flow, nominal/max (3/2)	kg/s	247/370
Tube OD	cm	2.54
Tube ID	cm	2.22
Average tube length	m	2.76
Temperature primary, hot	°C	700
Temperature primary, cold	°C	650
Temperature secondary, cold	°C	600
Temperature secondary, hot	°C	690
Primary side pressure drop, nominal	kPa	14
Secondary side pressure drop, nominal	kPa	66
Primary side velocity, nominal/max	m/s	1.1/1.65
Secondary side velocity, nominal/max	m/s	0.96/1.44
Heat transfer coefficient, primary	$W/(m^2 \cdot °C)$	3,400
Heat transfer coefficient, secondary	$W/(m^2 \cdot °C)$	3,500

5.3 DIRECT REACTOR AUXILIARY COOLING SYSTEM (DRACS) HEAT EXCHANGER AND LOOP

5.3.1 Overall DRACS Architecture

SmAHTR employs three DRACS loops in a two-out-of-three design approach; the core decay heat is designed to be removed with only two of the three DRACS loops operating.

Figure 5.5 is a simplified schematic of the DRACS cooling system. Table 5.2 shows the design parameters of the DRACS system. Each DRACS loop has been designed to remove 0.42 MW (0.33% of the total core thermal power) passively (by natural convection). Thus, the three DRACS will remove 1.26 MW, which is ~1% of the total core full power. Each DRACS loop removes decay heat passively to an outside natural draft air cooler that includes a 12 m high chimney (one cooler for each DRACS). The air coolers are located outside and elevated with respect to the reactor vessel in order to promote natural convection in the DRACS loop. Figure 5.6 shows the DRACS loop with the reactor vessel and the air cooler and tower. Dampers incorporated in the chimney inlet are used to control airflow to the finned air heat exchangers that are located inside the chimney. Figure 5.7 shows a closer view of the air cooler and how it is designed to operate.

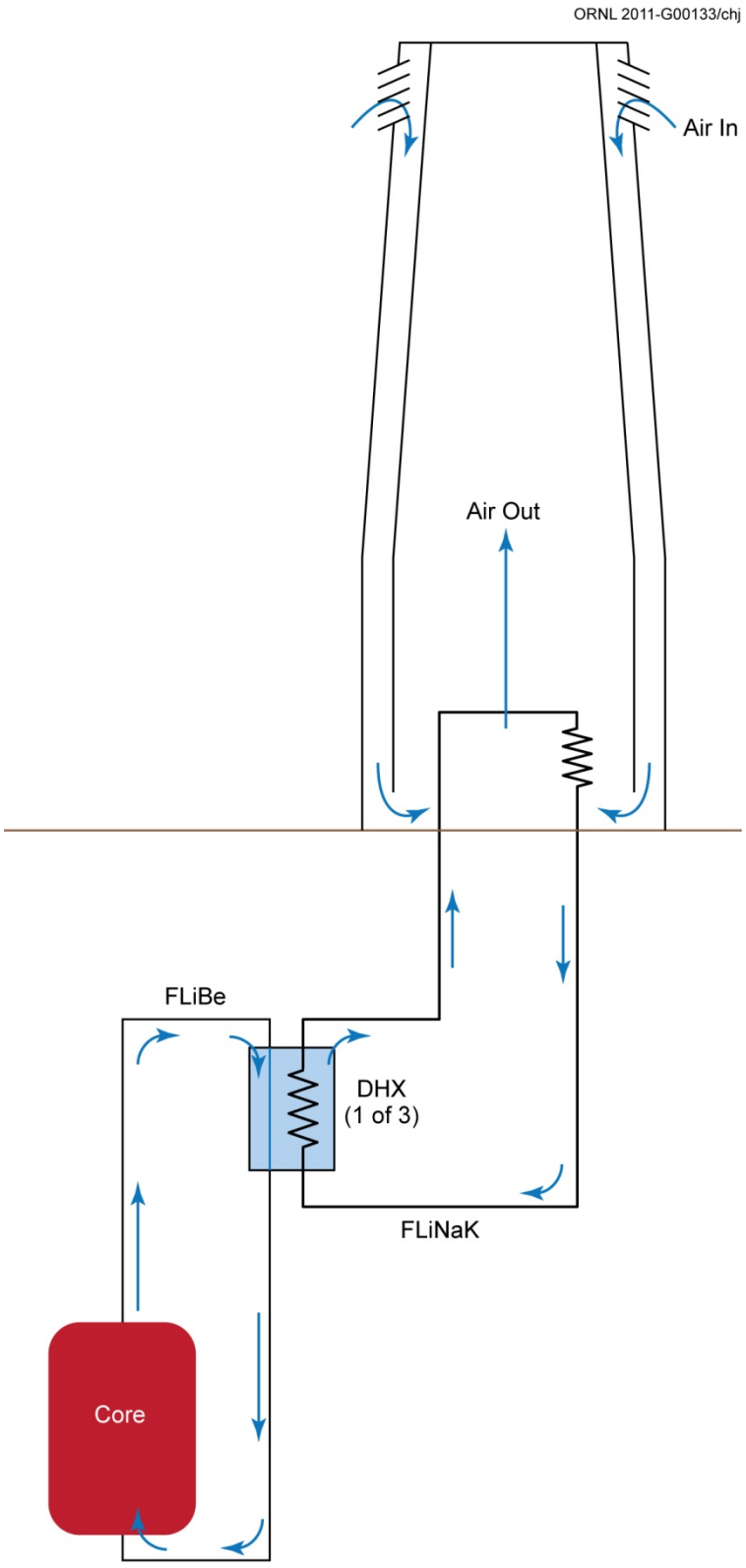

Fig. 5.5. Simplified schematic of the DRACS cooling system.

Table 5.2. DRACS design parameters

Variable	Units	Value
Cooling capacity, each	MW	0.42
Salt/salt (inside-vessel) HX		Vertical tubes
Secondary salt		FLiNaK
Elevation	m	0 (vessel annulus)
Number tubes		664
Tube length	m	2
Tube OD	cm	1.27
Tube ID	cm	1.021
Pitch		1.25
Primary side flow (per DRACS)	kg/s	9
Secondary side flow (per loop)	kg/s	7.2
Total core natural convection flow	kg/s	22–24 (two DRACS)
Primary side ΔT	°C	16
Secondary side ΔT	°C	30
Salt/air (inside tower) HX		Vertical tubes with fins
Elevation	m	+6
Number tubes		56
Tube length	m	2
Tube OD	cm	1.995
Tube, ID	cm	1.6646
DRACS piping, vertical	m	6×2
DRACS piping, horizontal	m	2×2
Air cooler (tower)		Vertical
Tower height	m	12
Gas flow area (horizontal)	m^2	4
Cooling gas		Air/nitrogen
Gas cold temperature	°C	30
Gas hot temperature	°C	205
Gas flow	kg/s	2.4

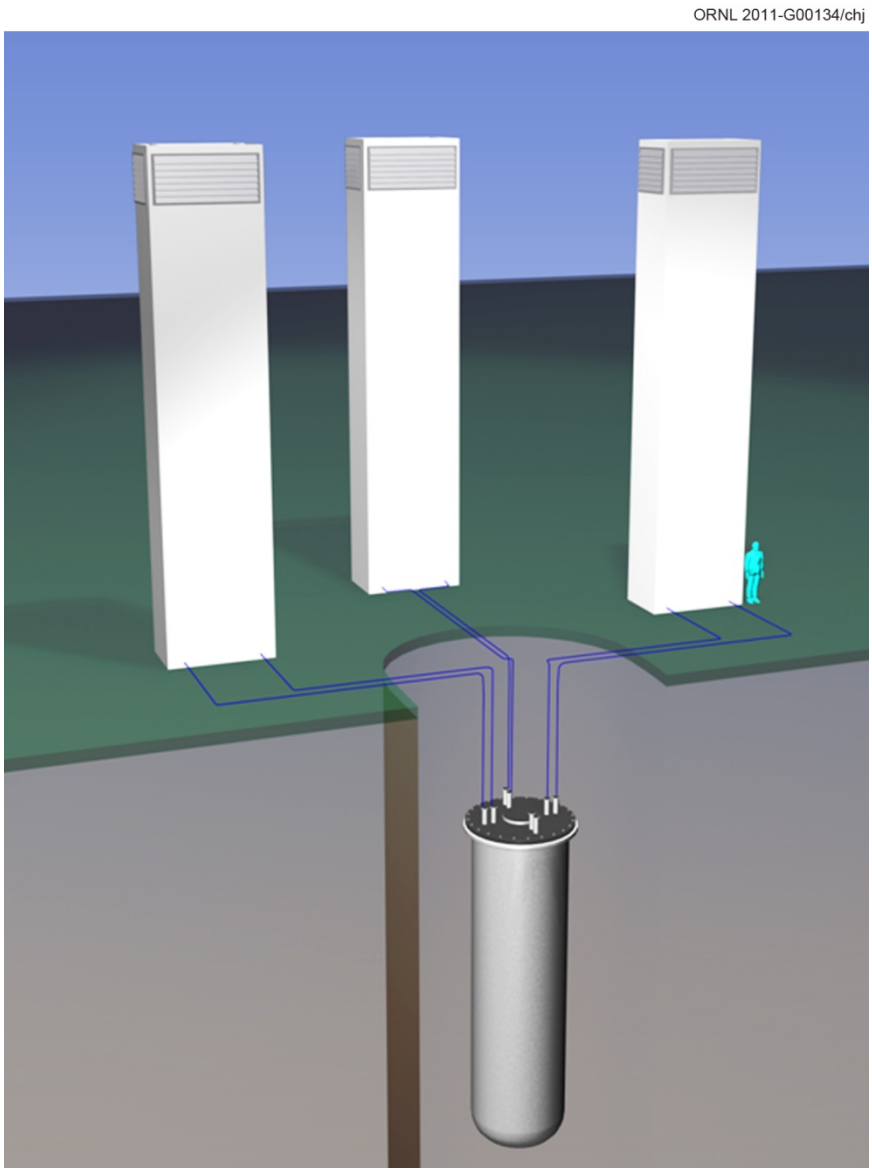

Fig. 5.6. View of the DRACS loops with the air coolers.

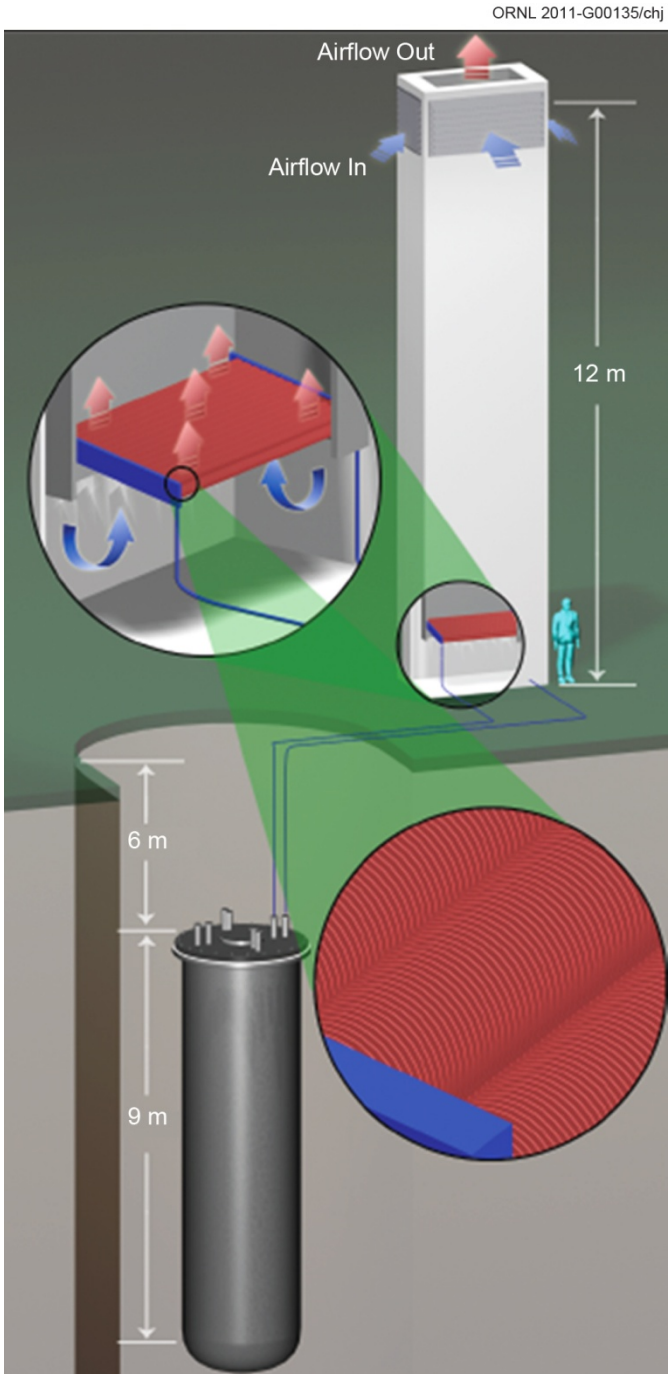

Fig. 5.7. DRACS loop and natural draft air cooler.

5.3.2 DRACS Salt Selection

Each DRACS loop has a heat exchanger (DHX) located inside the vessel annulus in contact with the primary coolant; the DRACS air radiator (DAR) is in contact with the outside cooling air. The DHX is a single-pass, shell-and-tube design, and the air heat exchanger (AHX) is a single-pass finned tube design. The salt selected for the coolant inside the tubes (the DRACS loop) is FLiNaK. This salt may not be the best choice as the coolant in this loop should have the lowest melting point in order to prevent salt freezing inside the loop, in particular at the air cooler. Therefore, a different coolant salt may be selected in the future. However, the salt selection for concept development purposes is sufficient to perform an initial design and assessment of the performance of DRACS. The material in contact with the salt is Hastelloy-N. The location of the DHXs inside the vessel is shown in Fig. 5.2.

The DRACS transfers heat from the primary coolant to ambient air via the in-vessel DHX and the external DAR. The requirements for the DRACS coolant are nearly identical to those for the secondary coolant with the exception of placing a higher value on a lower melting point to minimize the potential for salt freeze-up. Either FLiNaK or KF-ZrF_4 (43–57 mol % and a 430°C melting point) would be suitable salts for use in the DHX, with the FLiNaK providing somewhat improved heat-transfer performance and the KF-ZrF_4 providing a lower melting point while avoiding the possibility of diluting the primary salt lithium enrichment. KF-ZrF_4 is not currently in the RELAP code package. For this reason, FLiNaK was selected as the baseline coolant for the DRACS loop.

KF-ZrF_4 could also be employed in the secondary loop at an intermediate pressure between the power cycle and the power cycle loop. A pressurized intermediate loop would reduce the stress across the SHX, easing its design and fabrication. Further design trade studies will be required to evaluate which option would be preferred.

5.3.3 DRACS In-Vessel Heat Exchanger and Loop

The DHX is located inside the vessel annulus and is a single-pass, shell-and-tube cross flow heat exchanger. The secondary fluid (FLiNaK) flows inside the tubes, and the primary coolant (FLiBe) flows outside the tubes. The primary coolant flows downward during natural convection conditions (pumps off). During full-power operation, with the main pumps running, the primary coolant flow in the DHX is upward because of the pressure differential across the pump inlet and PHX. This flow results in a parasitic heat load on the system as any heat lost through the DRACS during normal operation is an overall system thermal loss, and results in less heat delivered to the intermediate loop. A vortex diode at the bottom of the DHX limits the amount of this upward flow. A vortex diode acts much like a leaky check valve; however, it has no moving parts. It has a high pressure drop in one direction (reverse) and a low pressure drop in the forward direction. Upward flow in the DHX during normal, pumped operation causes reverse flow in the diode, which reduces the total flow through the core.

The DHX consists of 664 vertical tubes, 2 m long (height), 1.27 cm (0.5 in.) OD, 1.021 cm ID, with a triangular pitch of P/D = 1.25. The AHX is located 6 m above the DHX (located inside the vessel annulus). The DRACS loop connecting both DHXs is 16 m long, consisting of two 6 m vertical runs and two 2 m horizontal runs. Total height of the DRACS loop is 8 m, including the 2 m high DHXs, one inside the vessel and the other inside the cooling tower, and the 6 m high vertical pipe. The horizontal pipe between both DHXs is 2 m, but other lengths may be required. Thus, one DRACS hot leg is 8 m vertically and 2 m horizontally with similar dimensions for the cold leg.

A rendering of the DHX is shown in Fig. 5.8. The design is similar to that of the PHX. Figure 5.8 shows horizontal tubes—the tube orientation could be either vertical or horizontal. As with the PHX, the secondary coolant, FLiNaK, is supplied to the bottom of the DHX through a down tube located at the right of the figure. The secondary flow exits at the left side of the DHX. For the DHX, the top of the heat exchanger is completely open to primary coolant flow. However, as discussed previously, a

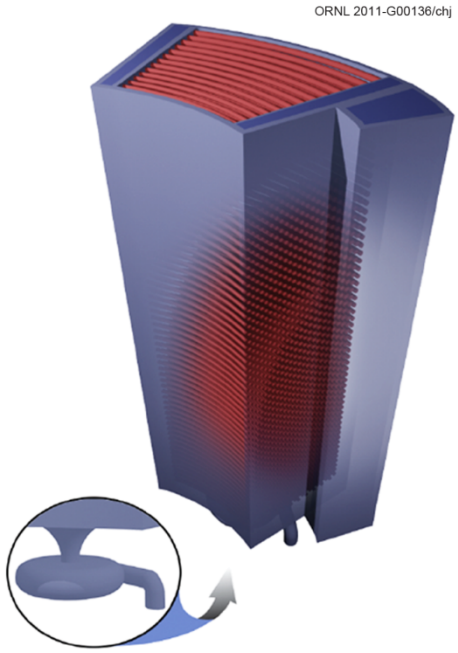

Fig. 5.8. DRACS salt-to-salt heat exchanger (DHX) showing incorporation of a vortex diode at the bottom.

vortex diode is located at the bottom of the heat exchanger to reduce reverse flow during normal operation. In this case, a vortex-type diode is included in the design.

5.3.4 Vortex Diode

The design of a vortex diode creates a vortex to increase the flow resistance in one direction. An example of the vortex diode is shown in Fig. 5.9. It is designed so that flow in the forward direction enters at the center of the device and exits at the tangential port (the diagram on the right of Fig. 5.9). In the reverse direction, flow enters the tangential port, induces a swirling flow in the diode, and then exits at the center port (diagram on the left of Fig. 5.9), increasing the pressure drop significantly over that in the forward direction.

Detailed parameters of the vortex diode, located at the base of each DHX inside the vessel, are not well known and can vary widely depending on the specific design, in particular the pressure drop in each direction and the diodicity. The diodicity of a vortex diode is defined as the ratio of the reverse-flow pressure drop (in the upward direction for the SmAHTR DRACS configuration—this is the large pressure drop) to the forward-direction pressure drop (natural convection pressure drop in the downward direction—this is the small pressure drop) for the same flow rate. Diodicity values of 400, 50, and 10 have been employed in RELAP5-3D and calculations to parametrically study the effect of different diodicity values. Form losses of $k = 1$ in the natural convection direction were used for the three cases. The form losses in the reverse direction were: $k = 400$, $k = 50$, and $k = 10$, to achieve the desired diodicities of 400, 50, and 10. The larger the value of diodicity, the smaller the calculated bypass or reverse up-flow. The smaller the bypass flow, the smaller the heat losses through the DRACS during normal operation at full power. In the RELAP5-3D model, the diodicity does not affect the DRACS natural convection flow because the natural convection flow form losses ($k = 1$) are the same for the three values of diodicity. Table 5.3 shows calculated bypass flow (or reverse flow), pump-flow/bypass-flow ratio, or P/B (the pump flow is always 350 kg/s), and heat losses for the three different diodicities used in these calculations. Both flow losses (bypass flows) and heat losses appear to be acceptable for the three diodicity values, with a DRACS power penalty of slightly over 1 MW during normal power operation. Additionally, dampers would be included in the air

Fig. 5.9. Forward (right) and reverse (left) operation of a vortex diode.

Table 5.3. Calculations with different diodicities

Valve diodicity	Bypass flow (kg/s/valve)	Bypass flow total (kg/s)	Core flow (kg/s)	Flow ratio P/B	DRACS losses (MW/DRACS)	Total DRACS loss (MW)
400	10.5	31.5	1,018.5	33.33	0.35	1.05
50	27	81	969	13	0.383	1.15
10	46.7	140	910	7.5	0.4	1.2

cooler design that would limit airflow to the DHX. This was not accounted for in these calculations but would reduce thermal losses even further.

During DRACS passive operation, the calculated natural convection flow is ~9 kg/s/DRACS. A value of the diodicity of 50 appears to be reasonable, based on available experimental data. Some calculations, like the loss of forced flow transient, employed a diodicity of 400.

5.3.5 DRACS Air Radiator

The DRACS air radiator or DAR (Fig. 5.7) inside the air cooler structure is also a single-pass, tube-and-shell, countercurrent flow device. The air circulates outside the tubes, upward, and the FLiNaK coolant inside the tubes, downward. The DAR consists of 56 vertical tubes with fins, 2 m long (height), 2.0 cm OD, and 1.66 cm ID. The air-cooled tower is 12 m in height, with a horizontal cross-sectional area of 4 m^2 for the airflow.

During decay-heat operation, three natural convection loops are interconnected for each DRACS: one inside the vessel primary system with FLiBe as the circulating fluid; another inside the DRACS loop with FLiNaK as the circulating fluid; and finally, the third loop inside the air cooler with air as the circulating fluid.

Typical natural convection flows expected during decay-heat operation in the DRACS system are 9 kg/s/DRACS of FLiBe through the primary side of the DHX inside the vessel, 7 kg/s of FLiNaK inside the DRACS loop, and 2.4 kg/s of air (or nitrogen) inside the air cooler.

5.4 INSTRUMENTATION AND CONTROL SYSTEM

5.4.1 Control System Overview

Functionally the instrumentation and controls for SmAHTR closely resemble those for any nuclear power plant, with temperature, pressure, flow, level, and neutron flux being the principal process variables monitored. SmAHTR's distinctive coolant, materials, temperature, and fuel, however, alter both the implementation of the process monitoring as well as key features of the control philosophy. The higher coolant operating temperature prevents direct use of almost any LWR instrumentation. Additionally, the conditionally corrosive nature of the fluoride salt coolant necessitates regular coolant chemistry monitoring.

Under normal operating conditions, the primary information transferred from the power or heat cycle to the nuclear plant control system is the heat demand. While SmAHTR is naturally load following due to its strong negative fuel temperature feedback coefficient, receiving a load request signal enables a more rapid nuclear plant response that minimizes temperature temporal variances and thereby decreases stress on the plant equipment. An erroneous load demand signal would result in increased stress on the plant equipment as the reactor inherent thermal feedback adjusts to the actual load.

The robust nature of the fuel, large fuel negative temperature feedback, and very large margin to coolant boiling, combined with the tolerance of the primary pressure boundary alloy for short-term temperature excursions, shifts the plant control focus from the core to the SHX. The SHX is the only

plant component that experiences both high temperatures and a large pressure differential along with having a functional requirement to minimize the internal wall thickness.

To minimize its size and cost, the SHX will operate near the design limits of its materials. Provided that proper chemistry control is maintained, the high-temperature effects on its structural alloys and joints will determine the lifetime of the SHX. The material creep (and thermal ratcheting) would be significantly accelerated by temperature excursions above the design limit while at operating differential pressure. Further, rapidly changing the temperature distribution within the SHX, as could occur with rapid flow or inlet temperature shifts, would result in excessively stressing the SHX internal structures, as its materials expand and contract. Thus a primary operational control objective would be to minimize the thermal excursions and resultant stresses on the SHX.

SmAHTR's control system design only exists at a primitive level. Knowledge of the core temperature feedback coefficient and the general stability of liquid-cooled reactor systems, however, provide confidence that a robust control system can be developed as a specific design emerges. The operational control systems available to SmAHTR are the direct reactivity control elements (rods or drums) and the heat removal system. A particular challenge for the detailed control design is that supercritical carbon dioxide power cycles, an attractive power cycle for use with SmAHTR, do not currently exist at industrial scales (beyond 1 MW); thus, their loop control technology has yet to be developed or demonstrated.

The overall reactor control system design intent is that during power operation the mean coolant core output temperature will be held constant at 700°C. Reactivity would be varied to maintain the constant temperature. Large power shifts would be accommodated using control element motion with smaller shifts performed by altering the coolant inlet temperature through flow control. Flow control technologies such as salt throttle valves or a heat exchanger bypass system, while conceptually achievable with current materials, have not been designed or demonstrated for FHRs. Alternatively, flow control could most directly be implemented by altering the pumping speed. Each of the three SmAHTR primary pumps will have a FLiBe flow capacity of 525 kg/s. A crude estimate of pump shaft power required to support this flow rate would be up to 200 kW combined shaft power for the three pumps. While variable speed motors in the 50–100 kW range are commercially available, variable speed primary pumps have not been previously used for nuclear power plants due to the low reliability of the required high-power control electronics. Over the past few decades, high-power solid-state electronics have undergone great improvements in their availability and reliability and might now be considered the preferred flow control methodology.

5.4.2 Process and Condition Measurement Instrumentation

5.4.2.1 Temperature

Temperature measurement is indicative of both process conditions and is a primary component of the energy transfer measurements necessary for efficient power plant operation. Thermocouples are the most common transducer for process temperature measurement. However, base metal thermocouples typically lack the long-term accuracy necessary for the heat balance measurements necessary for efficient process operation. Precious metal thermocouples are a possible alternative that may provide more accurate temperature measurements.

Type N (Nicrosil–Nisil) thermocouples were developed in the 1970s and 1980s as a lower drift alternative to other base metal (particularly Type K) thermocouples and may prove to be a suitable temperature measurement alternative.[1,2] Having achieved designation as a standard thermocouple type by the Instrument Society of America in 1983, Type N thermocouples have been in widespread use for more than 25 years. The Nicrosil and Nisil alloys contained in Type N thermocouples were developed after the instability mechanisms of other base-metal thermocouples were understood, specifically to overcome these instabilities. Nicrosil and Nisil alloy compositions feature increased component solute concentrations (chromium and silicon) in the nickel base to transition from internal

to surface modes of oxidation and include solutes (silicon and magnesium), which preferentially oxidize to form oxygen diffusion barriers.[3]

5.4.2.2 Flow

Liquid-salt-flow measurement will most likely be performed using either external, ultrasonic flowmeters or Venturi-type flowmeters that use differential pressure gauges as their active element. Ultrasonic flowmeters are currently gaining wide acceptance in LWRs as a primary coolant flowmeter due to their low uncertainty and high stability. SmAHTR's higher temperature requires the use of mechanical standoffs to limit the ultrasonic transducer temperature exposure. The mechanical standoffs required for high-temperature application are only becoming available, requiring additional design and development for confident application. The electronics for water and salt ultrasonic flowmeters would be essentially identical. The differential pressure gauges required for Venturi base flow measurement either require diaphragm deflection measurement tolerant of SmAHTR temperatures or impulse line interconnection between a high-temperature and a low-temperature diaphragm, which would be instrumented with conventional low-temperature diaphragm deflection technology. The impulse line fluid would be a lower melting point fluid such as a liquid metal. Both optically and capacitively based diaphragm deflection measurements are strong candidates for direct, high-temperature implementation. Specialized molten salt melt-compatible, diaphragm-deflection pressure gauges employing NaK (78% potassium, 22% sodium) impulse line isolation of the high-temperature diaphragm are becoming available.

5.4.2.3 Level

Several technologies are available for salt level measurement. Bubbler-type level measurements based upon the pressure required for minimal flow in a vertical tube are commercially available technology. Also, radar-type level measurements based upon reflection off the top surface of the salt are commercially available. The radar gun and electronics would be located in a standpipe above the fluid well outside of the high-temperature and high-radiation zones. Mechanical float-type level measurements can also be readily adapted to the salt loop by attaching a mechanical extension to a float on the surface of the salt. The mechanical extension would be configured such that it would extend into a nonmetallic standpipe above the vessel, enabling the position of the end of the mechanical extension to be determined magnetically. Heated lance-type level measurements within a salt-compatible sheath would also provide discrete position level measurement.[4]

5.4.2.4 Flux

High-sensitivity, high-temperature-tolerant neutron flux monitoring is necessary during the initial reactor approach to critical. The reflector and thick downcomer make monitoring the subcritical neutron flux outside the vessel impractical; thus, a high-sensitivity neutron detector is necessary in or near core during startup. Fission chambers are commercially available with temperature tolerances to ~550°C. An operational approach would thus be to achieve initial criticality with a salt temperature less than 550°C and to withdraw the startup detector before bringing the reactor to operating temperature. As requiring lower-temperature criticality is operationally limiting, development of higher-temperature flux monitoring is recommended.

Power-range neutron flux monitoring serves as an indication of unintended reactivity insertion as well as provides a cross check of the thermal measurement of reactor power. During power operation, the neutron flux is sufficiently large to make neutron flux measurements outside the reactor vessel using high sensitivity detectors. However, moving the flux measurements outside the core decreases the measurement fidelity in that the core interior flux will be spatially masked.

Local power-range monitors are used to provide an indication of the spatial flux distribution. Gamma thermometers are structurally similar to thermocouples and are thus anticipated to perform at FHR temperatures. While gamma thermometers have existed in some form since the 1950s[5] and indeed were approved by the U.S. Nuclear Regulator Commission (NRC) for local power measurement in pressurized water reactors (PWRs) in 1982, gamma thermometers are only now beginning to emerge in widespread use in commercial nuclear power plants. Gamma thermometers function based upon the heating of the sensor assembly by gamma rays and the subsequent controlled differential cooling of the sensor body. The temperature differential developed along the cooling path is proportional to the rate of heating by the incident gamma rays, which is in turn proportional to the local power-generation rate during power-range operation.

5.4.2.5 Salt chemistry

Maintaining the relatively low corrosivity of fluoride salts is critically dependent on controlling the reduction–oxidation state. The most readily oxidized component of Hastelloy-N is chromium. Monitoring the decay gamma rays from chromium activation within the primary coolant would provide an indication of chromium dissolution into the salt. The instrumentation required to characterize the detailed chemical state of fluoride salt exists as laboratory-type instrumentation and is not readily available in an industrial application. Electrochemical measurements are the standard technique for monitoring the redox condition of salt components. Optical absorption spectroscopy is also a potentially useful methodology for identifying trace chemical constituents and their valence state.[6] Optical access to the salt is most readily provided through a standpipe above the salt containing an inert gas bubble; a noble metal mirror within the salt would provide the optical return path.

5.5 REACTIVITY CONTROL SYSTEM

The SmAHTR Reactivity Control System (RCS) provides the capability to maintain control of the nuclear reactivity of the system during normal and off-normal operations. The RCS was not developed for SmAHTR, so several considerations must be taken into accout in its design. In a typical RCS, reactivity is controlled by a combination of fixed burnable absorbers, control rods (movable absorbers), and an inherent negative temperature feedback coefficient. Control rods are used during operation to offset reactivity changes from fuel burnup, fission product production (transient, such as xenon, and long term), and temperature variation during startup, operation, and shutdown. Burnable absorbers can also be used, and likely will be required, to control the large initial excess reactivity that exists in the SmAHTR single-batch long-life core. This section provides a discussion of the requirements for the RCS and proposed concepts for normal and off-normal operation.

5.5.1 RCS Purpose

The purpose of the RCS is allow for reactor reactivity control during normal operations, such as startup, steady state operation, changes in operating power and reactor shutdown, as well as off-normal operations requiring the ability to shutdown the reactor. The primary design requirements of the RCS have not been fully developed, but based on operational considerations and a review of the general design criteria (GDC) in 10 CFR 50 Appendix A for safety considerations, the following functional requirements have been developed.

1. Ensure that the reactor can be reliably shutdown and held in a safe shutdown configuration with the core in its most reactive state (e.g., cold configuration, no xenon).
2. Two physically diverse shutdown mechanisms must be provided to ensure that the reactor can be shutdown should one system fail.

3. The control system must be able to control reactivity during operation to account for fuel burnup, temperature feedback, and transient fission products (e.g., xenon).

5.5.2 Burnable Absorbers

The operational control of the reactor involves the startup, ascension to power, steady state operation, and orderly shutdown of the reactor system. This implies that sufficient reactivity control must be available to account for the temperature reactivity defect (cold-to-hot), changes of reactivity during operation (primarily due to fuel burnup and fission product poisons), and shutdown of the reactor. The need to change power in response to loads may also be required.

The strategy for controlling reactivity for SmAHTR is similar to other reactors in which the overall excess core reactivity (~27,000 pcm, as indicated in Sect. 4.3) is largely offset through the use of fixed burnable absorbers. Startup, changes in power level, and shutdown are generally accomplished through control rod movements, although the possibility of the use of reactivity feedback may allow variations in flow to change the temperature and therefore provide a means to adjust power.

Therefore, the use of fixed burnable absorbers will be used to manage the majority of the reactivity swing over the fuel cycle, which, as indicated above, is large given that the entire core is replaced. The goal in the design of the burnable absorber configuration, in terms of selection the burnable absorber type and amount, is to minimize the amount of excess reactivity that must be managed by the control rods, thereby minimizing the number of control rods and their reactivity worth. Common burnable absorbers for high-temperature reactors include boron carbide (possibly enriched in boron-10), gadolinium oxide and carbide, and erbium oxide and carbide. Combinations of these absorbers have been found to be effective in provide a means of controlling reactivity over time, with boron carbide as a thermal neutron absorber burning out relatively quickly and gadolinium and erbium as resonance-region absorbers burning out over a longer period of time. The boron carbide can be mixed directly with the graphite matrix, while gadolinium and erbium can consist of coated particles. Note, however, that if the absorbers do not fully burn out during the operation period, as the case may be with erbium, they will represent a reactivity penalty at end of life and shorten the overall fuel cycle length. In addition to providing reactivity control, burnable absorbers can also be used to provide power shaping, which may be useful in SmAHTR to flatten the radial and axial power profiles.

5.5.3 Operation Control Rods

Operation control rods will be required to adjust reactivity during startup and shutdown and to control transient reactivity changes not offset by burnable absorbers, such as responding to transient fission products, such as xenon-135. Safety shutdown (reactor scram) is not the primary function of these control rods, but they can be designed to drop into the core upon loss of power or other scram actuation. The specific number of controls and their absorber loading will be determined during the core design process to ensure that they are capable of managing the full reactivity swing from cold to hot and for buildup and decay of xenon-135. Additionally, the maximum worth of the control rod must be less than $1 of reactivity to ensure that a prompt critical excursion will not occur if the control rod is accidently withdrawn (control rod ejection, as it exists in LWRs, is not possible in low-pressure systems, such as SmAHTR, but uncontrolled withdrawal of the control rod cannot be ruled out). A typical design value would be less than $0.50. A control rod design based on that of the Gas-Turbine Modular Helium Reactor (GT-MHR) or Next-Generation Nuclear Plant (NGNP) can be adopted in which the control rod material is boron carbide (possible enriched) dispersed in graphite and clad with carbon–carbon composite materials. The control rod channels can also be formed with carbon–carbon composites, or the control must be design to be mechanically flexible to move thorough possibly offset channels resulting from graphite geometrical changes during operation. The

control rod drive motors can include magnetic release mechanisms as needed and springs or compressed nitrogen as can be used as a driving force to offset buoyancy in the liquid salt.

An additional means for operation control is the use of the inherently negative temperature reactivity feedback of the system. As shown in Table 4.4, the coolant reactivity coefficient is negative and therefore allows the possibility to effect reactivity changes through changes in the coolant temperature. This could occur passively by changes in the reactor load affecting heat removal from the reactor through the PHX or could occur directly by changes in the MCP speed resulting in changes in coolant flow (Sect. 5.4.1) and, therefore, changes in coolant temperature. Hence, the possibility of load-following operation and flow-based control exists but has not been investigated.

5.5.4 Reactor Shutdown System

A reserve shutdown system is necessary to provide a redundant system in addition to the operational reactivity control system. In SmAHTR, additional control rods, similar to other operational control rods, will be employed as a reserve shutdown system. These control rods are fully withdrawn during operation and are only allowed to release upon a loss of power or scram signal. Like the operational control rods, magnetic latches will be employed along with springs or compressed nitrogen gas to insert the control rods against the buoyancy forces of the salt.

The use of control drums in the reflector, as an alternative to rods, can also be considered. The drums are designed to have a portion of their surface with neutron absorbers that can be rotated towards the core to shut down the reactor, which in this case will result by basically blocking the reflector. The use of control drums minimize the above-core structures that are required but will require drive shafts that extend through the PHX, DHX region down to the reflector region.

Overall, the operational and reserve shutdown system must maintain the core in a fully subcritical configuration in the core's most reactive state, which is typically cold and xenon free at beginning of life, but may actually occur during the cycle if burnable absorbers are used. Further, it is typically assumed that the control rod of the highest worth is not inserted in the core. The amount of reactivity considered for the shutdown margin must include uncertainties associated with the prediction of the core reactivity, operational variations, and manufacturing tolerance.

5.5.5 Secondary Shutdown System

The GDC requires a physically diverse secondary shutdown system that operates on different design principles from the primary reactivity control system to ensure that the reactor can be maintain in a long-term shutdown mode. Several options that can be used for this secondary shutdown system, as briefly described.

Buoyancy driven control rods—the driving force of the control rods can be based on their buoyancy in the liquid salt, providing a fully passive shutdown mechanism in the event of loss of flow.

Absorber injection system—a strongly absorbing chemical can be injected into the coolant to provide shutdown of the reactor system. Several chemical options can be considered, but a primary concern is removal of the absorber from the expensive coolant salt. This would require a coolant salt chemical cleanup system that may be more substantial than that required for salt chemistry. Rather than inject the poison, a potentially passive means is to have a solid absorber in the core region that melts as the coolant reaches a certain temperature.

Absorber balls or pellets—a typical secondary shutdown system proposed for GT-MHR is the use of absorber balls or pellets that can be dropped in to the core. In the case of a liquid-salt system, these either need to have a higher density than the salt, be dropped into voided channels, or allowed to float up from the bottom of the core.

Expansion modules—another common passive reactivity control system, typically considered in fast reactors, is gas expansion modules or lithium expansion modules in which an absorber material

inserted in a tube within the core is compressed into a region above the core by the flow of the reactor coolant. Should the coolant stop flowing, the absorbtion expands into the core region, providing a means for shutdown.

5.6 REFERENCES

1. A.V. Belevstev, A.V. Karzhavin, and A. A. Ulanowsky, "Stability of a Cable Nicrosil-Nisil Thermocouple Under Thermal Cycling," pp. 453–7 in T*emperature: Its Measurement and Control in Science and Industry*, *Volume 7*, edited by Dean C. Ripple, AIP 2003.
2. J. Jablin, M. R. Storar, and P. L. Gray, "Improved Operating Efficiency Through the Use of Stabilized Thermocouples," *Journal of Engineering for Gas Turbines and Power* **122**, 659–63 (October 2000).
3. N. A. Burley, "Advanced Integrally Sheathed Type N Thermocouple of Ultra-High Thermoelectric Stability," *Measurement* **8**(1), 36–41 (January–March 1990).
4. K. Termaat, J. Kops, K. Ara, M. Katagiri, and K. Kobayashi, "Fabrication Tests of Tricoth-Type Reactor Water Level Sensor," *IEEE Transactions on Nuclear Science* **37**(2), 1024–1031 (April 1990).
5. R. H. Leyse and R. D. Smith, "Gamma Thermometer Developments for Light Water Reactors," *IEEE Transactions on Nuclear Science*, **NS-26**(1), 934–943 (February 1979).
6. J. P. Young and J. C. White, "Absorption Spectra of Molten Fluoride Salts," *Analytical Chemistry* **32**(7), 799–802 (June 1960).

6. SmAHTR SYSTEM SAFETY AND TRANSIENT BEHAVIOR

6.1 SAFETY/LICENSING PHILOSOPHY

The SmAHTR design takes advantage of the existing safety philosophy of several small modular reactors (SMRs).[1] The reactor uses passive decay-heat removal systems relying on natural convection, and the core is designed with large negative reactivity feedback coefficients. The core and all primary components are contained in the reactor vessel (integral design), which eliminates the possibility of a large break loss-of-coolant accident (LBLOCA) scenario. Only intermediate loop piping (ILP) carrying nonradioactive coolant penetrates the vessel. The passive decay-heat removal design eliminates reliance on off-site power, which is necessary if the reactor is to be sited in remote locations, and removes the need for safety-related emergency on-site AC power. The reactor can be viewed as having several barriers to fission product release in case of an accident, these being the coated particle fuel, the graphite moderator, the reactor vessel/guard vessel and the containment.

In addition to these barriers, the design has other safety features. The reactor will use TRISO-coated particle fuel, which not only acts as a fission product barrier but also has a failure point (>1,600°C). The use of molten salt coolant with a high boiling point and low vapor pressure allows near-ambient operating pressure. The good heat transport properties of the molten salt result in slow response to upset events without the need for active cooling systems. In addition, the molten salt coolant is transparent and chemically inert, allowing for easier refueling and in-service inspection.[2] SmAHTR uses seismic isolation to reduce the seismic fragility of the design. Below-grade construction reduces the vulnerability to aircraft impacts. The design will use risk-informed approaches to determine the level of defense in depth needed in the design to accommodate for uncertainties.[3]

These inherent safety design features combined with a small source term should lead to a reduced emergency preparedness zone, which would allow the reactor to be sited near other facilities that may need process heat, electricity, or both. Interfaces between the reactor and other facilities that may share the site will need to be accounted for in the safety analysis. Being a unique, first-of-a-kind system, sufficient data to support the safety case for SmAHTR will be necessary and will be obtained through a test program supported by detailed safety analysis. Many of the issues related to the use of a high-temperature molten salt coolant can be address through non-nuclear separate effects test programs in which component and thermal hydraulic tests with molten salt and/or simulant fluids are conducted. The data necessary to support the fuel qualification program can make use of data obtained by the NGNP program.

The passive decay-heat removal systems will need to be thoroughly analyzed, tested, and monitored or inspected to ensure they will meet the performance goals over the lifetime of the plant. Materials will be selected for compatibility with the high-temperature molten salt operation and for resistance to radiation damage.[4] Because the molten salt coolant has a relatively high melting point, special attention will be given to overcooling events which may cause coolant solidification to occur in some portions of the primary or intermediate coolant systems. A set of nuclear critical experiments will probably be necessary to quantify the reactivity feedback mechanisms. Because SmAHTR is a first-of-a-kind small reactor with limited source terms, it could be licensed as a prototype reactor,[5] allowing confirmatory data to be collected during operation of the first reactor.

As part of the conceptual design, a set of safety design criteria unique to SmAHTR will be developed that will be used in lieu of the “General Design Criteria” contained in 10 CFR 50 Appendix A to guide the design of the reactor. A probabilistic risk assessment (PRA) will be developed to determine the licensing bases events and classify the systems, structures, and components (SSC) as to their safety significance.[6] A phenomena identification and ranking table (PIRT) will be developed to assist in the event identification and SSC classification.

6.2 TRANSIENT BEHAVIOR

6.2.1 Introduction

The SmAHTR accident envelope can be defined by five types of transient conditions: transient over-power, loss of flow, loss of coolant inventory, overcooling, and loss of heat sink. These accidents are similar to those defined for a liquid-metal reactor (LMR) because the SmAHTR and the LMR have similar characteristics, mainly a coolant with high boiling point along with good heat transfer characteristics and low-pressure operating conditions. Given the similarities between a SmAHTR and LMR, it is likely that the design basis events will be defined by these five transients with scram. The Anticipated Transients without Scram (ATWS) will be considered beyond design basis events as agreed to by the regulators during the review of the Clinch River Breeder Reactor and the PRISM and Sodium Advanced Fast Reactor (SAFR) reactors.[7] In addition to the reactor transient accidents mentioned above, other accidents such as those that might occur during refueling and those generated from external events (seismic, fire, flood, and high winds) will be addressed as part of the design basis envelope. Time and resource constraints associated with this study have not permitted analyses of the five transient classes noted above; however, a preliminary analysis of the loss-of-flow transient has been completed and is discussed below.

6.2.2 Loss of Forced Flow with Scram

A loss of forced flow with scram was analyzed to determine whether the DRACS system as designed could remove the decay heat during a loss-of-flow event. This transient was performed based on the following assumptions.

(a) The reactor is initially at full-power operation (125 MWt) with the three pumps operating at full flow (350 kg/s/pump for cylindrical pin fuel).
(b) The transient is initiated at 500 s, when the power to the three pumps is lost, the pumps' coast downtime is 30 s, and the pumps' flow is reduced linearly to zero flow in 30 s.
(c) The reactor control system scrams the reactor; the reactor power is reduced to decay-heat levels in 4 s.
(d) Stringer (cylindrical pin) fuel was used in the core in this calculation.
(e) Only two of the three DRACS are operational, following the safety philosophy.
(f) The diodicity of the vortex valve is 400.

Calculations performed with the RELAP5-3D[8] code are presented in the following figures. Figure 6.1 shows the coolant flow through the core, which is reduced from the initial value of 1,018 kg/s (steady-state forced convection with the three pumps on) to a natural convection core flow of 24 kg/s. The natural convection flow consists of the flows through each of the two operational DRACS at 9 kg/s each plus the flow through the nonoperational DRACS at 6 kg/s. Figure 6.2 shows the flow through the core and through the DRACS after the transient is initiated.

Figure 6.3 shows the primary coolant flow through each of the DRACS during the complete transient. Before the transient is started, the flow through each DRACS is negative with a value of −10.5 kg/s. After the transient is initiated and natural convection is established, each operational DRACS has a flow of 9 kg/s while the nonoperational DRACS has a flow of 6 kg/s.

Figure 6.4 shows the natural convection flows calculated inside the DRACS loop and inside the air cooler (tower). The flow in the DRACS loop is 7 kg/s of FLiNaK, and in the air cooler it is 2.4 kg/s of nitrogen. (RELAP5 does not have the capability of using air as a fluid; however, it does have the capability of using nitrogen. Nitrogen was therefore used instead of air in these calculations.)

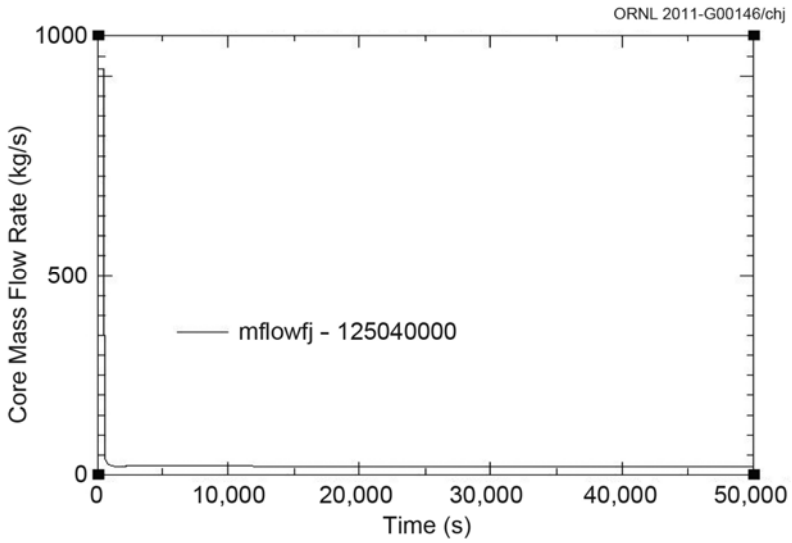

Fig. 6.1. Coolant flow through the core—transient initiated at 500 s.

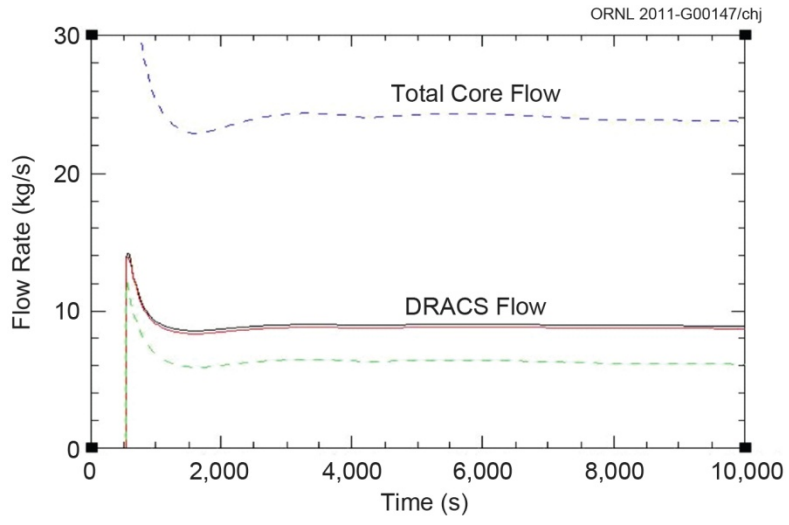

Fig. 6.2. DRACS flows and total flow through the core during natural convection conditions.

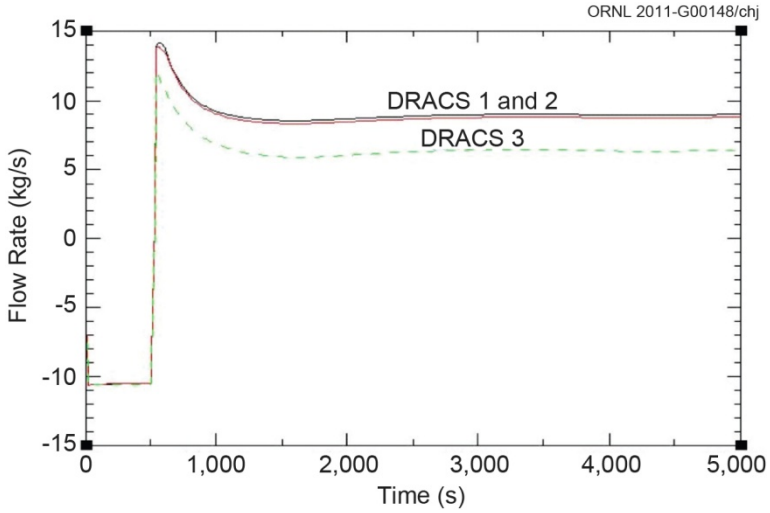

Fig. 6.3. Flows through each DRACS during forced convection (first 500 s) and during natural convection conditions.

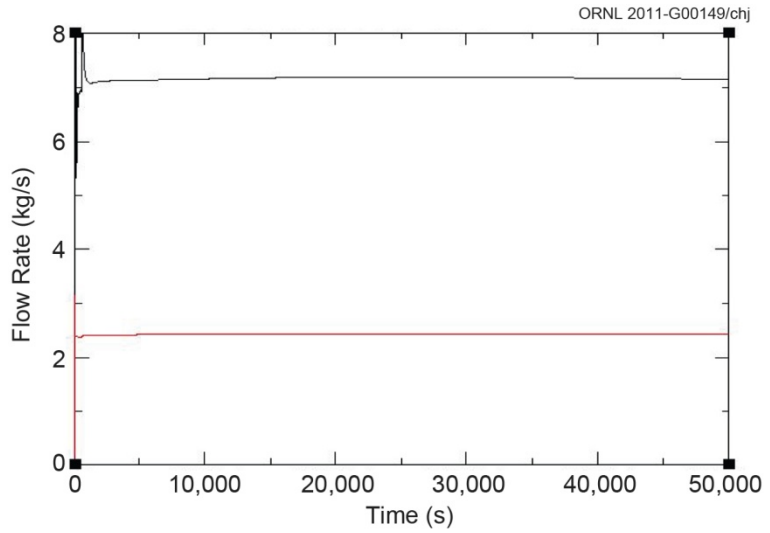

Fig. 6.4. Flows through the DRACS loop and through the air cooler.

Figure 6.5 shows the fuel centerline temperature for the hottest fuel assembly (center core) during the transient. The temperature before the transient was 1,178°C; it decreased to values between 715°C and 730°C after the transient was initiated.

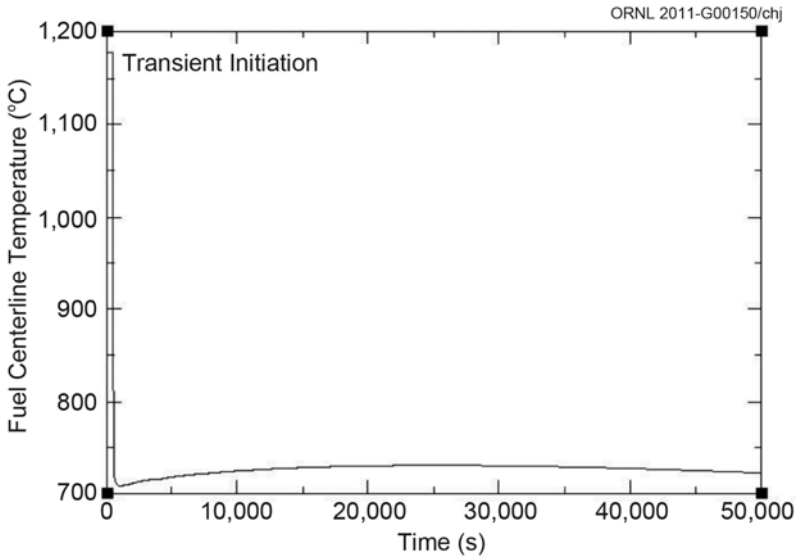

Fig. 6.5. Fuel centerline temperature during the complete transient.

Figure 6.6 shows the steady-state temperatures in the fuel (for the center assembly) at full power before the transient as calculated by RELAP5. The maximum centerline temperature is 1,178°C. A cosine shape is shown for the temperature, which reflects the axial cosine power distribution in the core.

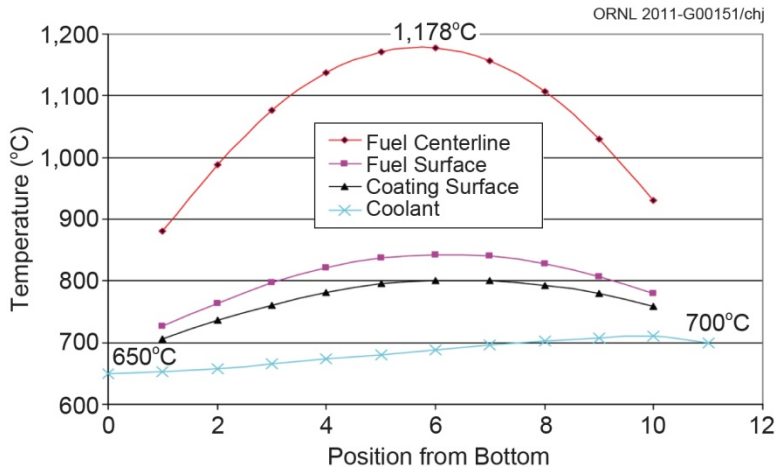

Fig. 6.6. Fuel and fuel surface coating temperatures calculated for the center.

Calculated coolant temperatures during the 50,000 s transient are shown in Fig. 6.7. The first 500 s are at full power—125 MWt—with decay heat values starting at 500 s. Coolant temperatures at full power are 650°C (inlet) and 700°C (outlet). During the first 26,000 s (7 hr) of the transient, the coolant temperature increases, decreasing afterwards when the DRACS removal capacity is larger than the core decay heat. Maximum calculated coolant temperature is 727°C, which is 27°C above the normal operation value. The cold inlet temperature increases up to 712°C; the value before the transient was 650°C. Fuel temperatures are always low (<750°C) during the transient. Only two out

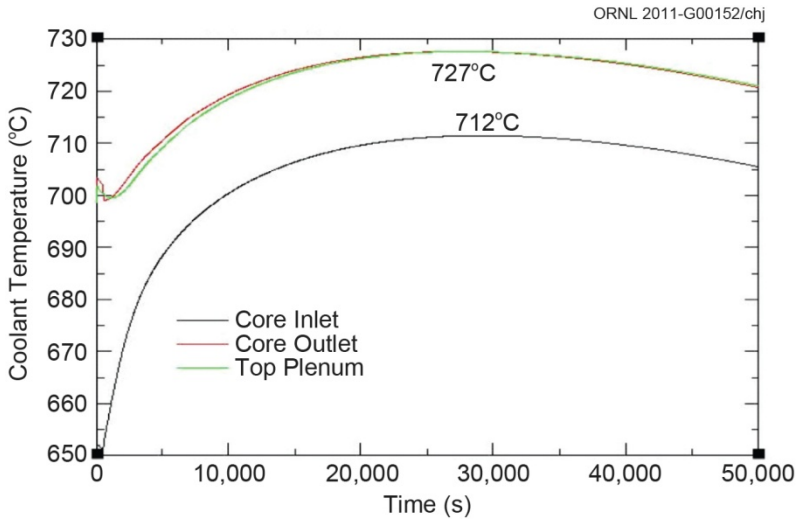

Fig. 6.7. Coolant temperatures calculated during DRACS natural convection conditions with only two DRACS operating.

of the three DRACS were operational in this decay-heat transient simulation, in accordance with the safety philosophy. If all three DRACS were operational, coolant temperature increases would be reduced. The calculated temperatures of both the fuel and the coolant were satisfactory during the complete transient, demonstrating the satisfactory operation of the DRACS loops.

6.3 SEISMIC SAFETY DESIGN CONSIDERATIONS

Seismic isolation will be used to reduce the seismic vulnerability of the plant. Seismic isolation systems have not been used in current GEN III+ designs but are expected to be reviewed by the regulator as part of the licensing process for some integral pressurized water reactors (iPWRs) and LMRs. Testing, analysis, and inspection requirements that arise as a result of these regulatory reviews will be directly applicable to SmAHTR, and the results of these reviews will be incorporated into the SmAHTR design as appropriate.

The below-grade design of SmAHTR, compared to current GEN III+ reactors, will require changes in the approach taken for seismic design of the reactor. The fact that several SMRs are expected to be located below grade will allow SmAHTR to take advantage of lessons learned during the regulatory review of these designs.

In addition to the below-grade seismic design and isolation issues, the effect of groundwater and hydrodynamic pressures associated with varying water tables will need to be considered in the design of below-grade reactors such as SmAHTR. As in the case of seismic design, lessons learned associated with the effects of water table variations and hydrodynamic pressure during licensing reviews of below-grade iPWRs and LMRs will be directly applicable to SmAHTR.

6.4 REFERENCES

1. Nuclear Energy Institute, *Small Reactors Provide Clean, Safe Power and Industrial Process Heat*, fact sheet, NEI (January 2010).

2. D. F. Williams, L. M. Toth, and K. T. Clarno, *Assessment of Candidate Molten Salt Coolants for the Advanced High-Temperature Reactor,* ORNL/TM-2006/12 (March 2006).

3. U.S. Nuclear Regulatory Commission, *Potential Policy, Licensing, and Key Technical Issues for Small Modular Nuclear Reactor Designs,* SECY 10-0034, Washington, D.C. (March 2010).

4. D. F. Wilson and W. R. Corwin, “Materials for a Small Salt-Cooled Modular, Advanced High Temperature Reactor (SmAHTR),” *ANS Transactions* (November 2010).

5. Code of Federal Regulations 10 CFR-50.43(e)(2).

6. U.S. Nuclear Regulatory Commission, *Feasibility Study for a Risk-Informed and Performance-Based Regulatory Structure for Future Plant Licensing* (2 vols.), NUREG-1860, Washington, D.C. (December 2007).

7. D. E. Carlson, *Preapplication Safety Evaluation Report for the Power Reactor Innovative Small Module (PRISM) Liquid-Metal Reactor,* NUREG 1368, Washington, D.C., U.S. Nuclear Regulatory Commission (February 1994).

8. Idaho National Laboratory, *RELAP5-3D Code Manual,* Rev. 2.4, INEEL-EXT-98-00834, Idaho (2006).

7. SmAHTR LIQUID-SALT THERMAL ENERGY STORAGE SYSTEM: THE "SALT VAULT"

7.1 INTRODUCTION

As noted previously, the SmAHTR concept has been developed with three potential operating modes and applications in mind: (1) process heat production, (2) electricity production, and (3) a combined cogeneration mode in which both electricity and process heat are produced. Chapter 4 of this report described the SmAHTR nuclear island structures and systems. This section introduces an innovative high-temperature thermal energy storage system intended to significantly extend the utility and range of potential process heat applications for multi-reactor SmAHTR installations.

The capability to cluster multiple reactors to meet energy demands greater than what could be met by a single reactor unit is an important design consideration for SMRs. This is certainly the case for any reactor concept designed for both electricity production and process heat applications. However, numerous questions and issues arise whenever multiple reactor units are interconnected. Only integration methods that do not compromise system safety or reliability can be considered. The interconnection or "ganging" of multiple reactor units to drive shared electrical power conversion systems has been widely discussed by reactor vendors and advanced concept developers for many years. However, the correct approach for clustering multiple small reactor units to meet intermediate-to-large process heat loads has received much less attention. This section discusses a novel method for clustering multiple SmAHTR reactor units to meet thermal energy loads greater than 125 MWt. The method not only provides the ability to meet larger thermal energy loads but, as will be discussed, offers the potential to enhance the robustness of the overall SmAHTR energy system by buffering interruptions in the thermal energy load from the reactors and/or buffering interruptions in one or more reactor operations from each other and from the thermal energy load.

The use of liquid salts as a thermal energy storage medium is not a new concept. Significant work has been done to explore the utility of liquid salts—particularly as energy storage media in solar thermal energy systems.[1,2] Indeed, the (3×50 MWe) Andasol solar thermal power plant in Spain, which began commercial operation in 2008, uses a two-tank (hot tank–cold tank) liquid-salt thermal energy storage system coupled to a steam–water Rankine power conversion system. The thermal storage salt medium (a 60% $NaNO_3$–50% KNO_3 mixture) used at Andasol is the same as that successfully demonstrated in the DOE Solar-I and Solar-II pilot plants in Barstow, California. The Andasol plant[3] stores thermal energy at 390°C in a 14 m high, 36 m diameter hot tank. The salt is pumped thorough a salt-to-water heat exchanger where it transfers its energy to a water loop, which then drives a traditional Rankine power conversion cycle to deliver 7.5 hr of electricity production from the fully charged hot tank. The salt is collected in the cold tank where it is reheated by the solar thermal system. These terrestrial systems typically use relatively low-temperature salts of various compositions and operate at temperatures up to 400°C—too low for optimal SmAHTR applications.

Higher temperature salts (including fluoride salts) have been explored for a number of years by the National Aeronautics and Space Administration as a medium for storing thermal energy for in-space solar dynamic power applications.[4,5]

7.2 THE SALT VAULT CONCEPT

Figure 7.1 is a simplified depiction of the SmAHTR "salt vault" thermal energy storage system with four SmAHTR units. (The salt vault heat exchanger configuration depicted in Fig. 7.1 is notional in nature. Considerable work remains to optimize the design of the salt vault system.) The cluster of SmAHTR units dumps its thermal energy into the salt vault, which in turn serves as a thermal energy reservoir for the process heat or power production customer. The simplistic salt vault concept

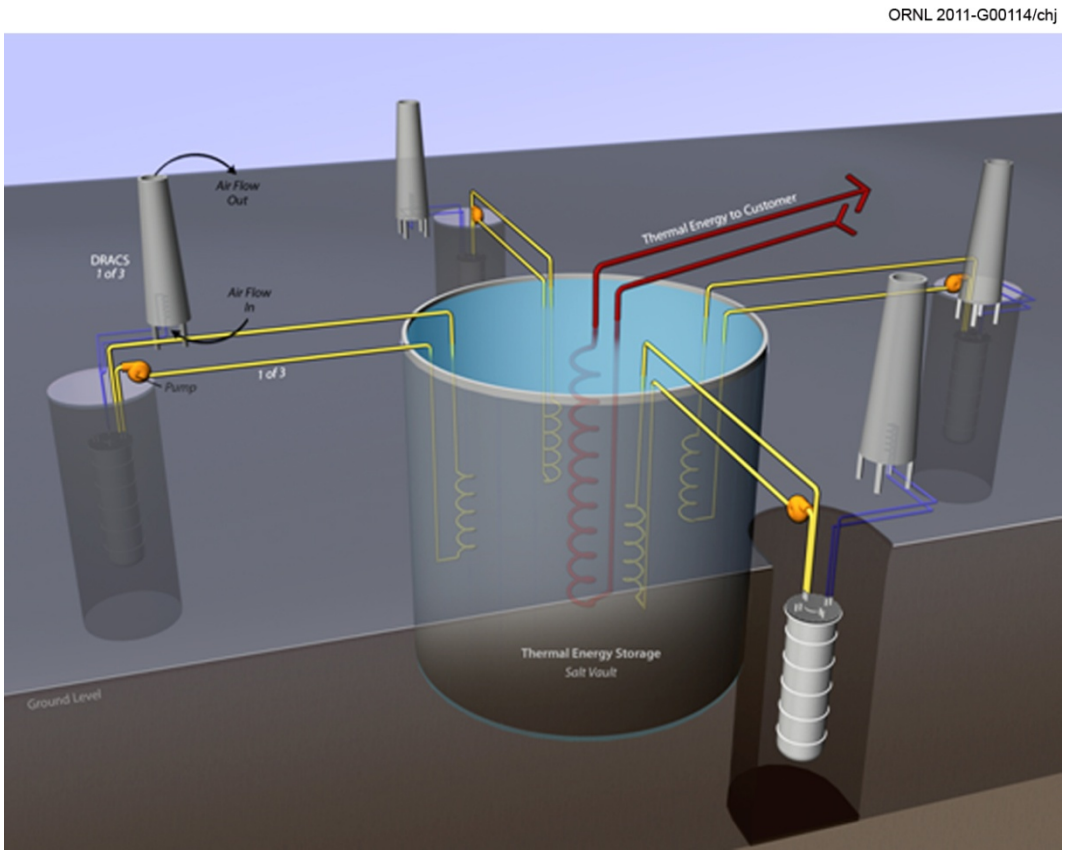

Fig. 7.1. SmAHTR salt vault thermal energy storage system.

depicted in Fig. 7.1 uses four charging heat exchangers (one from each SmAHTR unit) and one demand-side heat exchanger to convey the process heat to the customer (or potentially to a power conversion system).

7.3 EXTRACTING ENERGY FROM THE SmAHTR THERMAL ENERGY STORAGE SALT VAULT

There are a variety of process heat applications for SmAHTR reactors and potential methods for extracting energy from the salt vault. While it would be desirable from a thermal efficiency standpoint to locate the SmAHTR modules and salt vault energy storage system as close as possible to the process heat load, in practice it might be necessary to "ferry" heat for distances of a few kilometers. Figure 7.2 is a more detailed version of Fig. 7.1 that depicts some of these energy extraction and transport options.

Some SmAHTR process heat applications may be able to directly use the salt in the salt vault as the heat transport fluid in a directly coupled process heat demand loop (Loop A in Fig. 7.2). Other process heat applications might require an additional degree of isolation from the reactor intermediate cooling loop. Such applications could be handled via a second indirectly coupled process heat demand loop (Loop B in Fig. 7.2) that uses a demand-side heat exchanger in the salt vault. From a thermal efficiency standpoint, the indirect approach introduces an undesirable temperature drop across the intermediate loop heat exchanger in the salt vault and therefore reduces the temperature at which energy is supplied to the process heat customer.

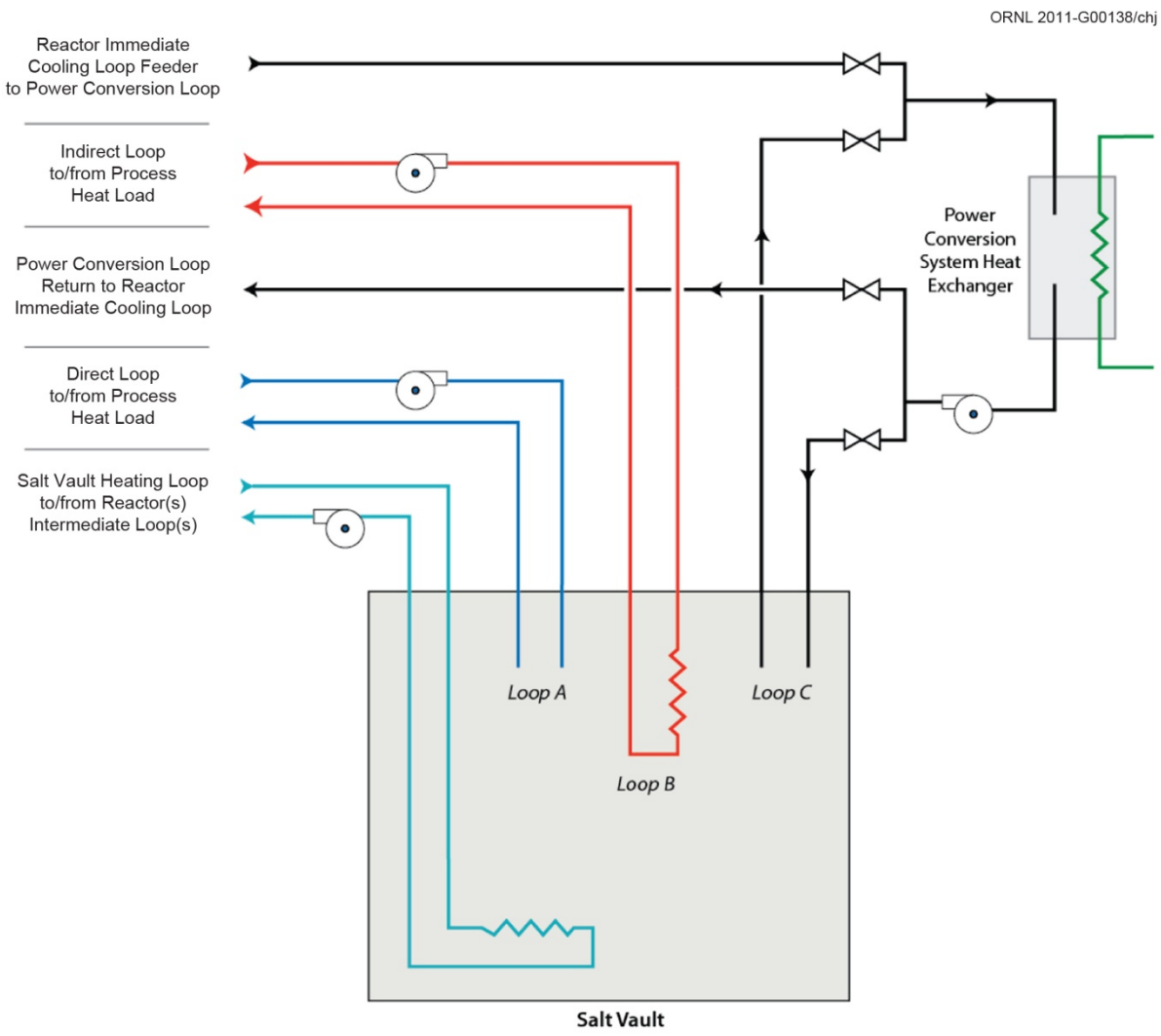

Fig. 7.2. SmAHTR salt vault thermal energy storage system with energy extraction subsystem details.

Finally, electrical power conversion subsystems may be interfaced either with the salt vault or directly with the reactor intermediate heat transport loops. As noted in the introduction to this section, the Solar-I and Solar-II demonstration projects and the more recent commercial experience of the Andasol solar thermal power station provide proof-of-concept for the industrial use of liquid-salt thermal storage and heat transport mediums—and the coupling of the thermal storage system with a power conversion system to produce electricity. Figure 7.2 depicts such a system, in which a dedicated energy extraction loop for electrical power production is added (Loop C). Salt from the salt vault is pumped via Loop C through a power conversion heat exchanger (where it transfers energy to the power conversion system working fluid) and then back either to the salt vault or, conceivably, directly to the intermediate heat transfer loop. Thus the power conversion system could be configured to draw its energy directly from one or more reactors or from the entire reactor cluster via the salt vault.

7.4 SmAHTR SALT VAULT THERMAL ENERGY STORAGE DESIGN CONSIDERATIONS AND FUNCTIONAL REQUIREMENTS

The SmAHTR salt vault concept provides, in principle, a number of desirable performance features:

- an elegantly simple way of combining the thermal output from multiple reactor units to meet larger heat loads,
- increased reliability on energy supply to the customer, and
- a softer system response to transients—both on the customer demand side and on the reactor supply side.

These benefits are gained at the cost of the additional system complexity required to couple the SmAHTR reactor modules and the customer demand to the salt vault. A number of questions are evident, including the following.

- Should the three intermediate heat transport loops from each reactor be ganged together at the reactor into a single-feed return line to and from the salt vault? This would necessitate only one supply-side heat exchanger in the salt vault per reactor but would eliminate the redundancy of three intermediate heat transport loops outside of the reactor.
- Should the intermediate loop circulating pumps be placed in the supply (hot) leg of the intermediate heat transport loop (and thus draw suction on the PHXs), or should they be placed in the return (cold) leg of the intermediate heat transport loop (and feed the PHXs)?
- Should the salt vault heat exchanger feed and return lines all enter the salt vault from the top, and if so, how does this influence the optimal design of the heat exchangers?
  - What is the optimal shape for the salt vault?
  - What is the optimal placement strategy for the heat exchangers within the salt vault?
  - What is the optimal approach for insulating the salt vault from its surroundings?

The trade studies necessary to address these issues and to develop an integrated set of criteria and guidelines for sizing the vault itself have not been performed at this point.

Several functional requirements and design constraints will impact the actual design of a specific salt vault system. Table 7.1 summarizes some of the more significant salt vault design considerations. Table 7.2 summarizes some very preliminary salt vault sizing analyses for salt vaults sized to provide 10,100 and 1,000 MWt-hr of energy while operating over a temperature range from 500°C to 600°C. (A salt vault sized to store 125 MWt-hr of energy could absorb or deliver 1 reactor-hr of the thermal output of a single SmAHTR unit.) All calculations assume no heat losses from the salt vault to its surroundings. While a broad range of candidate fluoride salts is available, the two salts selected for this analysis constitute a representative sample. The first conclusion that can be drawn from the analysis is that the physical size of the salt vaults is not large. A cubic salt vault measuring 10–11 m per side would be sufficient to store 100 MWt-hours of energy, and a cubic salt vault measuring 21–24 m per side would be large enough to store 1,000 MWt-hours of energy. A second conclusion from Table 7.2 is that the cost of the salt itself may not be prohibitive compared to the overall cost of the nuclear plant—on the order of $2 million to $23 million for a 100 MWt-hours vault and possibly as low as a few tens of millions of dollars for the 1,000 MWt-hours vault.

Tables 7.3 and 7.4 summarize the results of a simple analysis of the energy and time required to raise a salt vault sized to store 125 MW (1 reactor-hr) of SmAHTR thermal energy from a starting temperature of 20°C to the fluoride salt melting temperature, completely melt the salt, and raise the temperature of the entire salt vault from the melting temperature to the assumed 600°C salt vault operating temperature. Table 7.3 presents the results in terms of energy required. Table 7.4 presents the results in terms of reactor-hours required assuming the entire thermal output of a single 125 MWt

Table 7.1. SmAHTR salt vault thermal energy storage system design considerations

Salt vault design parameter	Comment
Thermal energy storage capacity (MW)	A function of process heat load (MW or Btu). A function of process heat load customer tolerance to energy supply interruptions (e.g., how long the process heat load facility requires for orderly shutdown in event of reactor trip). Directly impacts time required to heat salt vault to operational temperatures from cold start. Directly impacts time for salt vault to begin solidifying following reactor trip.
Salt vault salt selection	Melting point of the salt vault salt should be lower than that of the SmAHTR primary coolant if possible for operational flexibility. Boiling point of salt vault salt should be significantly higher than that of the reactor operating temperature. A major driver in the capital cost of the salt vault storage system—candidate fluoride salts vary greatly in cost. Low vapor pressure, high heat capacity, high thermal conductivity, and low corrosive activity salts are desirable.
Salt vault operating temperature range (T_{hot}–T_{cold})	A function of process heat customer user requirements. Larger allowable temperature swing reduces volume of salt required, physical size, and cost of the salt vault.
Salt vault shape and insulation	Long-term maintenance of the salt vault at elevated temperatures will necessitate a compact, thermally efficient design. A well-insulated, spherically shaped vault would be the most efficient shape from the thermal management standpoint but may not be possible due to the heat exchanger mechanical interface considerations.
Internal salt vault configuration and salt vault heat exchanger design and placement	Impacts operational characteristics of the salt vault, melt/freeze behavior, interfaces with multiple SmAHTR units, etc. The placement of the heat exchangers relative to each other and to the walls of the salt vault will be a critical optimization parameter.

Table 7.2. SmAHTR salt vault sizing analysis

Salt	Molar comp	Melting point (°C)	Salt heat capacity (MW-h/ M**3-°C)	Salt heat of fusion (MW-h/ M**3-°C)	Unit[a] salt price ($/L)	10 MWt-hr vault		100 MWt-hr vault		1,000 MWt-hr vault	
						Salt vault storage cube size (m per side)	Salt vault salt price ($)	Salt vault storage cube size (m per side)	Salt vault salt price ($)	Salt vault storage cube size (m per side)	Salt vault salt price ($)
LiF-NaF-KF	46.5-11.5-42	454	0.001057622	0.235	24.1	4.6	$2 million	9.8	$23 million	21.1	~$228 million
NaF-$NaBF_4$	8-92	385	0.0007322	0.089	1.5	5.1	$210,000	11.1	$2 million	23.9	~$21 million

[a]Estimated salt costs based on D. F. Williams, *Assessment of Candidate Molten Salt Coolants for the NGNP/NHI Heat-Transfer Loop*, ORNL/TM-2006-69 (June 2006).

Table 7.3. SmAHTR 125 MW salt vault dynamic heating/cooling analysis—energy requirements

Salt	Energy required to begin melting (MWt-hr)	Energy required to melt salt vault (MWt-hr)	Energy required to raise salt vault from melting to operating temperature (MWt-hr)	Total energy required to raise salt vault from ambient to operating temperature (MWt-hr)
LiF-NaF-KF	542.5	277.7	182.5	1,002.7
NaF-$NaBF_4$	456.3	151.9	268.8	876.9

Table 7.4. SmAHTR 125 MW salt vault dynamic heating/cooling analysis—time required based on a single 125 MWt SmAHTR

Salt	Time required to begin melting salt vault (hr)	Time required to completely melt salt vault (hr)	Time required to raise salt vault from melting to 600°C (hr)	Total time required to raise salt vault from ambient to 600°C (hr)
LiF-NaF-KF	4.3	2.2	1.5	8.0
NaF-$NaBF_4$	3.7	1.2	2.2	7.0

SmAHTR module was used to charge the salt vault. The conclusion from analysis of Table 7.4 is that the time for the salt vault to reach operational temperatures is reasonable (~7–8 hr or one shift), given that one would not expect the SmAHTR unit and the salt vault to undergo such start-up transients on a frequent basis.

7.5 REFERENCES

1. Pilkington Solar International GmbH, *Survey of Thermal Storage for Parabolic Trough Power Plants*, NREL/SR-550-27925, National Renewable Energy Laboratory (September 2000).
2. B. Kelly, H. Price, and D. Kearney, *Thermal Storage Commercial Plant Design Study for a 2-Tank Indirect Molten Salt System*, NREL/SR-550-40166, Golden, Colorado, National Renewable Energy Laboratory (July 2006).
3. Solar Millennium AG, *The Parabolic Trough Power Plants Andasol 1 to 3*, Erlangen, Germany, Solar Millennium (2008).
4. A. K. Misra and J. Whittenberger, *Fluoride Salts and Container Materials for Thermal Energy Storage Applications in the Temperature Range 973 to 1400 K*, NASA Technical Memorandum 89913 (AIAA-87-9226), National Aeronautics and Space Administration (August 1987).
5. D. E. Lacy, C. Coles-Hamilton, and A. Juhasz, *Selection of High Temperature Thermal Energy Storage Materials for Advanced Solar Dynamic Space Power System*, NASA Technical Memorandum 89886, National Aeronautics and Space Administration (August 1987).

8. SmAHTR ELECTRICAL POWER CONVERSION OPTIONS

8.1 INTRODUCTION

As a high-temperature system, SmAHTR is potentially compatible with several highly efficient (>40% thermal efficiency) power conversion technologies. The most attractive options for power conversion systems are Rankine and Brayton cycle technologies. One particularly appealing option is for the system to be coupled to a high-efficiency closed-cycle supercritical carbon dioxide ($S\text{-}CO_2$) power conversion system. $S\text{-}CO_2$ power conversion is an emerging technology that can potentially provide a combination of small system components and high operating efficiency even at modest operating temperatures.

Multi-reheat helium Brayton systems are also viable options, though they are less compact than the supercritical Brayton systems. Peterson and Forsberg[1] examined closed-cycle helium, open-air cycles, and $S\text{-}CO_2$ cycles for salt-cooled reactors at temperature ranges similar to those of the SmAHTR concept. Helium Brayton systems with the same conversion efficiency as $S\text{-}CO_2$ systems in the temperature range of interest (~700°C) are generally more complex and have larger components than $S\text{-}CO_2$ systems. The $S\text{-}CO_2$ systems can provide good efficiency at lower temperatures and have smaller and fewer components. Helium Brayton power conversion systems should provide better efficiency at higher temperatures, but to date, success with the large helium systems has been limited. Thus far based on preliminary screening, $S\text{-}CO_2$ systems appear to be the superior approach for a SmAHTR concept operating at ~700°C, while a multi-reheat helium Brayton system or even an open-air Brayton system would be the system of choice as the concept evolves to higher operating temperatures.

There are numerous ways to configure a $S\text{-}CO_2$ system. For this study, the recompression cycle was chosen for investigation because recent research suggests small-scale systems are relatively easy to control. However, significant development effort is required to develop the system to sizes applicable to SmAHTR. Heat exchangers represent the most significant technology development need if these systems are to be practical. Ongoing research[2] is being conducted to improve the performance (reduce the volume) of the printed circuit-board heat exchanger technology that will hopefully make it reliable and economical in the future. Small heat exchangers coupled with the small SmAHTR reactor and $S\text{-}CO_2$ turbo-machinery have the potential to make the SmAHTR a factory-built transportable system.

The use of $S\text{-}CO_2$ Brayton or Rankine cycles in binary geothermal power conversion cycles has the potential to generate electricity with relatively high efficiency using smaller turbo-machinery and is currently under investigation within DOE.[3] The key feature that allows higher efficiency conversion in a supercritical Brayton cycle is the rapid change in physical properties as a function of pressure near the critical point. For Rankine systems, it is waste heat rejection at constant and lower temperature coupled with reduced pumping power requirements in the liquid phase. Carbon dioxide is an excellent candidate for supercritical operation because it is stable and not very reactive at the temperatures of interest. Also, CO_2 has a low critical temperature (304 K). However, the drawback to using CO_2 as a supercritical fluid is its high critical pressure (7.4 MPa).

Gas Brayton power conversion has been proposed for a number of high-temperature reactor concepts, typically using helium as the working fluid. Helium is a low atomic mass gas, which requires that the turbo-machinery equipment be large and therefore expensive. It is also difficult to limit leakage, both within the system and out of the system. Helium is relatively expensive, but as an inert gas, it is promising for high-temperature applications. The efficiency of helium Brayton systems can exceed 50% at temperatures near 800°C.

Because of near-term material limitations, evolutionary reactor concepts like SmAHTR may enter the market at operating temperatures of ~700°C, below the longer term goals of 800–1,200°C. Figure 8.1 shows the predicted cycle efficiencies for various power conversion technologies as a

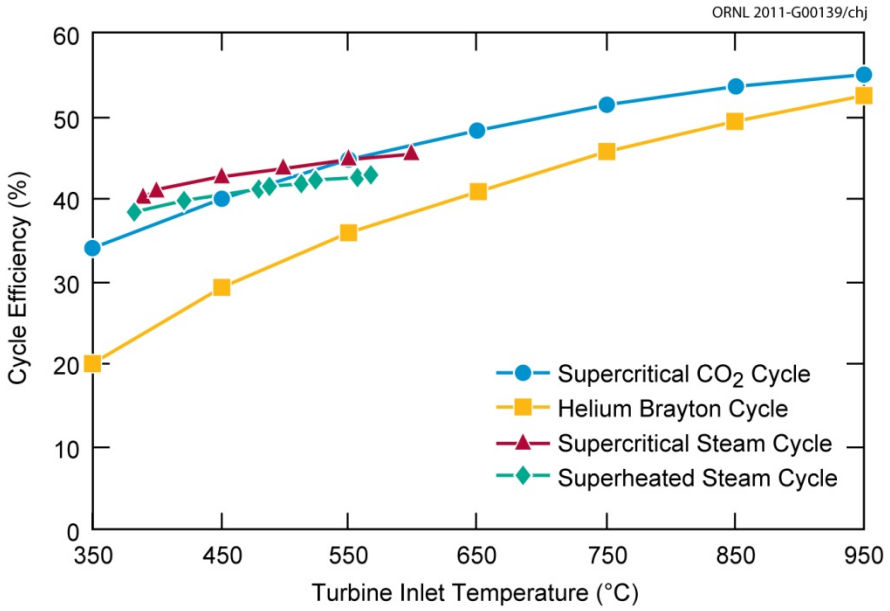

Fig. 8.1. Comparison of the S-CO_2 cycle with steam Rankine and helium Brayton cycles. Data obtained from W. S. Jeong et al., Potential Improvements of Supercritical CO_2, Korea Advanced Institute of Science and Technology.

function of turbine inlet temperature.[4] Below 500°C, steam systems and S-CO_2 systems are competitive. Steam systems however have limited evolutionary potential. S-CO_2 systems have the potential of achieving cycle efficiencies above 40% for temperatures greater than 450°C, while helium-based systems typically require an additional 200°C temperature increase to achieve the same cycle efficiency as a S-CO_2 system. It seems likely that helium systems can indeed evolve to higher temperatures than S-CO_2 systems due to the potential of CO_2 to dissociate; however, the S-CO_2 power conversion system appears to be the appropriate technology to consider for SmAHTR in an intermediate temperature variant.

8.2 SUPERCRITICAL CO_2 POWER CONVERSION SYSTEMS

The possibilities for combining SmAHTR reactors to S-CO_2 power conversion systems extend from multiple reactors feeding a single power conversion loop down to three 17 MWe power conversion loops coupled to the three independent loops of a single SmAHTR reactor. S-CO_2 power conversion is being tested today at power levels approaching 1 MW, and plans to build and test units in the range of 10 MWe are currently being considered, so this technology is already becoming relevant to the smaller power levels possible for SmAHTR. Conceptual designs have been developed for power levels as high as 300 MWe, and some current conceptual design studies are looking beyond 1,000 MWe.

In the SmAHTR-S-CO_2 concept, a salt-to-S-CO_2 heat exchanger transfers heat to the CO_2 working fluid. The supercritical pressure of the CO_2 in the heat exchanger is greater than 20 MPa. This high pressure along with the highest temperatures within the power conversion loop result in perhaps the major design challenge for the development of S-CO_2 power conversion system for use with reactors. Numerous arrangements of Brayton power systems are possible, and the options are similar to those of a traditional steam cycle including the number of turbines, shafts, and reheaters. For the S-CO_2 systems, current interest has focused on the recompression cycle, shown schematically in Fig. 8.2, as an attractive option in terms of a limited number of components and relatively high conversion. The S-CO_2 recompression Brayton system for SmAHTR incorporates a salt-to-gas heat exchanger, high-temperature and low-temperature recuperators, a waste heat rejection heat exchanger,

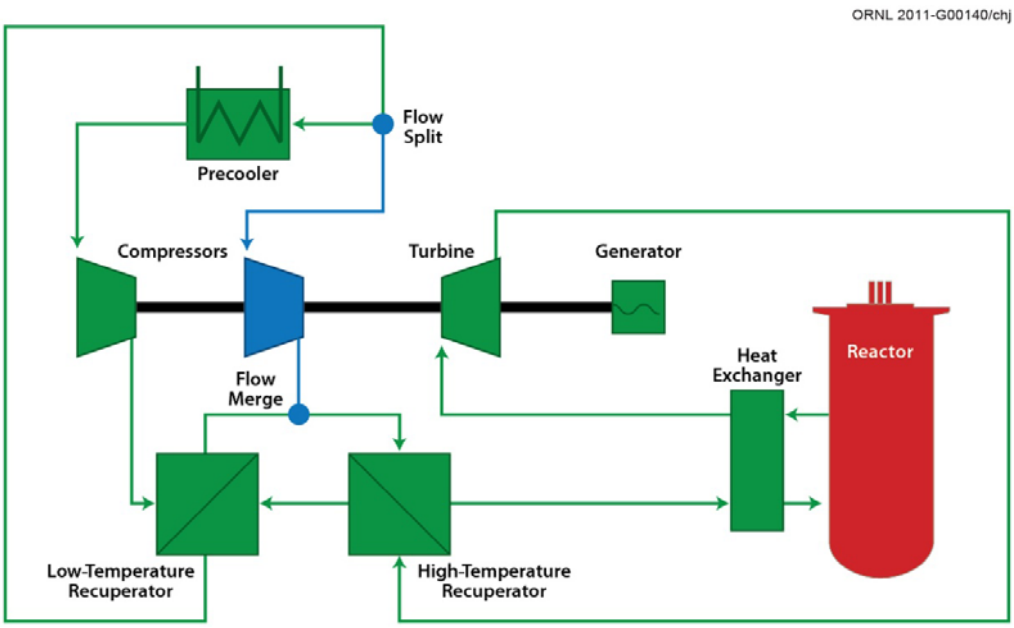

Fig. 8.2. Supercritical recompression Brayton cycle. Data obtained from W. S. Jeong et al., Potential Improvements of Supercritical CO_2, Korea Advanced Institute of Science and Technology.

and a single turbine and two compressors on a common shaft. This limited number of components can produce a cycle efficiency in excess of 40% at temperatures above 450°C and offers controllability through a single split flow valve. Depending on the size of the system, a gearbox may be required to couple the shaft to a 3,600 rpm generator.

In the recompression concept, the high-temperature recuperator transfers as much as three times the power input through the salt-to-CO_2 heat exchanger, so while the peak temperatures in the high-temperature recuperator are lower than those of the salt-to-CO_2 heat exchanger, it still has high pressure differential requirements and it transfers more power. The low-temperature recuperator transfers approximately one-third of the power of the high-temperature recuperator; however, due to the lower temperature potential available for a low-temperature recuperator, the recuperators are approximately the same size. The power conversion turbo-machinery and the system heat exchangers are the major power conversion system components, with the heat exchangers being larger in terms of both size and cost. The ability to develop affordable, compact heat exchanger technology to work with this power conversion system is an important development issue that is currently the focus of a significant amount of research.

The Printed Circuit Heat Exchanger© was developed by Heatric of Dorset, England, which is a division of the Meggitt Corporation. The concept uses chemically etched flow channels on a series of stacked plates. The plates are diffusion bonded, which currently limits the size of components. Over 400 units are reportedly operating worldwide for a broad of range of application up to 50 MPa and 800°C. Some units have reportedly been in service more than 12 years. Plate fin heat exchangers have been widely used as recuperators in the field of power generation. Ingersoll Rand Energy Systems in Portsmouth, New Hampshire, has developed plate fin heat exchanger technology in which the folded fins are brazed to the stamped plates to form unit cells. The unit cells can be stacked to form an entirely welded pressure boundary. The configuration is specifically designed to accommodate substantial thermal strain and therefore to tolerate the severe temperature gradients encountered during transient operations, which is important for any reactor concept.

Figure 8.3 shows a 20 MWe S-CO_2 power conversion system layout using compact heat exchanger technology[5] that could serve one of the three loops of the SmAHTR concept. Figure 8.4 shows a 50 MWe version based on the same technology that could serve all three loops of a single

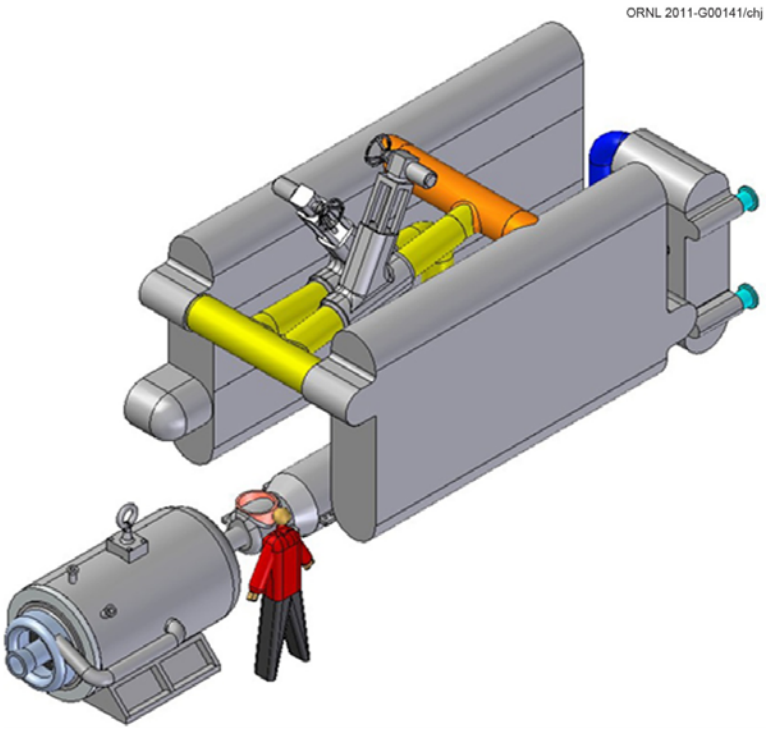

Fig. 8.3. A 20 MWe supercritical CO_2 power conversion system layout. *Source*: J. P. Gibbs et al., *Applicability of Supercritical CO_2 Power Conversion Systems to GEN IV Reactors*, Topical Report No. MIT-GFR-037, reprinted with permission.

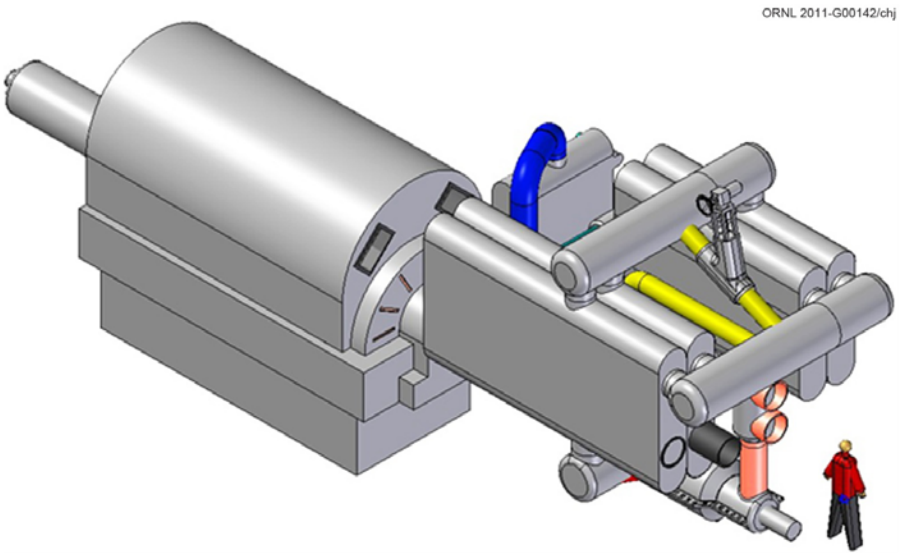

Fig. 8.4. A 50 MWe supercritical CO_2 power conversion system layout. *Source*: J. P. Gibbs et al., *Applicability of Supercritical CO_2 Power Conversion Systems to GEN IV Reactors*, Topical Report No. MIT-GFR-037, reprinted with permission.

SmAHTR reactor. In the single power conversion system approach, the three in-vessel salt-to-salt heat exchangers would transfer the heat from the primary salt coolant to a single intermediate salt.

Other pure fluids that are considered plausible for lower temperature supercritical power systems include methane, neon, ethane, propane, butane, pentane, hexane and sulfur hexafluoride (SF_6). These fluids all have physical characteristics that make them attractive working fluids; however, there are also concerns regarding system pressures, corrosiveness, flammability, health effects, and costs. Four candidate fluids, CO_2, SF_6, xenon, and propane, were evaluated as potential working fluids in low-temperature supercritical Brayton cycles. The values of the critical temperatures and pressures for these fluids are listed in Table 8.1.

Table 8.1. Critical temperatures and pressures of candidate fluids for low-temperature supercritical Brayton power conversion systems

	Critical temperature (K)	Critical pressure (KPa)
CO_2	304	7,377
SF_6	319	3,755
Xenon	290	5,842
Propane	370	4,247

The supercritical temperature and pressure of these fluids can be altered by mixing them.[6] Table 8.2 shows the estimated critical parameters of CO_2 mixed with 10% helium and with 10% hexane. Helium can lower the critical temperature, and hexane can raise it.

Table 8.2. Examples of how the critical temperature of fluids can be manipulated by mixing fluids

Critical values	CO_2 only	CO_2+He (10%)	CO_2 + 10% hexane
Critical temperature (K)	304	274	324
Critical pressure (kPa)	7,377	6,989	5,918

The ability to vary the critical temperature of supercritical working fluids can be very beneficial for power systems. Fluids can potentially be tuned to available sink and adjusted to accommodate seasonal or long-term changes in heat rejection conditions. Supercritical Rankine and Brayton cycles are being considered even for lower temperature applications such as LWRs and geothermal energy extraction because they potentially offer efficiency increases and component size reductions over competing steam and organic Rankine cycles (ORC). For the same turbine inlet temperatures, these advanced supercritical cycles offer the potential of more power with lower capital investment while rejecting less waste heat to the environment.

Eventually reactor power systems will advance to higher temperatures as new materials become available and our understanding of them improves. However, in the near term, reactor temperatures 200–300°C higher than today's LWRs are perhaps going to be considered advanced. S-CO_2 power conversion is an excellent matching technology to these intermediate reactor temperatures. It is however difficult to foresee a reactor concept being developed to work in conjunction with S-CO_2 power conversion until the technology matures. A demonstration of a S-CO_2 power system at a relevant power level, perhaps in the range of 10 MWe, coupled to a non-nuclear heat source is a plausible first step for demonstrating S-CO_2 power conversion systems. Once operating experience has been gained, the technology can be given serious consideration for operation with the next generation of advanced nuclear reactors. The experienced gained in lower risk and perhaps lower

temperature environments will be invaluable in moving the technology forward. It is recommended that nuclear and non-nuclear programs within DOE work together with industry to find the right opportunity to fund such an effort.

8.3 REFERENCES

1. C. W. Forsberg, P. F. Peterson, and R. A. Kochendarfer, "Design Options for the Advanced High-Temperature Reactor," paper 8026 in *Proceedings of ICAPP'08*, June 8–12, 2008, Anaheim, California.
2. K. Nikitin, Y. Katoa, and L. Ngoa, "Printed circuit heat exchanger thermal-hydraulic performance in supercritical CO_2 experimental loop," *International Journal of Refrigeration* **29**(5), 807–814 (August 2006).
3. S. A. Wright, R. F. Radel, M. E. Vernon, G. E. Rochau, and P, S. Pickard, *Operation and Analysis of a Supercritical CO_2 Brayton Cycle*, Sandia Report No. SAND2010-0171 (September 2010). Available at http://prod.sandia.gov/techlib/access-control.cgi/2010/100171.pdf
4. V. Dostal, M. J. Driscoll, and P. Hejzlar, *A Supercritical Carbon Dioxide Cycle for Next Generation Nuclear Reactors*, MIT-ANO-TR-100 (March 2004).
5. J. P. Gibbs, P. Hejzlar, and M. J. Driscoll, *Applicability of Supercritical CO_2 Power Conversion Systems to GEN IV Reactors*, Topical Report No: MIT-GFR-037.
6. W. S. Jeong et al., Potential Improvements of Supercritical CO_2 Brayton Cycle by Mixing of Other Gases with CO_2, Korea Advanced Institute of Science and Technology, Republic of Korea.

9. SmAHTR OPERATIONAL CONSIDERATIONS

9.1 INTRODUCTION

The SmAHTR preconceptual design has not matured to the point where the full spectrum of operational issues has been identified and resolved. The discussion that follows represents an initial effort to identify a workable methodology for performing the major tasks necessary for installing and operating a SmAHTR reactor. While no detailed planning has yet taken place for any of the individual tasks required and undoubtedly unanticipated challenges will arise, no major technological hurdles are apparent in any of the primary tasks evaluated.

9.2 TRANSPORT AND INSTALLATION

SmAHTR will be a small, modular nuclear power plant. The entire power plant is intended to be truck transportable, with no single component too large or heavy to fit on a flatbed truck. The largest power plant components will be the reactor vessel and the salt-to-gas SHX. The containment structure will be mostly below grade, and its design maximum loading requirements are dominated by impact or earthquake events since FHR-class reactors lack mechanisms to generate large pressures or significant projectiles. The resultant thinner (as compared to those required for LWRs) containment walls are well suited for “open-top-type” installation and steel-plate sandwich wall construction.

The SmAHTR reactor vessel will be transported to the site unfueled and unfilled. The reactor vessel has no penetrations and is thus essentially a large open pot. The vessel wall thickness is 25 mm, and the vessel mass is slightly less than 25 tons. All of the vessel internal structures are hung from the vessel top flange (Sect. 4.2). The reactor vessel flange assembly will be transported to the site separately from the vessel. The vessel central flange and SiC-SiC composite core hanging rods will be joined to the core top plate on site. Control rods will be placed in the core during factory assembly and attached to the vessel central flange as part of the mating process between the core and the vessel internals.

The reactor will be deployed into a below-grade metal-lined pre-stressed concrete silo. The silo will be thermally connected to the ground to maintain the concrete and liner well below 100°C during reactor operation. The silo serves three principal functions: (1) containment, (2) well to maintain the reactor salt above the top of the DHXs in case of vessel rupture, and (3) cooled boundary to trap tritium that has diffused through the hot reactor vessel.

The silo will have a relatively close fit to the exterior of the reactor vessel to minimize the amount of primary coolant salt that must be kept above the core to ensure that the DHXs remain covered in the event of vessel failure. Only sufficient space for automated access for in-service inspection will be provided. All but minor maintenance activities (insulation repair) will thus require lifting the reactor vessel for access.

The exterior of the reactor vessel will be wired with electrical heaters with sufficient power to heat the vessel to above the salt melting point. The vessel and heater assembly will be encased within a close-fitting insulator assembly. All reactor components will be well insulated on their exterior surface. The vessel, heaters, and insulation will be transported to the site as a single unit. High-sensitivity, power-range flux measurement instrumentation will be incorporated into the insulation assembly.

9.3 INITIAL FUELING AND HEAT-UP

The reactor core will be factory assembled, including both the core top and bottom support plates and structural skirting (Sect. 4.2). The core support rods are threaded at each end. The upper ends of the rods pass through the vessel central flange and are bolted externally. The lower ends of the rods

are screwed into the upper core support plate. The control rods are then mated to their drive mechanisms, and the in-core and top-core instrumentation (flux and temperature measurements) are slid into the guide tubes built into the core.

SmAHTR employs long-shaft, cantilevered primary pumps. All bearings and seals are located above the reactor vessel flange. The in-vessel heat exchangers, pumps, and instrumentation are all factory installed onto top vessel flange wedges. The reflector, core barrel, flow skirting, and top flange exterior rim structure will be factory preassembled and transported to the site as a single piece. The start-up source and fission chamber (not shown in Fig. 9.1) will be loaded into recesses in the reflector. Both will be withdrawn through the top of the reactor vessel once the reactor begins its ascent to power. The reflector assembly also includes a salt siphon tube that extends from above the top flange down to the bottom of the reactor vessel.

The reactor vessel assembly procedure begins by first lowering the reactor vessel onto its support brackets. Next the reflector package is lowered into place and bolted to the reactor vessel top flange. The heat exchangers and pump wedge segments are then lowered into the recesses provided for them in the top flange and bolted into place. The secondary side coolant piping and siphon tube are then bolted onto the piping stubs protruding from the vessel top flange, and the pumps are confirmed to be properly rotating. The core assembly structure is then lowered into the reactor vessel and the top flange bolted shut.

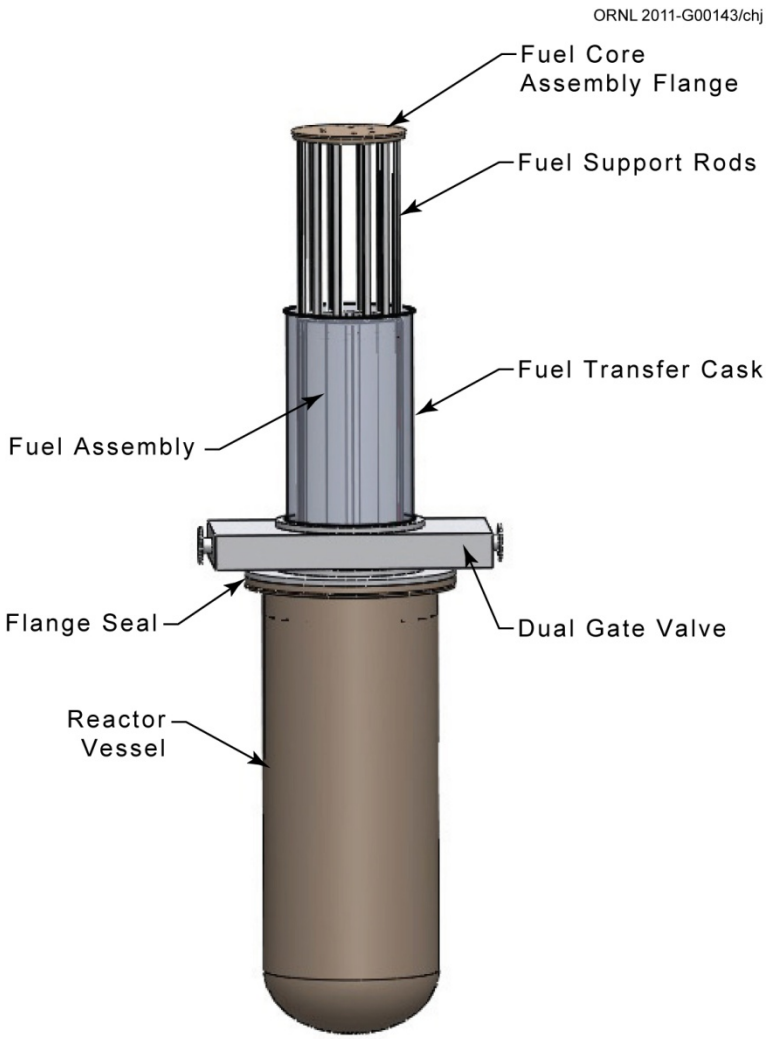

Fig. 9.1. SmAHTR core withdrawn into fuel transfer cask.

Once all of the structures inside the reactor vessel have been assembled and the top flange closed, the system will first be pressure checked by evacuating it through the gas control lines on the top flange. Dry helium will then be introduced into the vessel using the bottom siphon tube. Helium flow will be employed to dry out the moisture contained within the internal graphite during transport. The helium will be removed from the vessel using the cover gas control system piping. The vessel heaters will be employed to bring the interior structures to between 100°C and 150°C. Helium flow will be maintained until the gas exiting the core has no residual moisture. The siphon line will then be disconnected from the gas supply (to avoid the possibility of core voiding) and connected to the salt supply manifold emerging from the salt-handling tanks. The reactor vessel will then be heated to above the salt melting point (525°C nominally) using the external heaters.

9.4 SALT LOADING

The reactor salt inventory will be preloaded into salt-handling tanks. Between 50 and 60 m^3 of salt will be required for the initial primary inventory with additional primary salt required during refueling operation. The salt-handling tanks provide the volume necessary to store the primary salt inventory if the salt is ever siphoned from the reactor vessel for maintenance purposes. The salt-handling tanks will also incorporate a salt purification dip tube so that hydrogen fluoride and hydrogen can be bubbled through the salt to remove impurities in the salt accumulated during service.[1] The salt-handling tanks will also include helium sparging tubing to remove tritium from the salt.

The salt-handling tanks provide structured melting of the salt. Fluoride salts expand upon melting, and an important operational parameter is thus to melt the salt from a free surface. While conceptually the salt could be allowed to freeze within the reactor vessel and be melted from its top surface, the current operational intent is to never freeze the salt within the reactor vessel but instead to siphon the salt into handling tanks for any long-term cold shutdown events. Following initial start-up, decay heat and natural circulation will maintain the primary salt as a liquid for any anticipated operational occurrence.

All of the tubing interconnecting the salt-handling tanks to the reactor vessel siphon tube will be preheated to 550°C using external trace heating. Simultaneously all of the salt within the handling tanks will be melted using their structured heating systems. The pressure over the salt-handling tanks will then be increased one after another to siphon the salt from the tank into the reactor vessel. Once any one tank is emptied, its temperature will be lowered and a salt plug will formed in its dip tube to disconnect it from the reactor vessel. The reactor fill level will be monitored both by a radar-type level measurement system located in a standpipe above the top of the reactor vessel flange as well as thermocouples mounted to the exterior of the reactor vessel.

Cold (550°C) hydraulic and instrumentation validation testing will be performed once the salt has been introduced into the reactor vessel. The start-up neutron source and start-up fission chambers will then be introduced into the vessel through the in-reflector guide tubes, and cold subcritical neutronic measurements will be made. The reactor then will begin the initial approach to critical system validation path.

9.5 IN-SERVICE INSPECTIONS AND MAINTENANCE

Much of the in-service inspection and maintenance technology for SmAHTR power plants is directly analogous to that for LWRs. Motor current signature analysis will be applied to pumps as an indication of wear. Also, vibration measurements will be made on the external vessel structures to observe changes in performance. All of the reactor instrumentation signals will be evaluated for shifts in their noise and/or deviations from the anticipated signals based upon other measurements and the reactor performance model.

SmAHTR's containment outside the reactor vessel will be filled with dry nitrogen during operation. The nitrogen will be continuously circulated past a tritium-trapping organic catalyst similar to that used by heavy-water-moderated reactors to trap the emerging tritium. While both beryllium and tritium contamination will be almost certain (so contained breathing apparatus will be required), the space above the top flange of the reactor will not be acutely hazardous (either thermally or radioactively) during operation, and periodic access for component maintenance would be possible.

The primary salt chemistry control system will be employed to monitor the chromium and iron content of the primary salt as an indication of metallic corrosion. The primary salt chemistry control system provides access to the primary salt through tubes in the top flange. The salt chemistry control system enables reduction–oxidation state adjustment of the primary salt through contact with beryllium, much as was done during the MSRE.

In-service inspection of the in-vessel components will be primarily visual from above the salt surface. The salt is transparent, enabling visual access to immersed components via a window in the top flange. While the optical window will need to be mechanically wiped periodically to remove the salt vapor from its exposed surface, optical inspection should be possible on-line using a remote-controlled telescope and camera system. Once the reactor has been defueled, more detailed inspections of the reactor internals can be performed by raising the systems out of the salt or siphoning the salt from the vessel and lowering remote inspection equipment into the empty vessel.

9.6 REFUELING

SmAHTR features a cartridge core. The core is intended to be replaced as a unit and can be lifted from the vessel separately from the other in-vessel components. Refueling is performed with the salt maintained in liquid state, but at the reactor cold temperature (~550°C). At least 36 hr of core cooldown in the vessel is required before beginning core transfer to enable the core decay heat to fall below 1 MW. Refueling begins by unbolting the central top flange (that the core is hung from) from the reactor vessel flange.

A bottom-loading fuel transport cask is then positioned on top of the reactor vessel. The bottom of the transport cask is mated to the vessel flange with a seal at the interface and bolted down. Figure 9.1 shows the configuration of the refueling components and reactor vessel. The cask exterior surface will be covered with fins to enhance the natural convective heat transfer. Initial calculations indicate that for a reasonably sized transport cask (30 cm clearance from the core), natural draft cooling will provide 1 MW of decay heat removal at 650°C. The reactor vessel top plenum and fuel transfer cask are flooded with primary salt using the reactor salt-handling system prior to lifting the core.

The reactor core is then lifted into the fuel transfer cask, and the bottom cask closure dual gate valve is shut. The cask is then unbolted from the top of the reactor vessel and the core lowered onto the cask bottom. The bolts connecting the SiC-SiC core support cage to the central vessel top flange are then removed, and the central vessel top flange is lifted away. Next the core supporting rods are unscrewed from the top core support plate and lifted away. A top closure is then bolted to the fuel transfer cask. Figure 9.2 shows the closed fuel transfer cask on top of the reactor vessel. The entire fuel transfer cask is then immersed in the spent-fuel storage pool filled with a poisoned low-cost salt (such as europium-loaded KF-ZrF_4) and allowed to decay until just before the next core needs to be removed from the reactor.

The decay heat from the reactor core is less than 100 kW after 1–2 years of storage. At this point the core is removed from the transfer cask and placed directly into the storage pool filled with poisoned low-cost salt. Figure 9.3 shows the SmAHTR spent-fuel storage pool including both older cores in direct contact with the pool salt and a core still in its transfer cask. The transfer of the core out of the transfer cask occurs by first screwing a lifting structure to the core top plate and then lifting the core out of the top of the salt-filled transfer cask into an inert-gas-filled transfer channel. The large mass of the core and the low decay heat enable a slow (days) spent core transfer without

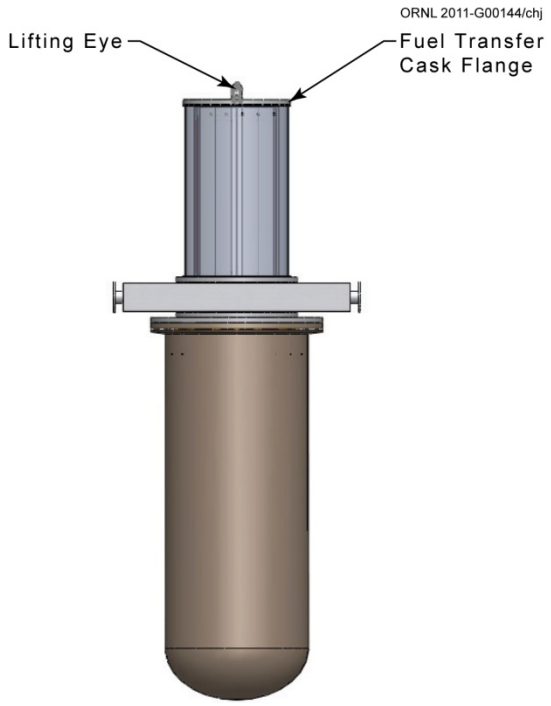

Fig. 9.2. Refueling cask prior to lifting from top of reactor vessel.

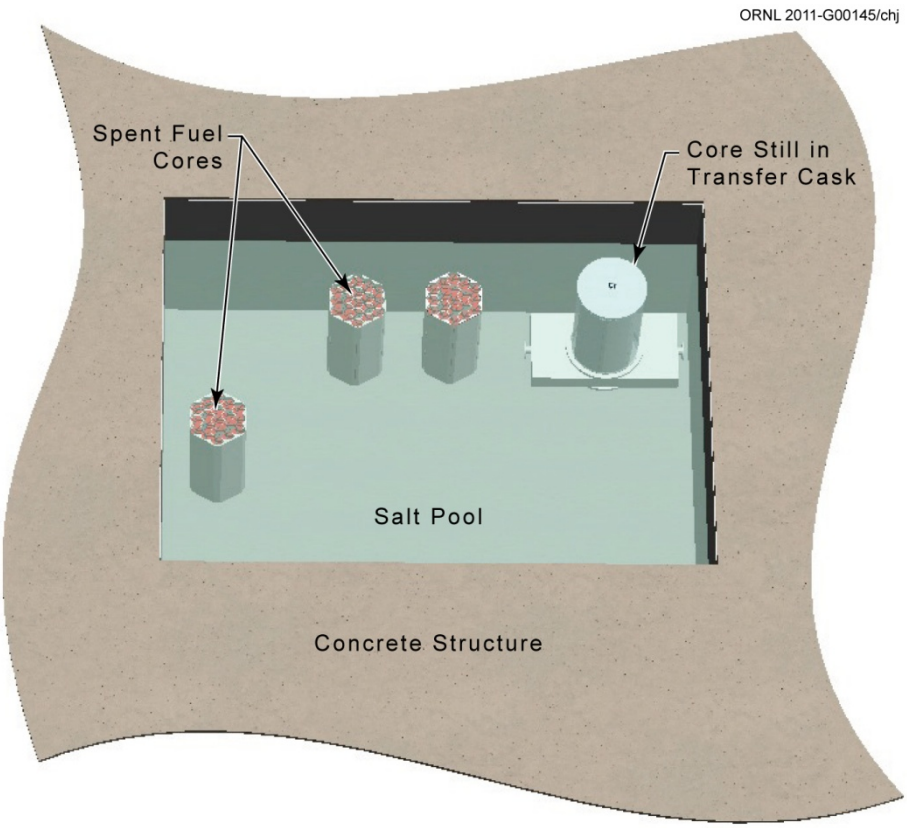

Fig. 9.3. Top view of SmAHTR spent core storage pool.

overheating the fuel. The expensive primary salt is then siphoned from the fuel transfer cask and recycled into the reactor primary salt-handling system, and the fuel transfer cask is reused to transfer the next spent core.

9.7 IN-VESSEL COMPONENT SERVICING AND REPLACEMENT

The reactor vessel internals are modular and designed to be independently replaceable. As discussed in Chaps. 4 and 5, the PHX and DHX are mounted to independent segments of the SmAHTR top flange. The primary pumps and in-vessel heat exchangers can be independently removed for inspection and maintenance by lifting from above using the fuel-handling crane. The primary coolant pump will be integrally mounted to the top of the PHX; thus, the two components will be withdrawn and serviced together.

9.8 REFERENCE

1. J. H. Shaffer, *Preparation and Handling of Salt Mixtures for the Molten Salt Reactor Experiment*, ORNL-4616 (January 1971).

10. SmAHTR UNIT CAPITAL AND OPERATIONS COST

10.1 SmAHTR COST AND ECONOMICS

Capital costs and economic performance of the SmAHTR reactor are a function of the specific deployment scenario. The initial SmAHTR concept focuses on transportability and ease of installation, with a cluster of small reactors intended to be brought into operation in a short time with minimal field construction or other infrastructure. Applications may be generation of electricity, high-temperature process heat for chemical processing, geologic materials extraction, or other processes. Because most existing reactors (aside from research and test reactors) have been built to generate electricity, this section discusses cost and economics in the context of electricity generation applications.

For electricity generation, SmAHTR is expected to deliver heat at a high temperature to a compact Brayton cycle turbine and generator. This report describes a reactor and supercritical CO_2 power conversion system that generate about 50 MWe in a single-unit application, or 200 MWe in a four-unit set, with a common salt vault. The motivation and economics for such a system can differ significantly from a large base-load plant, where the electrical output of a multi-unit site can exceed 3,000 MWe. Applications for electricity generation using a SmAHTR could include providing moderate amounts of secure power to a remote site, where other fuels may not be readily available or the electrical infrastructure does not support installation of a large generating facility. The cost of generating electricity with a small reactor is not expected to be will be comparable to the cost of electricity in a highly developed area. A complete estimate of capital and operating cost, leading to a life-cycle cost estimate or comprehensive economic model for supplying electricity or process heat, is not practical at the current level of system definition. Rather, various factors that drive cost relative to traditional LWRs are identified. Ease of implementation is impacted by the magnitude of capital cost required for design, licensing, fabrication, installation, and start-up of the plant. Financing must be identified, and in a commercial model, recovery of capital cost is a large portion of the cost of electricity. Manpower dominates the operations and maintenance cost for existing reactors, with fuel cost and other materials adding to the total. Ultimately, the cost of generating electricity is the sum of operating and capital recovery costs divided by the amount of electricity generated.

In applications where a larger amount of low-cost electricity is desired (as with most existing reactors), a larger AHTR may be more appropriate. Many of the cost factors identified in the following section would be applicable to both the SmAHTR and to large AHTRs. Several past efforts have identified cost differences between fluoride-salt-cooled reactors and other reactor systems. A comparison of cost factors, and rough costs, between a large AHTR, the liquid-metal-cooled S-PRISM, and the gas-cooled GT-MHR is found in Chap. 8 of Ref. 1.

10.2 UNIT CAPITAL COST CONSIDERATIONS

10.2.1 Favorable Cost Drivers

A number of considerations suggest the *n*th of kind production and capital costs of smarter modules can be attractive.

- High operating temperature, leading to high thermal efficiency and smaller equipment for the same electrical or useful thermal energy output.
- High operating temperature, enabling the use of Brayton cycle power-conversion equipment that is much smaller than typical Rankine steam-cycle equipment.
- Salt coolant with a high volumetric heat capacity and thermal conductivity, especially as compared to gas-cooled alternatives for high-temperature operation.

- Low operating pressure, leading to thinner walls in vessels and piping and reducing the physical energy that could cause or be released in accidents.
- Simplified containment system, avoiding the large pressurized containment vessels typical of existing LWRs.
- Separation of the safety significance of the reactor system from the power conversion system, especially through the use of the salt vault.
- Transparent coolant, simplifying visual inspection compared to liquid-metal-cooled reactors.
- Cartridge core, minimizing fuel handling facilities.
- Factory fabrication, with reduced cost and enhanced quality compared to field fabrication.
- Smaller structures, resulting from the use of Brayton cycle power equipment.
- Simplification of seismic design considerations, resulting from smaller equipment and structures.
- Transportation advantages, resulting from small reactor and power conversion equipment sizes and weights.

10.2.2 Unfavorable Cost Drivers

The favorable cost considerations noted above may be mitigated by the following unfavorable production and capital cost drivers.

- High-temperature equipment, requiring specialty alloys and equipment for salt-containing equipment and instrument penetrations.
- Advanced alloys, with limited sources of supply.
- Advanced power-conversion systems, such as supercritical CO_2 Brayton cycle equipment, for which little experience and manufacturing expertise exist.
- Establishment of a factory and tooling to enable factory fabrication cost savings.
- Dry core, preventing the use of water pools for refueling, inspection, and maintenance.
- Extensive pre-heat systems and insulation, with associated electrical power distribution systems.
- Cartridge core, in which a large shielded cask system is needed to remove and handle the core.
- Training of fabrication and construction labor force in working with unusual equipment and alloys.

Some of the favorable cost drivers will only appear as multiple units are built; similarly, several of the unfavorable cost drivers (such as experience with unusual materials) would decrease as the number of units increases. A key initial consideration is the investment needed to create a factory environment with appropriate tooling as compared to the opportunity for cost recovery until a larger number of units are built.

10.3 UNIT OPERATIONS AND MAINTENANCE COST CONSIDERATIONS

10.3.1 Favorable Cost Drivers

A number of considerations suggest the operations and maintenance costs of smarter modules can be attractive.

- High operating temperature, leading to better fuel utilization and reduced waste heat.
- Cartridge core, simplifying the refueling operation.
- Integrated reactor assembly designed for component removal and replacement.
- Simplified decay-heat-removal system, minimizing safety-related equipment maintenance and inspection.
- Small components, especially in the turbine hall.
- Transportable components, leading to the possibility of off-site factory refurbishment.

10.3.2 Unfavorable Cost Drivers

The favorable cost considerations noted above may be mitigated by the following unfavorable operations and maintenance cost drivers.

- Possibility of a large base-load staff in comparison to the amount of power generated, including operators, maintenance, fire brigade, security, and administration personnel.
- Need for operations and maintenance staff with special training in the application of unusual technologies.
- Handling of spent fuel as an intact assembly, using large shielded casks, as opposed to the familiar approaches of handling individual assemblies with simple equipment in a water pool.
- Impact of pre-heat systems and insulation on inspection and maintenance activities.
- As with capital cost, some of the unfavorable challenges fade as additional units come into operation, a larger trained labor pool is developed, and the availability of replacement components and appropriately equipped shop facilities grows.

10.4 SUMMARY

The previous discussion has noted a number of both favorable and unfavorable production, capital, operations, and maintenance cost drivers for SmAHTR modules. These cost considerations stem from both the generic attributes of FHRs and small modular reactors. Further exploration of the cost and economic performance of SmAHTR should be conducted following finalization of the reactor fuel and core configuration and further definition of the SmAHTR power conversion and salt vault energy storage systems.

10.5 REFERENCE

1. D. T. Ingersoll et al., *Status of Preconceptual Design of the Advanced High-Temperature Reactor (AHTR)*, ORNL/TM-2004/104 (May 2004).

11. SmAHTR DEVELOPMENT STRATEGY

11.1 INTRODUCTION

This section presents a brief assessment of the potential technology and system evolution possibilities for SmAHTR. As discussed in Chaps. 1 and 2, the initial evolution of the SmAHTR concept presented in this report is the product of a trade-space study of "small" fluoride-salt-cooled high-temperature reactors. In some sense SmAHTR and the original AHTR concept are "bookends" describing the very small and the very large FHR concept space. The numerous trade studies and compromises are embodied in the current SmAHTR concept. With respect to the potential evolution pathway for SmAHTR concepts, many questions are evident. Three major questions will be briefly discussed here.

- Should SmAHTR concepts grow to sizes larger than 125 MWt?
- Should SmAHTR concepts evolve to temperatures higher than 700°C, and if so, what are the reasonable design temperature evolution points?
- Should SmAHTR evolve to other power-conversion-system technologies?

With regard to the optimal size for SmAHTR, there appears to be no fundamental limit that requires the integral reactor power level be limited to 125 MWt. However, as discussed in previous sections, multiple SmAHTR units can be easily clustered together to meet higher thermal energy and electricity demands. Thus the prospects of relatively easy transport of a SmAHTR reactor to diverse field locations, coupled with the potential for cost advantages derived from factory fabrication of a smaller reactor, suggest that a detailed evaluation is necessary, before a decision can be made regarding optimization of SmAHTR's power level and the need for "larger SmAHTRs."

Concerning evolution of SmAHTR operating temperatures above 700°C, it is clear that FHR coolants and TRISO fuels employed in this initial SmAHTR evolutionary stage are capable of operating at much higher temperatures. However, the desire to avoid the unnecessary obstacle of creating an entirely new structural material in order to design and build the first SmAHTR prototype commends the more conservative approach of adopting only 700°C as the initial core outlet coolant temperature limit. Indeed, a pragmatic approach to SmAHTR demonstration would probably involve operating the reactor at temperatures as low as 600°C for a period of time prior to ascension to higher temperatures. The value of having a small, reliable very-high-temperature reactor operating at temperatures of 800°C, 900°C, or even 1,000°C would be significant, and perhaps transformational in terms of the architecture of our overall energy enterprise.

In a similar manner, the power conversion system embodied in the current SmAHTR evolution utilizes supercritical CO_2 Brayton technology, which, while well suited to the 700°C operating temperature of the current concept, is not appropriate for temperatures much above 800°C, where indirect-helium and direct-air Brayton technologies become more competitive. Hence, the selection of the power conversion technology for a very-high-temperature SmAHTR operating at 900°C or above would almost certainly be different from the that presented here.

With these considerations in mind, some thought has been given to the central question of the materials performance barriers currently evident that limit SmAHTR to the 700°C operating range, and how these materials challenges can be addressed to enable SmAHTR concepts with much higher operating temperatures.

11.2 MATERIALS CONSIDERATIONS FOR TEMPERATURE EVOLUTION OF SmAHTR

The materials of construction for the primary and secondary systems of SmAHTR will be required to have adequate strength, toughness, corrosion resistance, and radiation tolerance. Based on

currently available metallic materials limitations, the early vision for SmAHTR is a reactor with a maximum coolant outlet temperature of 700°C, with subsequent advancements to outlet temperatures up to 850°C and perhaps even 950–1,000°C. These advancements require a materials evolution strategy, which is outlined in this section.

For the existing suite of high-temperature structural alloys, protection from the service environment is afforded by the development of stable, slow-growing oxide layers, which are typically chromia at temperatures up to around 850°C and alumina at higher temperatures. These layers reduce alloy wastage and internal oxidation and allow for acceptable service lifetimes. As fluoride salts flux oxide layers, this approach to alloy protection is not applicable. Instead, protection depends on achieving thermodynamic stability and low solubility of alloying elements in the fluoride salts.

Pure nickel and alloys with very high nickel contents, and a sufficiently low content of certain other constituents, have been shown to have excellent resistance to environmental attack in liquid-fluoride-salt environments. However, if these materials are to provide simultaneously protection in oxidizing environments, such as air or gases for a Brayton-cycle turbine for production of electricity (helium, supercritical CO_2, etc.), they must develop a stable oxide layer in that environment as well. Hastelloy-N (originally called INOR-8), a commercially available, nickel-based alloy (Ni7Cr--16Mo-1Si), was originally developed by the ORNL in conjunction with the MSRE in the 1960s. Over 200,000 lb of Hastelloy-N were produced and used for construction of major MSRE components and was explicitly designed for compatibility with molten fluoride salts. Its chromium content is low but still sufficient to provide oxidation resistance in air. It is a solid-solution-strengthened (with molybdenum) alloy that does not embrittle upon aging and has limited contents of aluminum, titanium, and carbon to minimize fabrication and corrosion problems.

For the majority of uncooled metallic components for the 700°C outlet-temperature design (RPV, core barrel and other metallic internals, IHXs, DRACS), it is expected that Hastelloy-N will be used as a material of construction. Hastelloy-N has the designation of USN N10003 and has been incorporated into ASME Boiler and Pressure Vessel (B&PV) Code, Section II, Part D, Table 1B for service up to 704°C (1,300°F) for welded construction under Section VIII, Division 1 rules. Product forms covered include seamless and welded fittings (SB-366), plate, sheet, and strip (SB-434), and rod (SB-573), all in annealed condition. However, Hastelloy-N is not explicitly approved for nuclear construction within ASME's Section III, and significant additional materials property testing and analysis would be required to develop and support changes to the ASME Code (i.e., either a Code Case or modification of the main Code language in Section III) to cover such usage. Notwithstanding, Hastelloy-N has adequate strength and excellent salt and air compatibility up to 704°C and has been successfully used in construction of both of the molten salt reactors developed at ORNL. It should perform well in SmAHTR.

Raising the outlet temperature above about 700°C will preclude the use of Hastelloy-N for most uncooled components because its high-temperature strength drops precipitously above that temperature. Achieving relatively small incremental increases in operating temperature up to 750°C or slightly above may be possible using other existing commercial high-nickel alloys, such as Haynes 242 (a Ni-8Cr-25Mo-2.5Co-0.8Si age-hardenable alloy). However, Haynes 242 has not been used for nuclear service, and significant materials qualification testing would be needed to ensure its applicability. Other high-temperature alloys with much higher levels of chromium such as Haynes 230 (22Cr and 5Co) may also be applicable if suitable approaches to controlling the Lewis acidity of the salt (which affects alloying element solubility in the salt) can be developed.

For higher temperatures, structural alloys that can be used include nickel-clad or weld overlaid superalloys such as alloys 800H, 617, or 230. For the near term, insulated structures can be used, and for the longer term, newly developed, higher strength nickel-base alloys or even refractory-metal-based alloys will be available.

If a coated or layered structure is used, a number of issues must be considered. First is the question of the adequacy of the high-nickel layer to provide protection for the microstructure of the underlying superalloy. Evaluation of diffusion through the surface layer of various alloying elements and environmental impurities (e.g., oxygen and carbon) to and from the free surface of the layered component must demonstrate stability of both the high-temperature properties of the superalloy and the integrity of the layer (see Fig. 11.1). Fabricability is clearly an issue. Simple geometries can be fairly easily obtained via co-extrusion, roll bonding, weld overlay cladding, etc., but complex geometries such as tube-to-tube sheet, manifolds and headers, compact heat exchangers, etc., will be a much more significant challenge. Long-term integrity of the surface layer bond and inspectability of the layered component must be ensured.

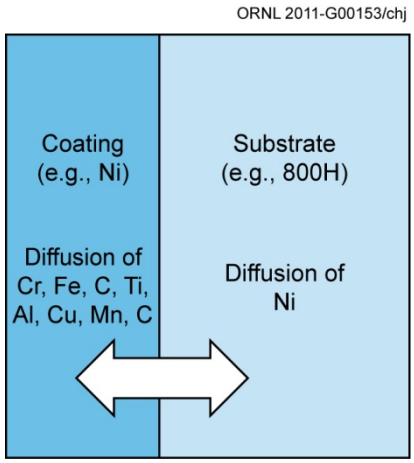

Fig. 11.1. Schematic representation of diffusion through the protective surface layer in a layered metallic structure.

For external components, such as the RPV or piping, it may be possible and desirable to internally insulate the component, allowing the use of a lower service temperature alloy, such as A508 or A533B steel, for the pressure boundary. This approach would require an engineering solution to corrosion protection on the inside surface of the component and an insulation layer sufficient to limit the operating temperature of the alloy used to an acceptable range, such as that schematically depicted in Fig. 11.2. With such an approach, it would be possible to increase the operating temperature of the coolant to 850°C or significantly beyond and still enable the use of existing structural alloys codified for nuclear service, but only for components with a coolable surface. Reactor internals, such as the core barrel or control rods, or heat exchangers that would have to operate at temperatures at or near that of the coolant would still require materials of construction with higher usage temperatures.

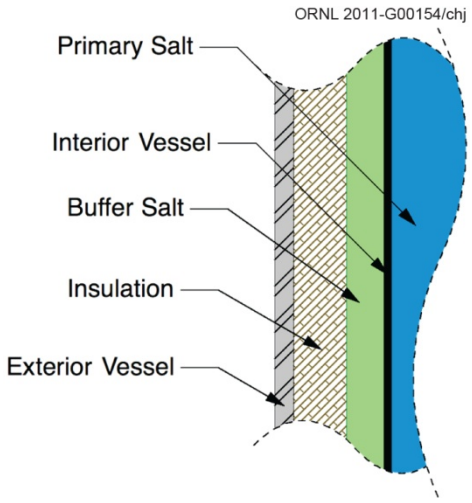

Fig. 11.2. Use of insulated structures for pressure boundaries.

The long-term solution for higher temperature operation of SmAHTR up to 850°C or slightly higher will likely require the development of a new superalloy with both adequate mechanical properties at the operating temperature and sufficient compatibility with the liquid salt and other required environments. Given the major overall advances in materials science and especially in predictive thermodynamic-based modeling tools for alloy development and evaluation, this is a very realistic possibility but would still likely require several years of development and qualification before such an alloy could be codified for nuclear service.

Alternately, the use of carbon–carbon or SiC-SiC composites or monolithic SiC would allow for uncooled components to temperatures up to and beyond 1,000°C, but would include very significant qualification, codification, and regulatory activities for the design and use of such materials, as well as ways to ensure the limited permeability needed for any pressure boundary applications. It is also expected that the radiation resistance of this class of materials would be adequate for use in the reactor internals for virtually all of the conditions envisioned for SmAHTR.

SmAHTR's graphite structures are expected to be of the fixed prismatic type with fairly fine webs, so the use of a high-strength, fine-grained graphite will be needed. Two grades of Toyo Tanso

graphite (IG110 or 430) that are currently being qualified for use in high-temperature gas-cooled reactors, such as the NGNP, would be well-qualified candidates. These materials are expected to pose no significant challenges associated with increasing reactor coolant temperature up to 1,000°C.

The leading candidate materials for various components of the SmAHTR operating at a range of output temperatures are summarized in Table 11.1.

In summary, the performance limits of structural materials available for use in near-term SmAHTR demonstrations would limit their operating temperature to ~700°C. In the longer term, materials evolution strategies that would enable SmAHTR operations at 850°C and above are evident.

Table 11.1. Leading candidate materials for selected SmAHTR reactor components operating at various reactor output temperatures

Component	700°C	850°C	950–1000°C
Graphite internals	Toyo Tanso IG110 or 430	Toyo Tanso IG110 or 430	Toyo Tanso IG110 or 430
RPV	Hastelloy-N	Nickel weld-overlay cladding on 800H, insulated low-alloy steel, new nickel-based alloy	Interior insulated low-allow steel
Core barrel and other internals	Hastelloy-N	C-C composite, new nickel-based alloy	C-C or SiC-SiC composite, new refractory alloy
Primary heat exchanger	Hastelloy-N	New nickel-based alloy, double-sided nickel cladding on 617 or 230	C-C or SiC-SiC composite, monolithic SiC
DRACS	Hastelloy-N	New nickel-based alloy, double-sided nickel cladding on nickel-based superalloy (e.g., 617 or 230)	C-C or SiC-SiC composite, monolithic SiC
Pump	Hastelloy-N, Ti-mod Hastelloy-N	Moly-alloy or ceramic-coated nickel-based superalloy	Moly-alloy or ceramic-coated nickel-based superalloy
Control rods and internal drives	C-C composites, Hastelloy-N, Nb-1Zr	C-C composites, Nb-1Zr	C-C composites, Nb-1Zr
Secondary loop piping	Interior insulated low-alloy steel, Hastelloy-N	Interior insulated low-alloy steel, new nickel-based alloy	Interior instulated low-alloy steel
Secondary heat exchanger (salt to salt)	Hastelloy-N	New nickel-based alloy, limited permeability C-C composite	Limited permeability C-C composite
Secondary heat exchanger (salt to gas)	Coaxially extruded tubes, 800H with nickel-based layer	New nickel-based alloy, coaxially extruded tubes, 800H with nickel layer, limited permeability C-C composite	Unknown at this time, due to very high strength requirements at this temperature

12. SUMMARY

12.1 SmAHTR 1.0

During the spring of 2010, a small team was assembled at Oak Ridge National Laboratory to explore the feasibility of fluoride-salt-cooled small modular high-temperature reactors. The goals of the team were (1) explore the technology and system architecture design trade space for such concepts and (2) develop an initial design evolution to serve as a vehicle for understanding the potential performance attributes of such systems and their developmental challenges. The SmAHTR reactor and thermal energy system presented in this report are the results of this study.

SmAHTR is a 125 MWt, integral primary system reactor concept, designed to operate with a core outlet temperature of 700°C and a refueling interval of 3–4 years. The reactor vessel is sufficiently small to accommodate transport to the deployment site by standard tractor-trailer vehicles.

Four SmAHTR reactor core concepts are under consideration: (1) solid cylindrical fuel pellets in removal stringer fuel assemblies, (2) hollow annular fuel pellets in removal stringer fuel assemblies, (3) removal fuel assemblies utilizing fuel plates or "planks," and (4) pebble-bed cores. The first three options were evaluated in this initial study. While the focus has been on "cartridge core" designs that enable rapid removal and reloading of the entire core as an integrated unit, none of the fuel designs considered to date preclude the more traditional approach of insertion and removal of individual fuel assemblies. All fuel designs use coated-particle graphite (TRISO) fuel very similar to that specified for a Next-Generation Nuclear Plant (NGNP).

SmAHTR employs a "two-out-of-three" concept for operational heat removal and shutdown decay-heat removal. Three 50% capacity systems operate in parallel at all times—only two of which are required for complete functionality. The transition from operation model to shutdown decay-heat-removal mode is accomplished without resorting to active system components.

The preliminary investigation of SmAHTR's transient response and safety attributes indicates the system is well behaved and transitions smoothly from operations to shutdown mode while maintaining substantial fuel temperature margins. The combination of low power density, passive heat removal, robust coated-particle graphite fuel, low primary system operating pressure, high coolant volumetric heat capacity, and fission product retention capability of the coolant presents a package of performance attributes that enable a high degree of safety.

In addition to the SmAHTR reactor system itself, a very preliminary concept has been developed for a "salt vault" high-temperature thermal energy storage system. The integration of multiple SmAHTR modules with the salt vault not only increases the size of the supportable energy demand beyond that which can be met by a single unit but also provides significant additional benefits with respect to "buffering" the customer energy demand from the reactors as a group, and the individual reactors from each other.

This initial SmAHTR concept evolution is not sufficiently detailed to support in-depth capital and operating-cost analyses. However, the intrinsic attributes of the SmAHTR system (low pressure, compact system with efficient heat transport characteristics), considered on balance, offer the prospect of attractive *n*th-of-kind capital costs and competitive unit operating costs both for electricity production and process heat applications for deployment scenarios in the 2030 time period and beyond.

SmAHTR's operating temperature is currently constrained by the performance limits of the structural materials used in the reactor vessel and non-fuel internal structures. This limitation restricts near-term SmAHTR concepts to operating temperatures of ~700°C. With this in mind, and in view of the benefits to be gained from higher system operating temperatures, a preliminary two-step materials development strategy has been formulated. This strategy targets expansion of the SmAHTR concept to 850°C and ~1,000°C in the coming decades.

12.2 SmAHTR CONCEPT EVOLUTION

The SmAHTR concept presented here is but a snapshot of a complex technology and system architecture trade space. SmAHTR and the SmAHTR salt vault thermal energy system described in this report are not optimized systems. Additional concept-definition work to be done includes the following:

- Optimization of the fuel and core design
- Further definition of the reactivity and instrumentation and control system
- Expanded transient and safety analyses (including generation of a pre-conceptual phenomena identification and ranking table, or PIRT, as soon as the concept is sufficiently defined to enable the exercise)
- Optimization of the in-vessel PHX and DHX designs
- Optimization of the salt vault system design and its interface with the reactors
- Optimization of the SmAHTR electrical power conversion system design and the interface to it
- Preliminary SmAHTR capital cost estimates

Modest investment in these activities will significantly expand our understanding of the feasibility of the SmAHTR concept, its performance attributes, and its principal development challenges.

12.3 ENABLING RESEARCH AND DEVELOPMENT

System concept development activities are essential elements of integrated advanced reactor development programs because *it is in the system concept that the value and promise of scientific research and technology development are made manifest*. Concept development provides the basis for prioritizing and guiding both basic technology development and enabling component development activities. With this in mind, a focused research, technology development, and component demonstration program is needed to enable FHR and SmAHTR development. A focused R&D program would include the development and optimization of fluoride-salt coolants, TRISO fuel forms, salt-compatible structural materials (graphites, composites, metals), critical components (pumps, heat exchangers, and valves), and high-temperature instrumentation. Based on the work performed to date, priority must be placed on the development of compact salt-to-salt and salt-to-gas heat exchangers. Other key component development priorities include liquid-salt pumps and the vortex diodes that can operate in high-temperature liquid-salt environments. All of these activities will be complemented by a basic focus on the development of high-performance, high-temperature nuclear materials, as discussed previously.

Finally, it should be noted that SmAHTR and FHRs in general benefit from and leverage much ongoing fuels and materials work in the DOE Office of Nuclear Energy NGNP and AGR fuels programs.

APPENDIX A. SmAHTR FUEL TECHNOLOGY CONSIDERATIONS

APPENDIX A. SmAHTR FUEL TECHNOLOGY CONSIDERATIONS

A.1 COATED-PARTICLE FUEL TECHNOLOGY

The fuel form of choice for high-temperature reactors specifically designed for high-efficiency electricity generation and high-temperature heat applications is a coated particle fuel that consists of a small spherical core or kernel of nuclear material surrounded by pyrocarbon and SiC coatings designed to retain the fission products during normal operation and all licensing basis events. The fuel kernel is typically fabricated using sol-gel techniques, resulting in a high-density ceramic that retains most of the fission products. The most common coated particle design, under development since the early 1960s and referred to as TRISO (tri-isotropic), is typically fabricated by chemical vapor deposition of the successive layers in a fluidized bed furnace. The innermost layer or buffer layer is porous, low-density (~0.95 g/cc) pyrocarbon, which provides volume to accommodate kernel swelling, fission gases, and fission dependent gases (CO and CO_2) and sufficient mass to absorb fission product recoil momentum to protect the structural layers. Three structural layers are then applied: (1) a gas-tight high-density pyrocarbon layer (~1.95 g/cc) whose primary function is to serve as a substrate for the SiC layer, protect the kernel from chlorine generated during SiC deposition, and hold the SiC layer in compression; (2) a high-density SiC layer (~3.2g/cc) to serve as the primary "pressure vessel" and fission product barrier layer to retain the metallic fission products that diffuse through the inner pyrocarbon (IPyC) layer at high temperature; and (3) another high-density pyrocarbon layer (~1.95 g/cc) whose primary function is to protect the SiC layer during further fuel fabrication steps, help keep the SiC under compression during service, and provide a final barrier to fission product release.

This fuel form is extremely versatile; for a given fast or thermal reactor mission, the TRISO coating design remains essentially the same while the kernel's metal loading and composition is varied: U for energy production, U/Th for resource sustainability, and U/Pu/minor actinides for used fuel management. Coated particle fuel is one of the few fuel forms that can be applied to high-temperature and high-burnup applications and has the potential to achieve burnups and temperatures significantly beyond current experience. As a result of about 50 years of research and development worldwide, standard uranium-based TRISO fuel can now be fabricated with acceptable performance for nominal operating conditions with roughly 800°C core outlet temperature in a helium-cooled reactor.

A.2 SmAHTR FUEL DESIGN CONSIDERATIONS

While the specific fuel particle design depends on the required fuel service conditions, a representative coated particle design that could readily be adopted for use in the Small modular Advanced High-Temperature Reactor (SmAHTR) is the Advanced Gas Reactor-1 (AGR-1) fuel, recently demonstrating excellent fission product retention to 4×10^{25} n/m^2 peak fast fluence [E > 0.18 MeV, 19% peak fissions per initial metal atom (FIMA), and 16% average FIMA] during a 610 effective full-power-day irradiation test in the Idaho National Laboratory's Advanced Test Reactor.[A.1] Figure A.1 is a cross section of a typical AGR-1 particle. Table A.1 provides the fuel product specifications and typical batch values for coating thickness, density, microstructure, and anisotropy. The AGR-1 fuel test is the first test in a series of irradiation tests planned to support licensing of the Next-Generation Nuclear Plant (NGNP). Two high-temperature gas-cooled reactor (HTGR) concepts are currently being considered for the NGNP: the pebble-bed reactor and the prismatic-block reactor. If the NGNP uses a pebble-bed design, the coated particle fuel will have a UO_2 kernel. If the prismatic-block design is selected, the coated particle fuel kernel will be composed of a mixture of UO_2 and UC_2 (also referred to as "uranium oxicarbide" or UCO) designed to mitigate kernel migration at higher burnup, a known failure mechanism for HTGR designs having a

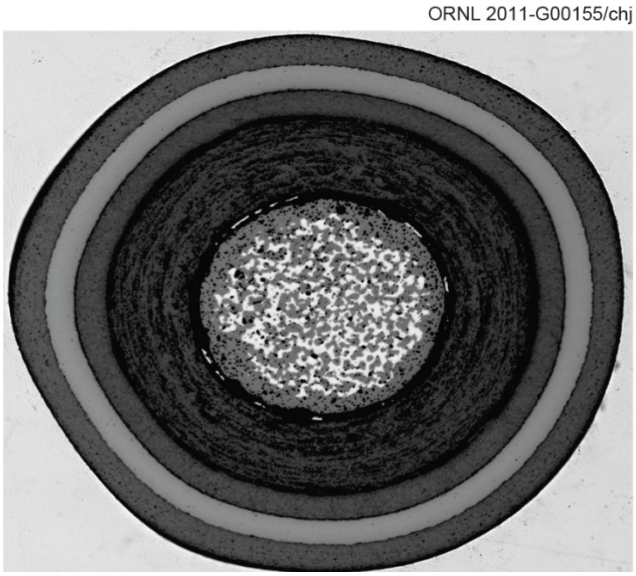

Fig. A.1. Cross section of an AGR-1 TRISO fuel particle with a mixed uranium oxide–uranium carbide (UCO) fuel kernel.

Table A.1. Advanced Gas Reactor-1 (AGR-1) fuel product specifications and typical batch values for coating thickness, density, microstructure, and anisotropy

Fuel layer	AGR-1 composite specification	Typical batch
Buffer		
Thickness	100 ± 15 mm	103 ± 8 mm
Density	1.05 ± 0.15 g/cc	1.10 ± 0.05 g/cc
Inner pyrolytic carbon		
Thickness	40 ± 4 mm	40 ± 2 mm
Density	1.9 ± 0.05 g/cc	1.90 ± 0.02 g/cc
Anisotropy factor (BAFo)	<1.024	<1.015 ± 0.002
Silicon carbide		
Thickness	35 ± 3 mm	35 ± 1 mm
Density	≥3.19 g/cc	3.205 ± 0.001 g/cc
Microstructure	No large columnar grains extending through the SiC layer	No large columnar grains extending through the SiC layer
Outer pyrolytic carbon		
Thickness	40 ± 4 mm	41 ± 2 mm
Density	1.9 ± 0.05 g/cc	1.91 ± 0.01 g/cc
Anisotropy factor	<1.035	<1.007

sufficiently high thermal gradient in the fuel body. Kernel migration, or the "amoeba effect," is the result of the transfer of carbon from the hot side of the kernel-buffer surface to the cold side of the kernel-buffer surface, which causes the kernel to propagate up the temperature gradient through the buffer and IPyC and damage the SiC layer. Careful control of the oxygen-to-metal ratio in the kernel has been shown to eliminate kernel migration, but this adds to the complexity of the kernel fabrication process and requires storage of the finished product in an inert atmosphere before coating. Including carbon in the kernel controls the oxygen chemical potential ($UC_2 + O_2 \rightarrow UO_2 + 2C$), thereby minimizing the oxygen chemical potential and shutting down the carbon transport.

Another approach to controlling the oxygen potential is to include an oxygen getter to bind up the oxygen released from the fission of uranium (e.g., $SiC + O_2 \rightarrow SiO_2 + C$). While kernel migration has been observed in pebble-bed designs, it is effectively controlled by limiting the maximum power in the sphere and by the continuous movement of the sphere through the core. These controls result in thermal gradients in the pebble that are smaller than the gradients in a prismatic fuel compact, and UO_2 kernel migration is negligible. Therefore, depending on the details of the SmAHTR design, the kernel could be exclusively UO_2 or could be designed using the AGR-1 fuel design, either of the two current NGNP designs, or a design incorporating SiC or ZrC in a UO_2 kernel to serve as an oxygen getter. Incorporating SiC into the kernel is the current choice of the U.S. Department of Energy Office of Nuclear Energy, Deep Burn program.[A.2]

Table A.2 provides a comparison of the fuel service conditions among various high-temperature reactor concepts. Note that the SmAHTR conceptual design may require fuel operating at a power density outside the bounds that have been demonstrated to date. Should this be the case, consideration should be given to research and development to demonstrate adequate TRISO performance at high power density. In addition, it may be that the fission product retention requirements placed on the TRISO fuel to support gas-cooled reactor operation may be too stringent for liquid-salt-cooled applications, where any fission products released to the coolant can be extracted using previously demonstrated technology.

Table A.2. Comparison of fuel service conditions for normal operation[a]

HTGR[a] concept	Mean power density MW/m^3	Discharge burnup (% FIMA)		Discharge fast fluence, E > 0.1 MeV (10^{21} n/cm^2)		Temperature (°C)	
		Core average value	Maximum value	Core average value	Maximum value	Core average value	Maximum value
AVR	2.6						
NGNP[b] pebble bed	3.4	8.31	8.75	2.01	2.39	644	1,048
NGNP prismatic			17		5	1,250[b]	1,400
SmAHTR	9.4						1,250

[a]HTGR = high-temperature gas-cooled reactor, FIMA = fissions per initial metal atom, AVR = Arbeitsgemeinschaft Versuchsreaktor (German prototype pebble-bed reactor), NGNP = Next-Generation Nuclear Plant, SmAHTR = Small modular Advanced High-Temperature Reactor.

[b]NGNP values are maximum time averaged.

Following fabrication and acceptance testing of the TRISO particles, the next step in the fuel fabrication process is forming the particles into a suitable matrix for in-core service. Unlike light water reactor fuels in which the oxide fuel pellet is protected from the reactor coolant water by a metal cladding, the TRISO fuel could be in direct contact with the gas or salt coolant. Given their small size (<1 mm diameter), direct contact between the fuel particles and the salt coolant may not be desirable; therefore, the TRISO particles are usually consolidated into a carbonaceous matrix material and pressed into a form suitable for the particular reactor design. Typical forms are pebbles

(Germany, China), right circular cylinders (United States), or annular cylinders (Japan); however, other forms, including cruciform, curved plates, and planks, could be envisioned. Whatever the final form, the method currently preferred for preparing the core particles for molding is to first apply a thin layer of a matrix precursor material to the TRISO particle and then compress the overcoated fuel particles into the desired shape. The overcoat performs two functions: (1) it distributes compacting forces to minimize the probability of fracturing the TRISO particle during the compacting process, and (2) it controls the loading fraction of the nuclear material.

The matrix for the NGNP fuel is a mixture of graphite and a binding material (thermosetting resin) that is deformable at processing temperatures (room temperature to ~150°C depending on the resin). To fabricate a cylindrical compact, the overcoated particles are poured into a cylindrical die and compressed in the axial direction by a single or double acting plunger. The overcoating material flows into the interstitial spaces resulting in a fuel compact composed of TRISO particles surrounded by a void-free matrix. The mass of the overcoat is carefully controlled to provide the desired matrix density and packing fraction and hence the fissile loading. The thickness of the overcoat for the AGR-1 fuel compacts (165 μm) provides a packing fraction of 35%. Work by Morris and Pappano indicated the maximum practical compact packing fraction is most likely in the 40–50% range.[A.3] While recent production level targets have been ~40%, packing fractions up to 50% have been reported in the literature.[A.4] Figure A.2 shows an AGR-1 fuel compact and an annular compact fabricated by the Japanese for the High-Temperature Test Reactor (HTTR). [A.5]

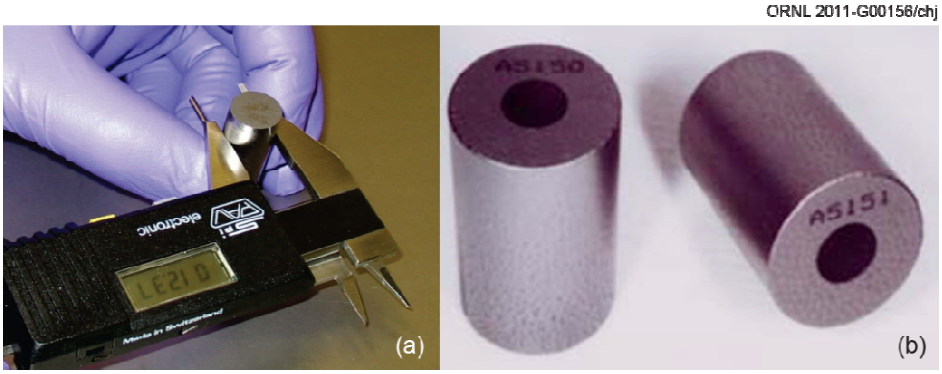

Fig. A.2. Photographs of (a) an AGR-1 fuel compact and (b) a Japanese HTTR annular fuel compact.

To fabricate annular compacts for the SmAHTR, the same graphite-resin matrix formulation used for the AGR-1 fuel compacts could be used. While the dimensions of the SmAHTR's annular compact are larger than typical HTGR fuel compacts, they are of the same order of magnitude and do not require any new equipment beyond a new die set; therefore, fabrication is not expected to present any undue difficulty. Given the paucity of mechanical strength data available in the literature, measurements of SmAHTR compact properties should be performed and factored into the mechanical and fluid dynamics model to ensure in-service conditions do not exceed material performance capabilities.

As discussed in Sect. 4.3, an interesting alternative SmAHTR fuel design would use TRISO fuel consolidated into fuel "planks" approximately 2.8 cm thick by 23 cm wide by 4 m long (Fig. A.3). While fabrication of this fuel form would provide a challenge due to its large size relative to traditional HTR fuel forms, incorporation of TRISO particles into a suitable plank is feasible. An assessment of the fabrication steps required to fabricate a fuel plank (Table A.3) indicates that while new equipment would be required, the fabrication steps are expected to be very similar to those of other fuel forms. Owing to the large fuel plank dimensions; lack of mechanical strength data as a

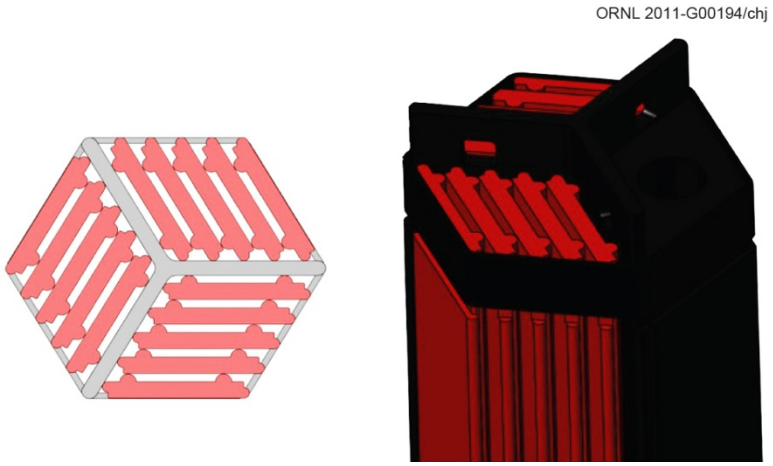

Fig. A.3. Conceptual sketch of an innovative plank fuel form.

Table A.3. Comparison of fuel compact and fuel plank fabrication steps

Process step	AGR-1 compact	SmAHTR plank
Matrix production	Natural graphite, synthetic graphite, thermosetting resin wet-mixed together to form "resinated" powder	Similar if not identical materials
Overcoating	Overcoat TRISO particles in spinning canister	Same process used for fluoride-salt-cooled high-temperature reactor (FHR); large-scale overcoater has been demonstrated at Vector Corp.
Fuel form fabrication	Press overcoated particles in cylindrical die	Requires research and development; forming is feasible; maintaining the physical integrity of the plank after fabrication will require specially designed handling fixtures and procedures Probably vibro-mold FHR planks in rectangular mold; same principle used to make NBG-18 graphite for Pebble-Bed Modular Reactor
Carbonizing (baking)	Green fuel form baked to 950°C to set and carbonize the resin	Same process for fuel planks but specialized furnace to minimize handling and accommodate plank dimensions
Final heat treatment	Baked fuel form high temperature to 1,800°C for impurity reduction	Same process for fuel planks (again specialized furnace)

function of packing fraction; and questions regarding the structural integrity of a long, thin plank, it is anticipated that handling of the plank would require specialized fixtures.

The development of the plank fuel form and the transition from laboratory scale to industrial scale can be expected to required the following major steps.

- Install a small-scale vibro-molding station (~1/10 scale).
- Fabricate planks and determine optimal packing fraction to toughness ratio. (NOTE: forming the plank is one part of the project; ensuring that it does not crack under its own weight during handling will be the key issue.)
- Characterize planks for broken particles and erosion properties.
- Determine best forming method and "recipe" for strong planks.
- Transition to large-scale equipment; will most likely need a conveyer system between molding, baking, and final heat treatment.

In addition, fuel form erosion studies are needed to ensure adequate performance in the SmAHTR fuel configuration. Matrix production and overcoating is already well understood and is being done at large scale.

A.3 REFERENCES

A.1. U.S. Department of Energy, Generation IV Nuclear Energy Systems, "Advanced Gas Reactor Fuel Program's TRISO Particle Fuel Sets a New World Record for Irradiation Performance," November 2009, available at http://www.ne.doe.gov/geniv/neGenIV9.html

A.2. R. D. Hunt, J. D. Hunn, J. F. Birdwell, T. B. Lindemer, and J. L. Collins, "The addition of silicon carbide to surrogate nuclear fuel kernels made by the internal gelation process," *J. Nucl. Mater.* **401**, 55–59 (2010).

A.3. R. N. Morris and P. J. Pappano, "Estimation of Maximum Coated Particle Fuel Compact Packing Fraction," *J. Nucl. Mater*. **361**(1), 18–29 (March 2007).

A.4. E. H. Voice and D. W. Sturge, *Advances in HTR Matrix Technology*, D. P. Report 867 (February 1974).

A.5. "Fuel Researches in the HTTR project" Shohei UETA, Nuclear Science and Energy Directorate, Nuclear Applied Heat Technology Division, High Temperature Fuel & Material Group, Japan Atomic Energy Agency (JAEA), IAEA International Conference on Non-Electric Applications of Nuclear Power: Seawater Desalination, Hydrogen Production and other Industrial Applications, April 16–18, 2007, JAEA Oarai R&D Center, Oarai, Japan.

APPENDIX B. SmAHTR RELAP5-3D MODEL

APPENDIX B. SmAHTR RELAP5-3D MODEL

B.1 SmAHTR SYSTEM MODEL DESCRIPTION

RELAP5-3D/ATHENA, Version 2.4.2, was used to perform thermal hydraulic evaluations of the SmAHTR concept. RELAP5-3D[B.1] includes properties for four salts: FLiBe, FLiNaK, $NaBF_4$-NaF, and NaF-ZrF_4. For the calculations presented here, FLiBe is used for the primary coolant and FLiNaK for the secondary coolant [for the secondary of both the primary heat exchanger (PHX) and the direct reactor auxiliary cooling system (DRACS)].

The RELAP5-3D nodalization of the primary system is shown in Fig. B.1. A cross section of the various core designs was presented in Sect. 4.3. Each of the core designs was divided radially into three rings with 1, 6, and 12 assemblies (volumes 116, 117, and 118) moving from the core centerline to the outer radius. Each ring had an assumed radial and axial (cosine) power distribution. A flat radial power profile has also been used in some of the models.

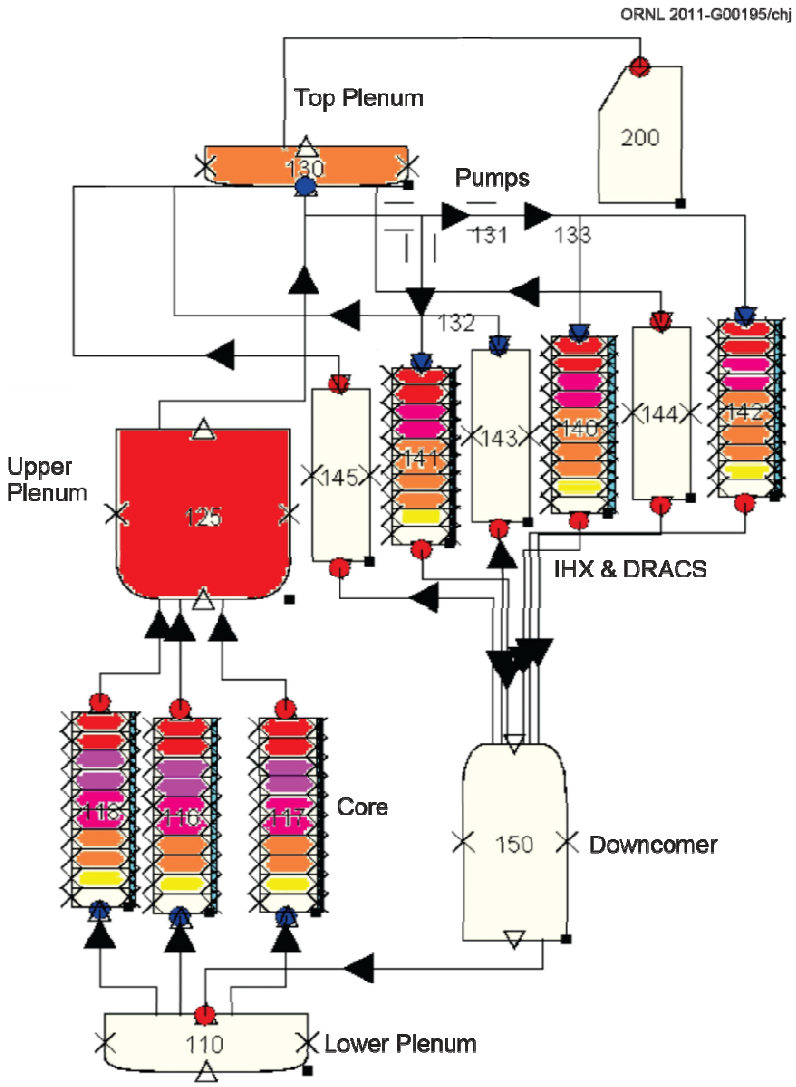

Fig. B.1. RELAP5-3D nodalization of the SmAHTR primary system.

The primary system includes the lower plenum (volume 110); upper plenum (volume 125); top plenum (volume 130) with the open gas volume (connected to volume 200); three pumps (junctions 131, 132, and 133); three PHXs (volumes 140, 141, and 142); three DRACSs (volumes 143, 144, and 145); and finally, the downcomer (volume 150). The colors in each control volume are indicative of the temperature of the coolant inside the control volume during normal operation. Yellow is cold (650°C), and red is hot (700°C). The arrows also show the direction of the flow during normal operation. The flow in the DRACS (reverse flow) is up, while the flow in the intermediate heat exchangers (IHXs)is down.

RELAP5 "heat structures" in contact with volumes 116, 117, and 118 model the fuel pins, graphite pins, and graphite blocks within the reactor core. Heat structures in contact with volumes 140, 141, and 142 model the PHXs. Finally, the DRACS heat exchangers are the heat structures in contact with volumes 143, 144, and 145.

The different fuel designs were modeled by changing the hydraulic volumes 116, 117, and 118 and the respective heat structures in contact with them (modeling fuel and graphite pins and reflector/moderator). The three different fuels analyzed (cylindrical pins, annular pins, and plates) have been modeled separately. For the annular fuel, two channels representing the inside and the outside of the annulus were required for each ring for a total of six parallel channels in the core. The RELAP5 nodalization for the annular fuel is shown in Fig. B.2. The remainder of the model for annular fuel is the same as Fig. B.1.

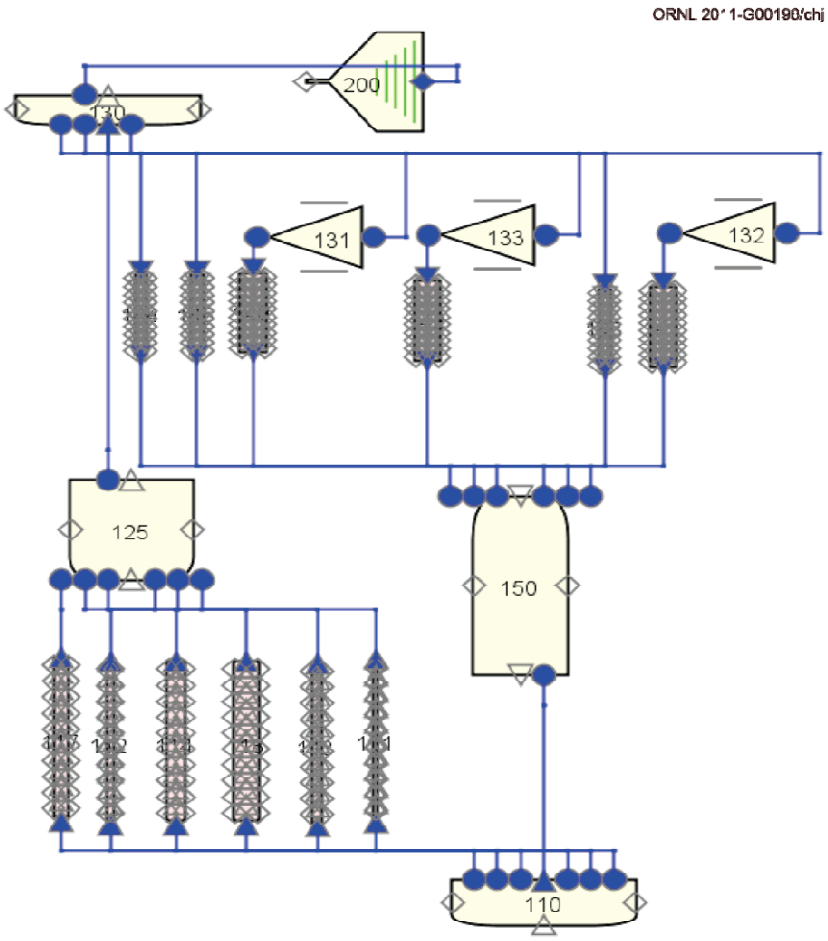

Fig. B.2. RELAP5-3D nodalization for the annular fuel. Core with six channels between the lower plenum (110) and the upper plenum (125).

Secondary systems (or intermediate loops) were also modeled for each of the three PHXs and for each of the three DRACSs. Furthermore, each DRACS loop is connected to an air cooler; the DRACS loop and the air cooler are also represented in the RELAP5-3D model.

Figure B.3 is an isometric view of the primary system model generated by the RELAP-3D graphics processor showing the temperatures of the coolant in the outside volumes of the vessel during normal operation. The top plenum, PHXs, downcomer, and lower plenum can be seen in the figure. The coolant temperature is hotter at the top (at 700°C), decreasing as the coolant goes through the PHXs, and is constant at the temperature of 650°C in the downcomer and in the lower plenum. The larger diameters of the lower plenum and the top plenum in Fig. B.3 are artifacts of the larger horizontal flow areas of those two volumes when compared to the smaller horizontal flow areas of the PHX and downcomer. Also, the hemispherical lower plenum volume must be represented as a cylinder in the RELAP-3D model.

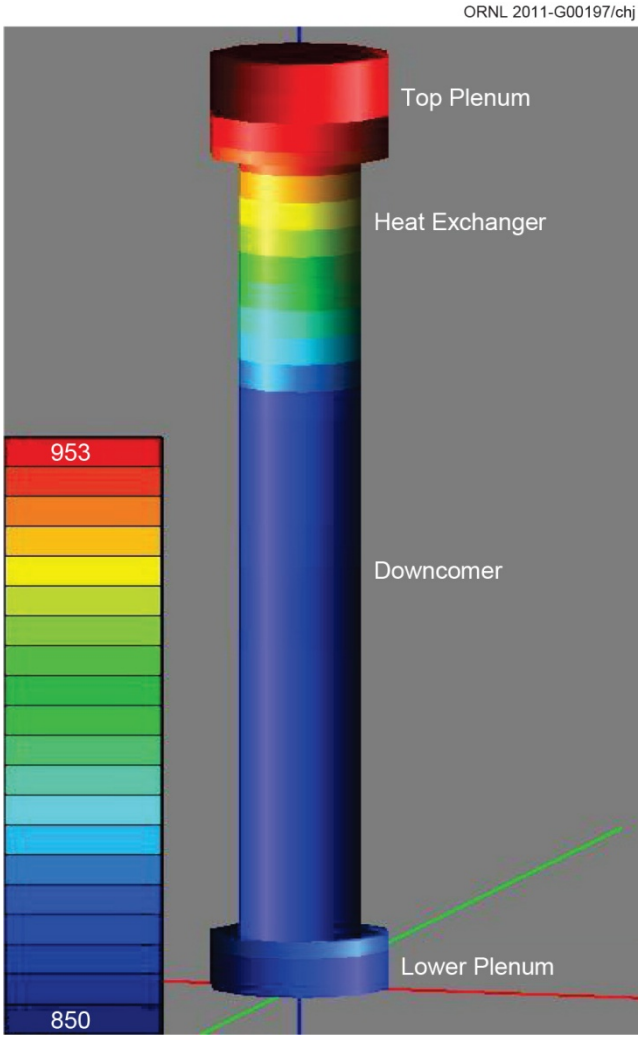

Fig. B.3. Isometric view of the SmAHTR vessel generated by RELAP5.

B.2 REFERENCES

B.1. Idaho National Laboratory, *RELAP5-3D Code Manual*, Rev. 2.4, INEEL-EXT-98-00834, Idaho (2006).

INTERNAL DISTRIBUTION

1. S. J. Ball
2. G. L. Bell
3. K. J. Beierschmitt
4. S. M. Bowman
5. E. C. Bradley
6. J. J. Carbajo
7. M. S. Cetiner
8. D. A. Clayton
9. W. R. Corwin
10. R. A. Crone
11. G. F. Flanagan
12. J. C. Gehin
13. S. R. Greene
14. D. E. Holcomb
15. J. D. Hunn
16. D. Ilas
17. D. T. Ingersoll
18. G. T. Mays
19. P. J. Pappano
20. C. V. Parks
21. F. J. Peretz
22. A. L. Qualls
23. L. L. Snead
24. V. K. Varma
25. D. F. Wilson
26. G. L. Yoder
27. S. J. Zinkle

EXTERNAL DISTRIBUTION

28. P. B. Lyons (DOE/NE)
29. R. S. Johnson (DOE/NE)
30. J. E. Kelly (DOE/NE)
31. D. C. Welling (DOE/NE)
32. S. J. Golub (DOE/NE)
33. R. A. Kendall (DOE/NE)
34. M. P. Crozat (DOE/NE)
35. P. Finck (INL)
36. K. McCarthy (INL)
37. K. Pasamehmetoglu (INL)
38. R. N. Hill (ANL)
39. C. Grandy (ANL)
40. G. E. Rochau (SNL)
41. P. F. Peterson (UCB)
42. A. T. Cisneros (UCB)
43. E. D. Blandford (UCB)
44. C. W. Forsberg (MIT)
45. N. E. Todreas (MIT)
46. C. Rodriguez (GA)
47. R. Schleicher (GA)
48. J. E. Goossen (Westinghouse)
49. M. G. Anness (Westinghouse)
50. Paul Murray (AREVA)
51. Kim Stein (AREVA)
52. Bojan Petrovic (GIT)